From the Core of Red Giant Stars to the Edge of the Tumors

César Domingo Pardo
IFIC (CSIC-University of Valencia)

"Anselm Kiefer (German artist) is fascinated by the night sky and its different interpretations throughout history, particularly those describing it as a divine, mysterious kingdom recalling our origins and fate."

GSI-FAIR Colloquium, Darmstadt, 11/02/2025

A. Kiefer (Guggenheim M.)

Outline

- Heavy elements nucleosynthesis: How stars make gold (r-process) and lead (s-process)?
- Neutron-capture experiments at CERN n_TOF: Red-Giant stars in the lab
- Enhancing detection sensitivity in neutron capture TOF experiments
- Beyond the limits: r-process neutron-reactions in the lab?
- From stars to tumors: ion-range & dose monitoring in hadron therapy
- Summary & Outlook

PERIODIC TABLE

Atomic Properties of the Elements

NIST | NATIONAL INSTITUTE OF STANDARDS AND TECHNOLOGY
U.S. DEPARTMENT OF COMMERCE

Physical Measurement Laboratory www.nist.gov/pml
Standard Reference Data www.nist.gov/srd

FREQUENTLY USED FUNDAMENTAL PHYSICAL CONSTANTS[§]

1 second = 9 192 631 770 periods of radiation corresponding to the transition between the two hyperfine levels of the ground state of ^{133}Cs

speed of light in vacuum	c	299 792 458 m s^{-1}	(exact)
Planck constant	h	$6.626\ 070\ 15 \times 10^{-34}$ J Hz^{-1}	(exact)
elementary charge	e	$1.602\ 176\ 634 \times 10^{-19}$ C	(exact)
Avogadro constant	N_A	$6.022\ 140\ 76 \times 10^{23}$ mol^{-1}	(exact)
Boltzmann constant	k	$1.380\ 649 \times 10^{-23}$ J K^{-1}	(exact)
electron volt	eV	$1.602\ 176\ 634 \times 10^{-19}$ J	(exact)
electron mass	m_e	$9.109\ 383\ 71 \times 10^{-31}$ kg	
energy equivalent	m_ec^2	0.510 998 951 MeV	
proton mass	m_p	$1.672\ 621\ 926 \times 10^{-27}$ kg	
energy equivalent	m_pc^2	938.272 089 MeV	
fine-structure constant	α	1/137.035 999	
Rydberg energy	$R_\infty hc$	13.605 693 1230 eV	
Newtonian constant of gravitation	G	6.674×10^{-11} $m^3\ kg^{-1}\ s^{-2}$	

[§] For the most accurate values of these and other constants, visit pml.nist.gov/constants.

- ⬜ Solids
- 🟪 Liquids
- 🟥 Gases
- 🟦 Artificially Prepared

Period	Group 1 IA	2 IIA	3 IIIB	4 IVB	5 VB	6 VIB	7 VIIB	8 VIII	9	10	11 IB	12 IIB	13 IIIA	14 IVA	15 VA	16 VIA	17 VIIA	18 VIIIA
1	1 $^2S_{1/2}$ **H** Hydrogen 1.008 $1s$ 13.5984																	2 $^1S_0$ **He** Helium 4.0026 $1s^2$ 24.5874
2	3 $^2S_{1/2}$ **Li** Lithium 6.94 $1s^22s$ 5.3917	4 $^1S_0$ **Be** Beryllium 9.0122 $1s^22s^2$ 9.3227											5 $^2P^\circ_{1/2}$ **B** Boron 10.81 $1s^22s^22p$ 8.2980	6 $^3P_0$ **C** Carbon 12.011 $1s^22s^22p^2$ 11.2603	7 $^4S^\circ_{3/2}$ **N** Nitrogen 14.007 $1s^22s^22p^3$ 14.5341	8 $^3P_2$ **O** Oxygen 15.999 $1s^22s^22p^4$ 13.6181	9 $^2P^\circ_{3/2}$ **F** Fluorine 18.998 $1s^22s^22p^5$ 17.4228	10 $^1S_0$ **Ne** Neon 20.180 $1s^22s^22p^6$ 21.5645
3	11 $^2S_{1/2}$ **Na** Sodium 22.990 [Ne]$3s$ 5.1391	12 $^1S_0$ **Mg** Magnesium 24.305 [Ne]$3s^2$ 7.6462											13 $^2P^\circ_{1/2}$ **Al** Aluminum 26.982 [Ne]$3s^23p$ 5.9858	14 $^3P_0$ **Si** Silicon 28.085 [Ne]$3s^23p^2$ 8.1517	15 $^4S^\circ_{3/2}$ **P** Phosphorus 30.974 [Ne]$3s^23p^3$ 10.4867	16 $^3P_2$ **S** Sulfur 32.06 [Ne]$3s^23p^4$ 10.3600	17 $^2P^\circ_{3/2}$ **Cl** Chlorine 35.45 [Ne]$3s^23p^5$ 12.9676	18 $^1S_0$ **Ar** Argon 39.95 [Ne]$3s^23p^6$ 15.7596
4	19 $^2S_{1/2}$ **K** Potassium 39.098 [Ar]$4s$ 4.3407	20 $^1S_0$ **Ca** Calcium 40.078 [Ar]$4s^2$ 6.1132	21 $^2D_{3/2}$ **Sc** Scandium 44.956 [Ar]$3d4s^2$ 6.5615	22 $^3F_2$ **Ti** Titanium 47.867 [Ar]$3d^24s^2$ 6.8281	23 $^4F_{3/2}$ **V** Vanadium 50.942 [Ar]$3d^34s^2$ 6.7462	24 $^7S_3$ **Cr** Chromium 51.996 [Ar]$3d^54s$ 6.7665	25 $^6S_{5/2}$ **Mn** Manganese 54.938 [Ar]$3d^54s^2$ 7.4340	26 $^5D_4$ **Fe** Iron 55.845 [Ar]$3d^64s^2$ 7.9025	27 $^4F_{9/2}$ **Co** Cobalt 58.933 [Ar]$3d^74s^2$ 7.8810	28 $^3F_4$ **Ni** Nickel 58.693 [Ar]$3d^84s^2$ 7.6399	29 $^2S_{1/2}$ **Cu** Copper 63.546 [Ar]$3d^{10}4s$ 7.7264	30 $^1S_0$ **Zn** Zinc 65.38 [Ar]$3d^{10}4s^2$ 9.3942	31 $^2P^\circ_{1/2}$ **Ga** Gallium 69.723 [Ar]$3d^{10}4s^24p$ 5.9993	32 $^3P_0$ **Ge** Germanium 72.630 [Ar]$3d^{10}4s^24p^2$ 7.8994	33 $^4S^\circ_{3/2}$ **As** Arsenic 74.922 [Ar]$3d^{10}4s^24p^3$ 9.7886	34 $^3P_2$ **Se** Selenium 78.971 [Ar]$3d^{10}4s^24p^4$ 9.7524	35 $^2P^\circ_{3/2}$ **Br** Bromine 79.904 [Ar]$3d^{10}4s^24p^5$ 11.8138	36 $^1S_0$ **Kr** Krypton 83.798 [Ar]$3d^{10}4s^24p^6$ 13.9996
5	37 $^2S_{1/2}$ **Rb** Rubidium 85.468 [Kr]$5s$ 4.1771	38 $^1S_0$ **Sr** Strontium 87.62 [Kr]$5s^2$ 5.6949	39 $^2D_{3/2}$ **Y** Yttrium 88.906 [Kr]$4d5s^2$ 6.2173	40 $^3F_2$ **Zr** Zirconium 91.224 [Kr]$4d^25s^2$ 6.6341	41 $^6D_{1/2}$ **Nb** Niobium 92.906 [Kr]$4d^45s$ 6.7589	42 $^7S_3$ **Mo** Molybdenum 95.95 [Kr]$4d^55s$ 7.0924	43 $^6S_{5/2}$ **Tc** Technetium (97) [Kr]$4d^55s^2$ 7.1194	44 $^5F_5$ **Ru** Ruthenium 101.07 [Kr]$4d^75s$ 7.3605	45 $^4F_{9/2}$ **Rh** Rhodium 102.91 [Kr]$4d^85s$ 7.4589	46 $^1S_0$ **Pd** Palladium 106.42 [Kr]$4d^{10}$ 8.3368	47 $^2S_{1/2}$ **Ag** Silver 107.87 [Kr]$4d^{10}5s$ 7.5762	48 $^1S_0$ **Cd** Cadmium 112.41 [Kr]$4d^{10}5s^2$ 8.9938	49 $^2P^\circ_{1/2}$ **In** Indium 114.82 [Kr]$4d^{10}5s^25p$ 5.7864	50 $^3P_0$ **Sn** Tin 118.71 [Kr]$4d^{10}5s^25p^2$ 7.3439	51 $^4S^\circ_{3/2}$ **Sb** Antimony 121.76 [Kr]$4d^{10}5s^25p^3$ 8.6084	52 $^3P_2$ **Te** Tellurium 127.60 [Kr]$4d^{10}5s^25p^4$ 9.0098	53 $^2P^\circ_{3/2}$ **I** Iodine 126.90 [Kr]$4d^{10}5s^25p^5$ 10.4512	54 $^1S_0$ **Xe** Xenon 131.29 [Kr]$4d^{10}5s^25p^6$ 12.1298
6	55 $^2S_{1/2}$ **Cs** Cesium 132.91 [Xe]$6s$ 3.8939	56 $^1S_0$ **Ba** Barium 137.33 [Xe]$6s^2$ 5.2117		72 $^3F_2$ **Hf** Hafnium 178.49 [Xe]$4f^{14}5d^26s^2$ 6.8251	73 $^4F_{3/2}$ **Ta** Tantalum 180.95 [Xe]$4f^{14}5d^36s^2$ 7.5496	74 $^5D_0$ **W** Tungsten 183.84 [Xe]$4f^{14}5d^46s^2$ 7.8640	75 $^6S_{5/2}$ **Re** Rhenium 186.21 [Xe]$4f^{14}5d^56s^2$ 7.8335	76 $^5D_4$ **Os** Osmium 190.23 [Xe]$4f^{14}5d^66s^2$ 8.4382	77 $^4F_{9/2}$ **Ir** Iridium 192.22 [Xe]$4f^{14}5d^76s^2$ 8.9670	78 $^3D_3$ **Pt** Platinum 195.08 [Xe]$4f^{14}5d^96s$ 8.9588	79 $^2S_{1/2}$ **Au** Gold 196.97 [Xe]$4f^{14}5d^{10}6s$ 9.2256	80 $^1S_0$ **Hg** Mercury 200.59 [Xe]$4f^{14}5d^{10}6s^2$ 10.4375	81 $^2P^\circ_{1/2}$ **Tl** Thallium 204.38 [Hg]$6p$ 6.1083	82 $^3P_0$ **Pb** Lead 207.2 [Hg]$6p^2$ 7.4167	83 $^4S^\circ_{3/2}$ **Bi** Bismuth 208.98 [Hg]$6p^3$ 7.2855	84 $^3P_2$ **Po** Polonium (209) [Hg]$6p^4$ 8.4181	85 $^2P^\circ_{3/2}$ **At** Astatine (210) [Hg]$6p^5$ 9.3175	86 $^1S_0$ **Rn** Radon (222) [Hg]$6p^6$ 10.7485
7	87 $^2S_{1/2}$ **Fr** Francium (223) [Rn]$7s$ 4.0727	88 $^1S_0$ **Ra** Radium (226) [Rn]$7s^2$ 5.2784		104 $^3F_2$ **Rf** Rutherfordium (267) [Rn]$5f^{14}6d^27s^2$ 6.02	105 $^4F_{3/2}$ **Db** Dubnium (268) [Rn]$5f^{14}6d^37s^2$ 6.8	106 $_0$ **Sg** Seaborgium (269) [Rn]$5f^{14}6d^47s^2$ 7.8	107 $_{5/2}$ **Bh** Bohrium (270) [Rn]$5f^{14}6d^57s^2$ 7.7	108 $_4$ **Hs** Hassium (269) [Rn]$5f^{14}6d^67s^2$ 7.6	109 **Mt** Meitnerium (277)	110 **Ds** Darmstadtium (281)	111 **Rg** Roentgenium (282)	112 **Cn** Copernicium (285)	113 **Nh** Nihonium (286)	114 **Fl** Flerovium (290)	115 **Mc** Moscovium (290)	116 **Lv** Livermorium (293)	117 **Ts** Tennessine (294)	118 **Og** Oganesson (294)

Lanthanides	57 $^2D_{3/2}$ **La** Lanthanum 138.91 [Xe]$5d6s^2$ 5.5769	58 $^1G^\circ_4$ **Ce** Cerium 140.12 [Xe]$4f5d6s^2$ 5.5386	59 $^4I^\circ_{9/2}$ **Pr** Praseodymium 140.91 [Xe]$4f^36s^2$ 5.4702	60 $^5I_4$ **Nd** Neodymium 144.24 [Xe]$4f^46s^2$ 5.5250	61 $^6H^\circ_{5/2}$ **Pm** Promethium (145) [Xe]$4f^56s^2$ 5.5819	62 $^7F_0$ **Sm** Samarium 150.36 [Xe]$4f^66s^2$ 5.6437	63 $^8S^\circ_{7/2}$ **Eu** Europium 151.96 [Xe]$4f^76s^2$ 5.6704	64 $^9D^\circ_2$ **Gd** Gadolinium 157.25 [Xe]$4f^75d6s^2$ 6.1498	65 $^6H^\circ_{15/2}$ **Tb** Terbium 158.93 [Xe]$4f^96s^2$ 5.8638	66 $^5I_8$ **Dy** Dysprosium 162.50 [Xe]$4f^{10}6s^2$ 5.9391	67 $^4I^\circ_{15/2}$ **Ho** Holmium 164.93 [Xe]$4f^{11}6s^2$ 6.0215	68 $^3H_6$ **Er** Erbium 167.26 [Xe]$4f^{12}6s^2$ 6.1077	69 $^2F^\circ_{7/2}$ **Tm** Thulium 168.93 [Xe]$4f^{13}6s^2$ 6.1844	70 $^1S_0$ **Yb** Ytterbium 173.05 [Xe]$4f^{14}6s^2$ 6.2542	71 $^2D_{3/2}$ **Lu** Lutetium 174.97 [Xe]$4f^{14}5d6s^2$ 5.4259
Actinides	89 $^2D_{3/2}$ **Ac** Actinium (227) [Rn]$6d7s^2$ 5.3802	90 $^3F_2$ **Th** Thorium 232.04 [Rn]$6d^27s^2$ 6.3067	91 $^4K_{11/2}$ **Pa** Protactinium 231.04 [Rn]$5f^26d7s^2$ 5.89	92 $^5L^\circ_6$ **U** Uranium 238.03 [Rn]$5f^36d7s^2$ 6.1941	93 $^6L_{11/2}$ **Np** Neptunium (237) [Rn]$5f^46d7s^2$ 6.2655	94 $^7F_0$ **Pu** Plutonium (244) [Rn]$5f^67s^2$ 6.0258	95 $^8S^\circ_{7/2}$ **Am** Americium (243) [Rn]$5f^77s^2$ 5.9738	96 $^9D^\circ_2$ **Cm** Curium (247) [Rn]$5f^76d7s^2$ 5.9922	97 $^6H^\circ_{15/2}$ **Bk** Berkelium (247) [Rn]$5f^97s^2$ 6.1979	98 $^5I_8$ **Cf** Californium (251) [Rn]$5f^{10}7s^2$ 6.2819	99 $^4I^\circ_{15/2}$ **Es** Einsteinium (252) [Rn]$5f^{11}7s^2$ 6.3684	100 $^3H_6$ **Fm** Fermium (257) [Rn]$5f^{12}7s^2$ 6.50	101 $^2F^\circ_{7/2}$ **Md** Mendelevium (258) [Rn]$5f^{13}7s^2$ 6.58	102 $^1S_0$ **No** Nobelium (259) [Rn]$5f^{14}7s^2$ 6.6262	103 $^2P^\circ_{1/2}$ **Lr** Lawrencium (262) [Rn]$5f^{14}7s^27p$ 4.96

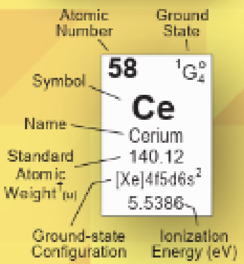

For the most precise values and uncertainties visit ciaaw.org and pml.nist.gov/data.

---

† Based upon ^{12}C. () indicates the mass number of the longest-lived isotope.

NIST SP 966 (June 2024)

The origin of the elements:

Making Gold (r-process) and Lead (s-process)

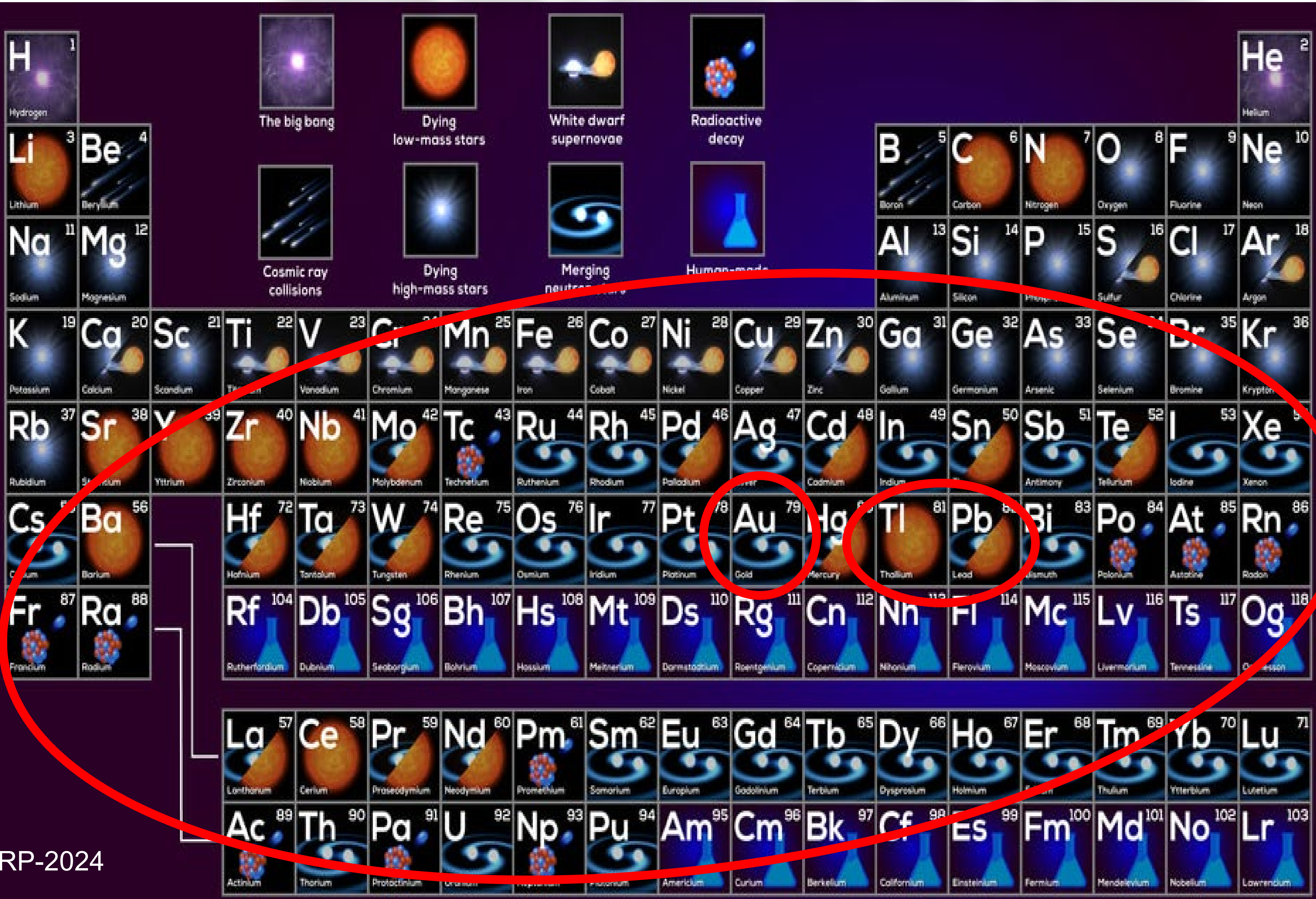

LRP-2024

Heavy Elements Nucleosynthesis: Making Gold (r-process)

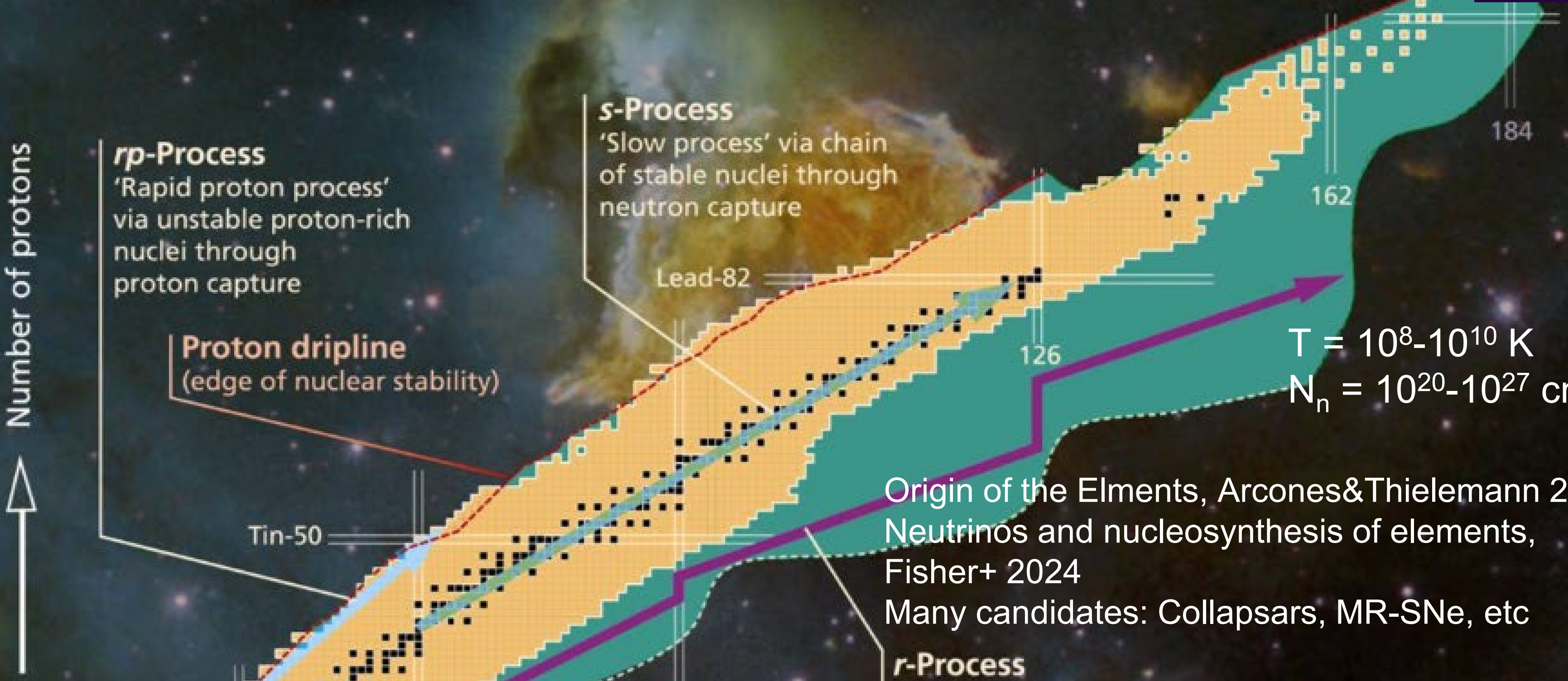

$T = 10^{8}$-10^{10} K

$N_n = 10^{20}$-10^{27} cm^{-3}

Origin of the Elments, Arcones&Thielemann 2023

Neutrinos and nucleosynthesis of elements, Fisher+ 2024

Many candidates: Collapsars, MR-SNe, etc

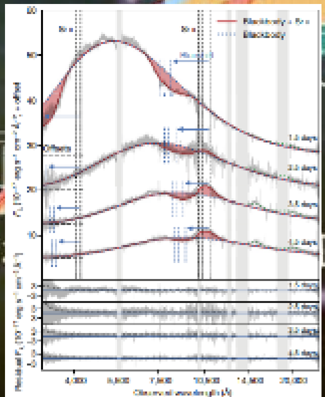

Article

Identification of strontium in the merger of two neutron stars

D.Watson+ 2019

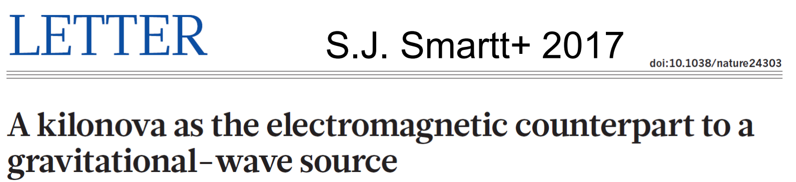

LETTER

S.J. Smartt+ 2017

doi:10.1038/nature24303

A kilonova as the electromagnetic counterpart to a gravitational-wave source

The r-process: all elements at once, in a few seconds

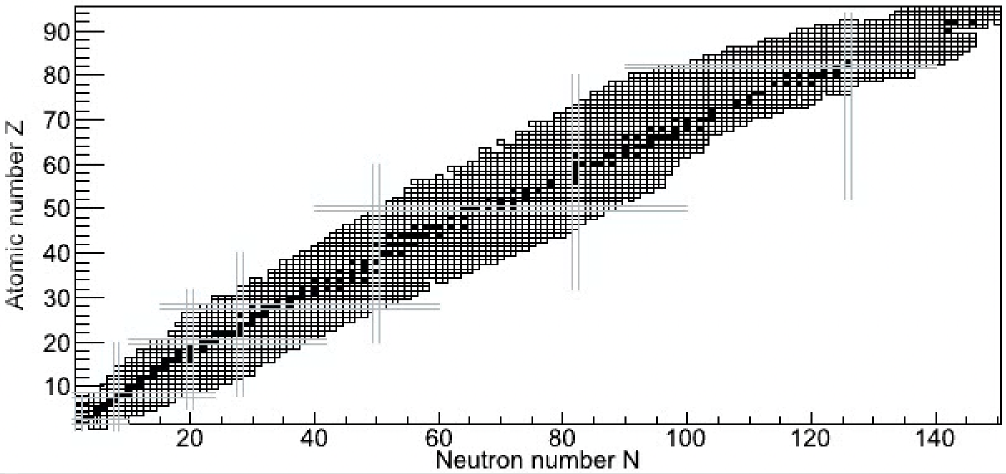

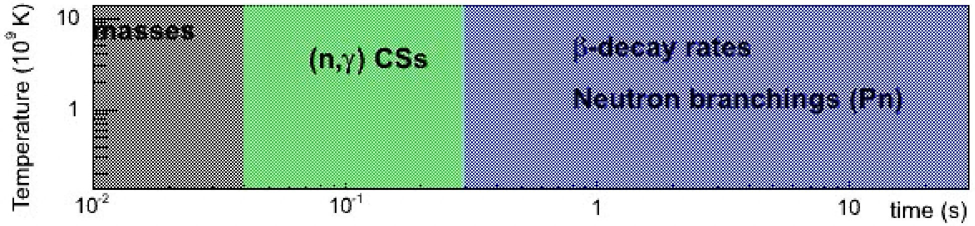

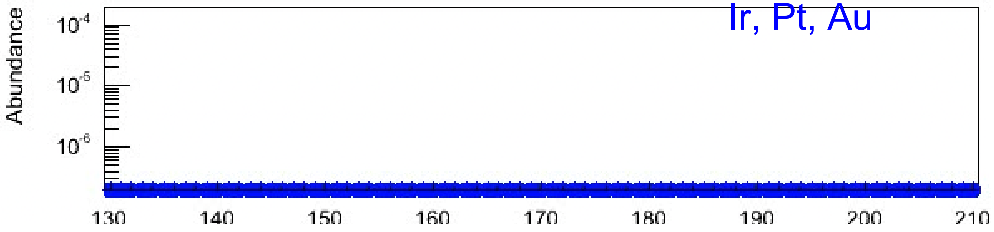

By CDP with ROOT, modSN-Thermotrajectory from AA+GMP'21,
NucNet network code, B. Meyer et al., Clemson University
FRDM+QRPA (P. Möller) + JINA Reaclib Database

Most recent advanced NS-toolkit:

OPEN ACCESS

The Nuclear Reaction Network WinNet

M. Reichert, C. Winteler, O. Korobkin, A. Arcones, J. Bliss, M. Eichler, U. Frischknecht, C. Fröhlich, R. Hirschi, M. Jacobi, J. Kuske, G. Martínez-Pinedo, D. Martin, D. Mocelj, T. Rauscher, and F.-K. Thielemann

The r-process: all elements at once, in a few seconds

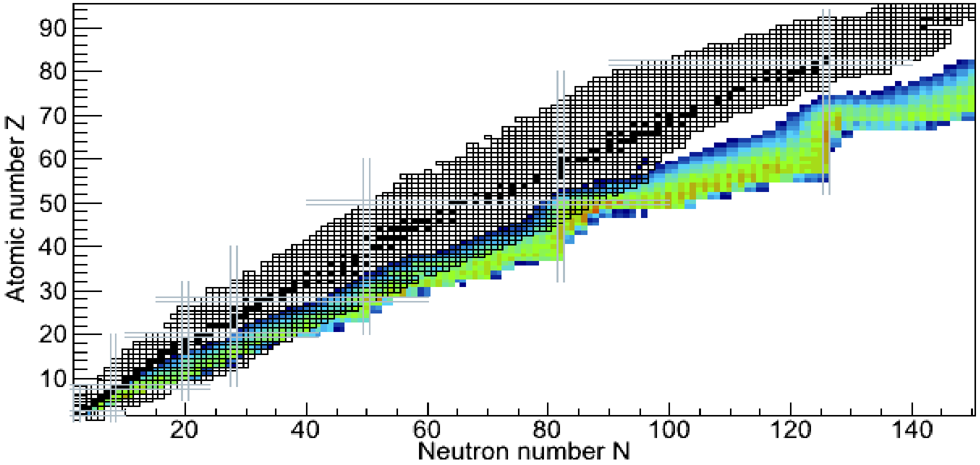

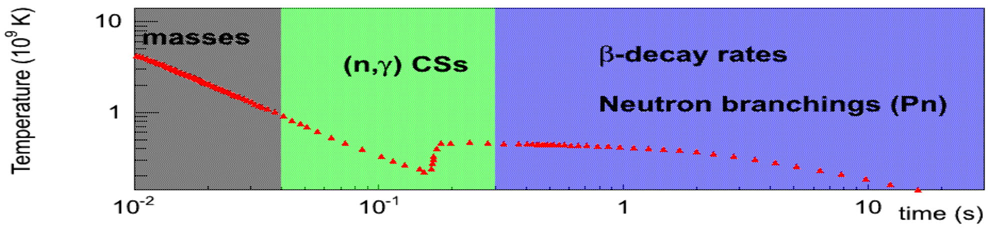

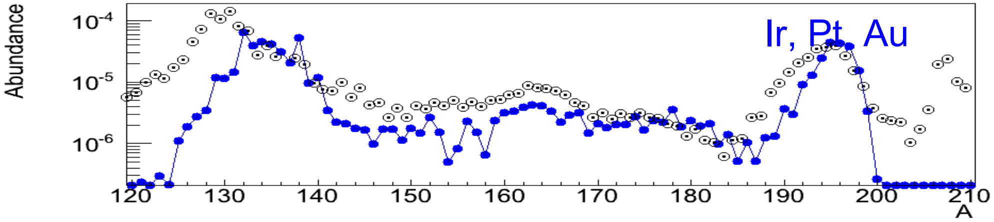

By CDP with ROOT, modSN-Thermotrajectory from AA+GMP'21,
NucNet network code, B. Meyer et al., Clemson University
FRDM+QRPA (P. Möller) + JINA Reaclib Database

Important neutron-capture isotopes:

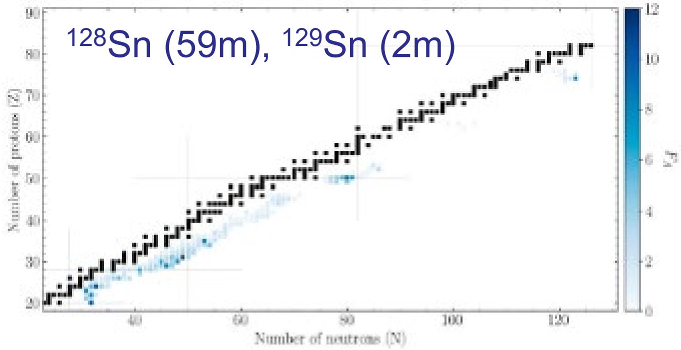

Vescovi+2022

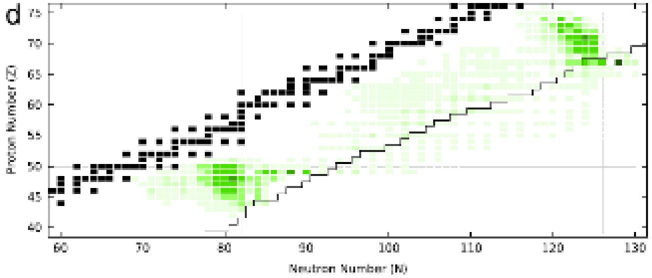

Mumpower+2016

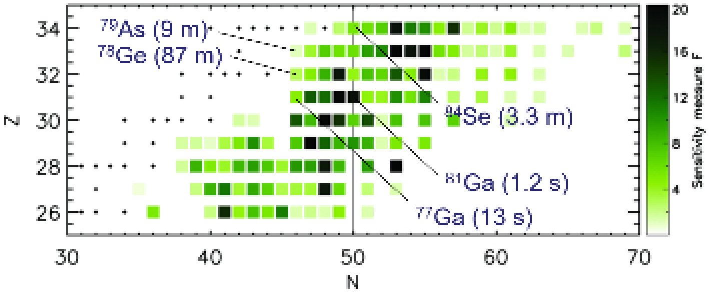

Surman+2014

The r-process: How much gold is produced in one event?

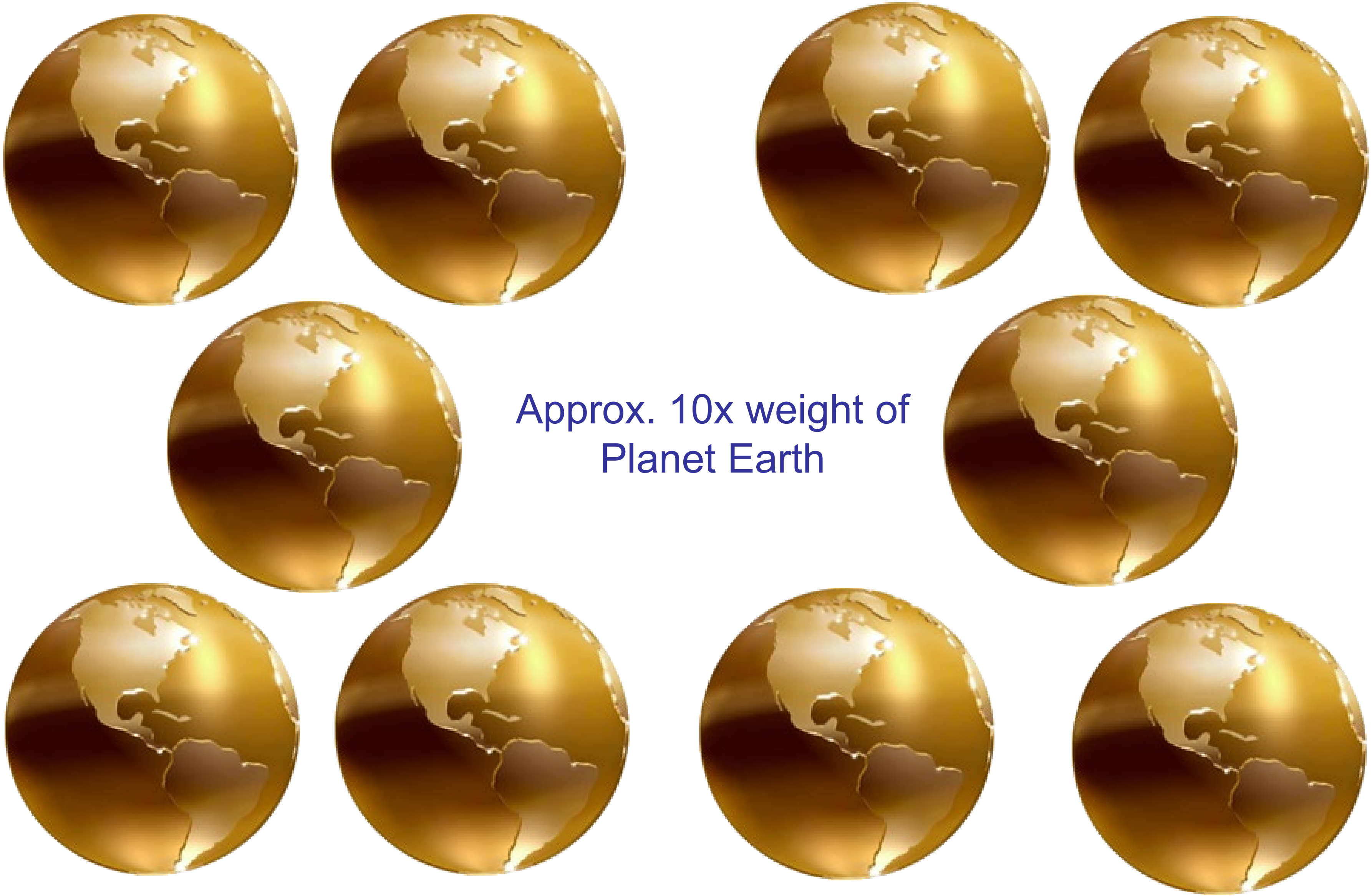

Approx. 10x weight of
Planet Earth

The r-process: How much gold is produced in one event?

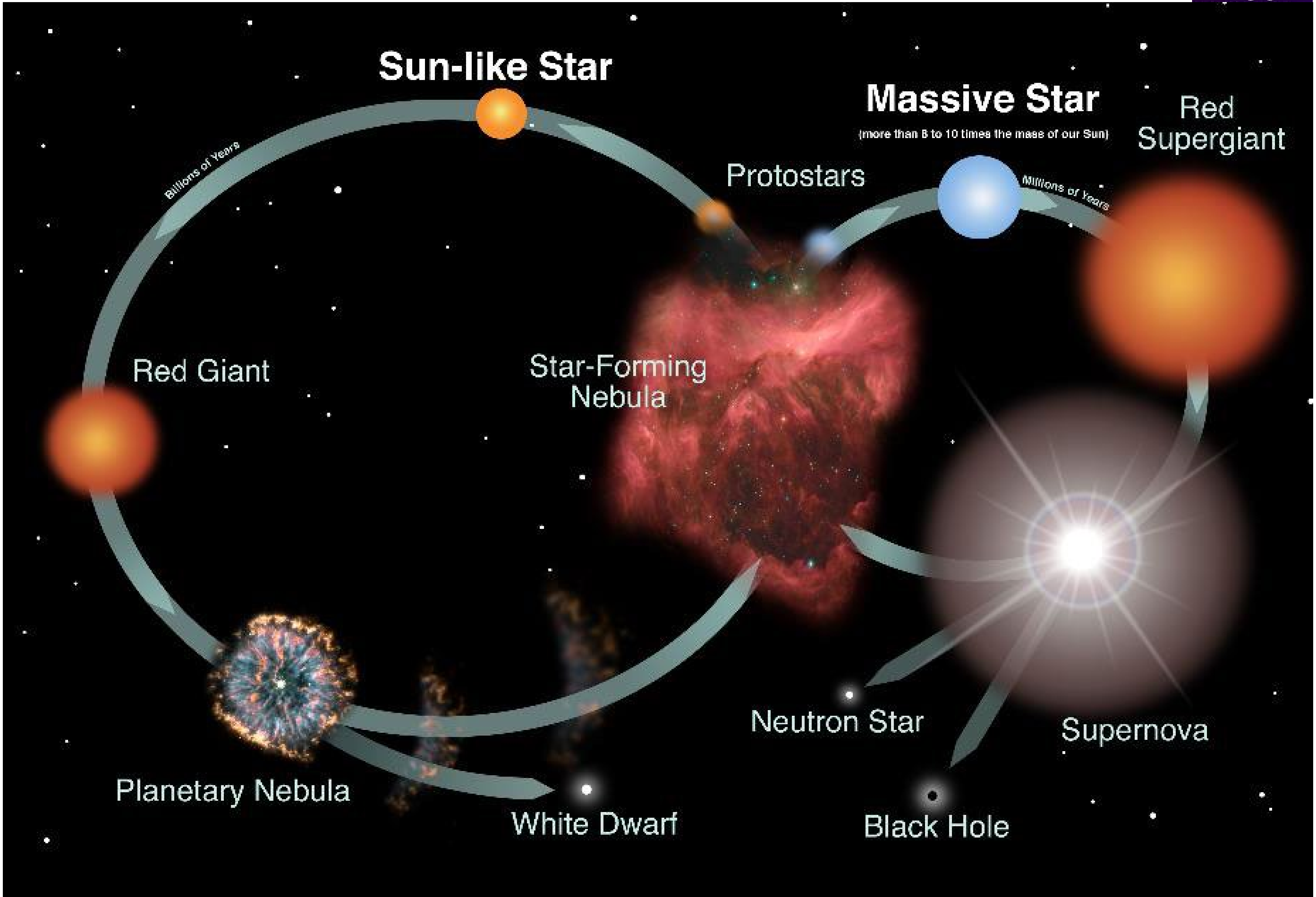

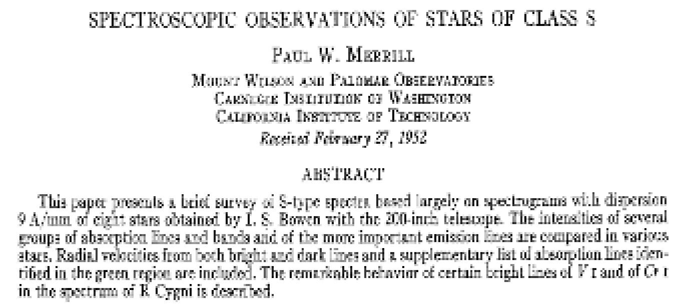

SPECTROSCOPIC OBSERVATIONS OF STARS OF CLASS S

Paul W. Merrill

Mount Wilson and Palomar Observatories
Carnegie Institution of Washington
California Institute of Technology

Received February 27, 1952

ABSTRACT

This paper presents a brief survey of S-type spectra based largely on spectrograms with dispersion 9 A/mm of eight stars obtained by I. S. Bowen with the 200-inch telescope. The intensities of several groups of absorption lines and bands and of the more important emission lines are compared in various stars. Radial velocities from both bright and dark lines and a supplementary list of absorption lines identified in the green region are included. The remarkable behavior of certain bright lines of *V* I and of *Cr* I in the spectrum of R Cygni is described.

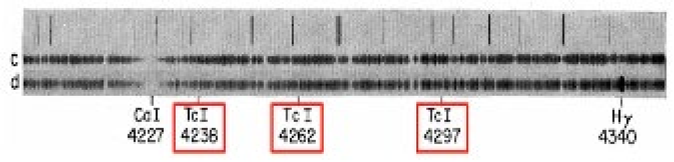

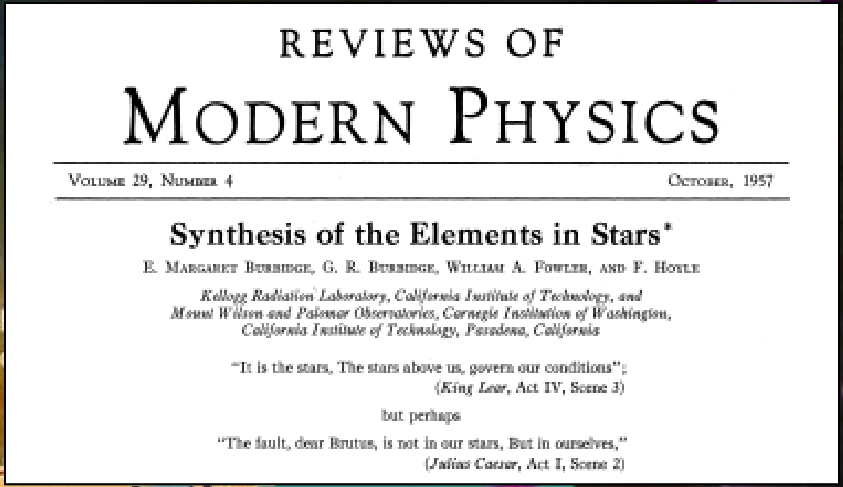

REVIEWS OF
MODERN PHYSICS

Volume 29, Number 4 October, 1957

Synthesis of the Elements in Stars*

E. Margaret Burbidge, G. R. Burbidge, William A. Fowler, and F. Hoyle

Kellogg Radiation Laboratory, California Institute of Technology, and Mount Wilson and Palomar Observatories, Carnegie Institution of Washington, California Institute of Technology, Pasadena, California

"It is the stars, The stars above us, govern our conditions";
(*King Lear*, Act IV, Scene 3)

but perhaps

"The fault, dear Brutus, is not in our stars, But in ourselves,"
(*Julius Caesar*, Act I, Scene 2)

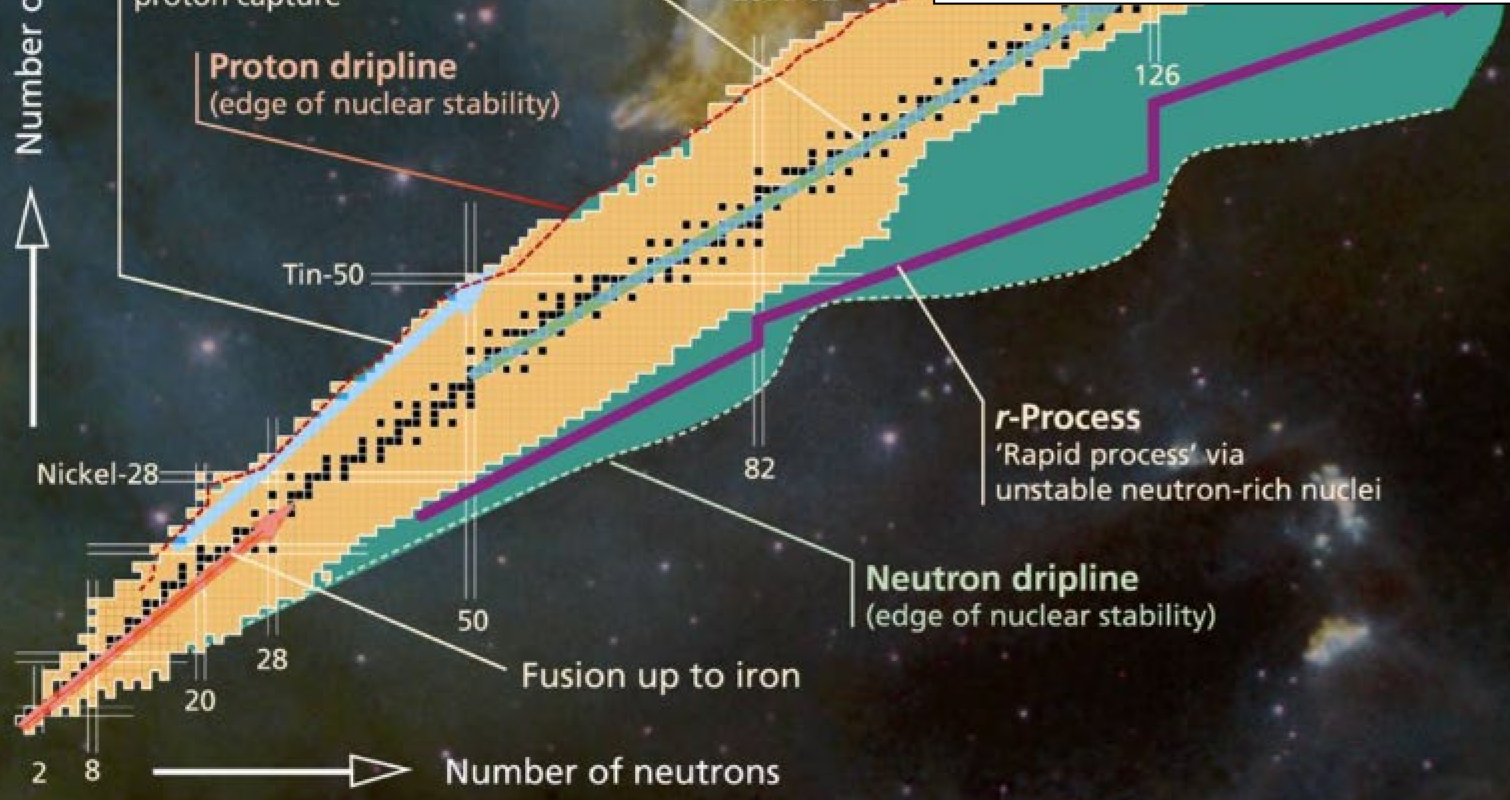

The slow neutron-capture process (s-process) mechanism: Fe to Pb-Bi

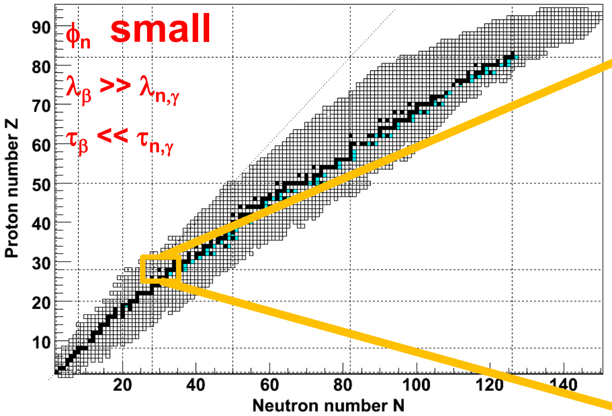

s process in Massive Stars (Red Giants)

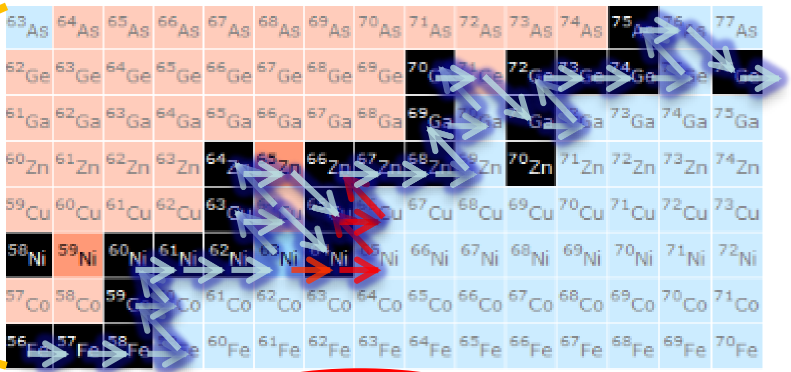

^{63}As	^{64}As	^{65}As	^{66}As	^{67}As	^{68}As	^{69}As	^{70}As	^{71}As	^{72}As	^{73}As	^{74}As	^{75}As	^{76}As	^{77}As
^{62}Ge	^{63}Ge	^{64}Ge	^{65}Ge	^{66}Ge	^{67}Ge	^{68}Ge	^{69}Ge	^{70}Ge	^{71}Ge	^{72}Ge	^{73}Ge	^{74}Ge	^{75}Ge	^{76}Ge
^{61}Ga	^{62}Ga	^{63}Ga	^{64}Ga	^{65}Ga	^{66}Ga	^{67}Ga	^{68}Ga	^{69}Ga	^{70}Ga	^{71}Ga	^{72}Ga	^{73}Ga	^{74}Ga	^{75}Ga
^{60}Zn	^{61}Zn	^{62}Zn	^{63}Zn	^{64}Zn	^{65}Zn	^{66}Zn	^{67}Zn	^{68}Zn	^{69}Zn	^{70}Zn	^{71}Zn	^{72}Zn	^{73}Zn	^{74}Zn
^{59}Cu	^{60}Cu	^{61}Cu	^{62}Cu	^{63}Cu	^{64}Cu	^{65}Cu	^{66}Cu	^{67}Cu	^{68}Cu	^{69}Cu	^{70}Cu	^{71}Cu	^{72}Cu	^{73}Cu
^{58}Ni	^{59}Ni	^{60}Ni	^{61}Ni	^{62}Ni	^{63}Ni	^{64}Ni	^{65}Ni	^{66}Ni	^{67}Ni	^{68}Ni	^{69}Ni	^{70}Ni	^{71}Ni	^{72}Ni
^{57}Co	^{58}Co	^{59}Co	^{60}Co	^{61}Co	^{62}Co	^{63}Co	^{64}Co	^{65}Co	^{66}Co	^{67}Co	^{68}Co	^{69}Co	^{70}Co	^{71}Co
^{56}Fe	^{57}Fe	^{58}Fe	^{59}Fe	^{60}Fe	^{61}Fe	^{62}Fe	^{63}Fe	^{64}Fe	^{65}Fe	^{66}Fe	^{67}Fe	^{68}Fe	^{69}Fe	^{70}Fe

⇨ $= {}^{A}Z(n,\gamma)^{A+1}Z$

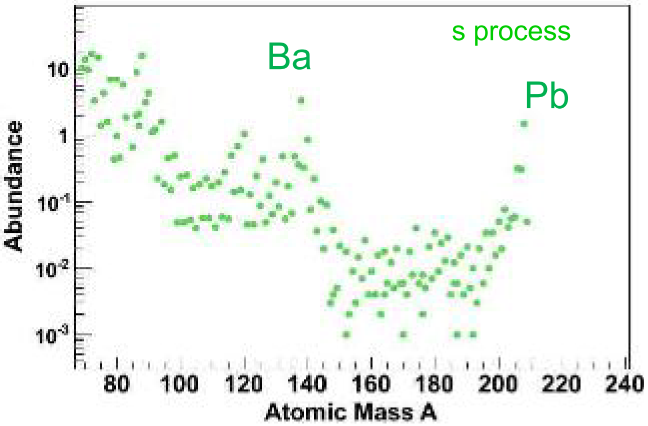

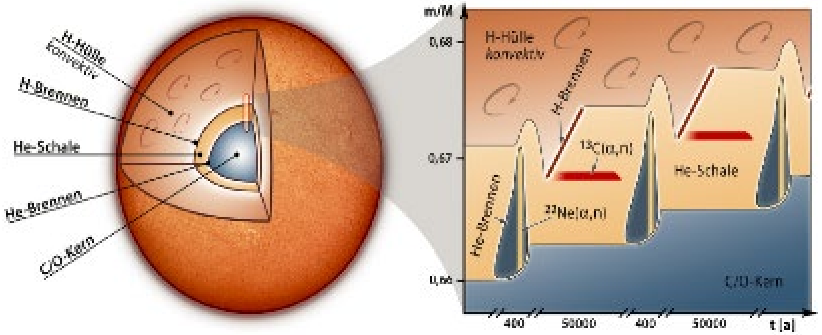

Massive Stars ($M>8M_\odot$)

core He-burning	shell C-burning
$3\text{-}3.5\cdot10^{8}$ K	$\sim1\cdot10^{9}$ K
kT=25 keV	kT=90 keV
10^{6} cm^{-3}	**$10^{11}\text{-}10^{12}$ cm^{-3}**

$^{22}Ne(^{4}He,n)^{25}Mg$

Low-Mass AGB Stars $1.5\ M_\odot < M < 3M_\odot$

shell H-burning	He-flash
$0.9\cdot10^{8}$ K	$3\text{-}3.5\cdot10^{8}$ K
kT=8 keV	kT=23 keV
$10^{7}\text{-}10^{8}$ cm^{-3}	$10^{10}\text{-}10^{11}$ cm^{-3}
$^{13}C(^{4}He,n)^{16}O$	**$^{22}Ne(^{4}He,n)^{25}Mg$**

Many open questions in s-process nucleosynthesis

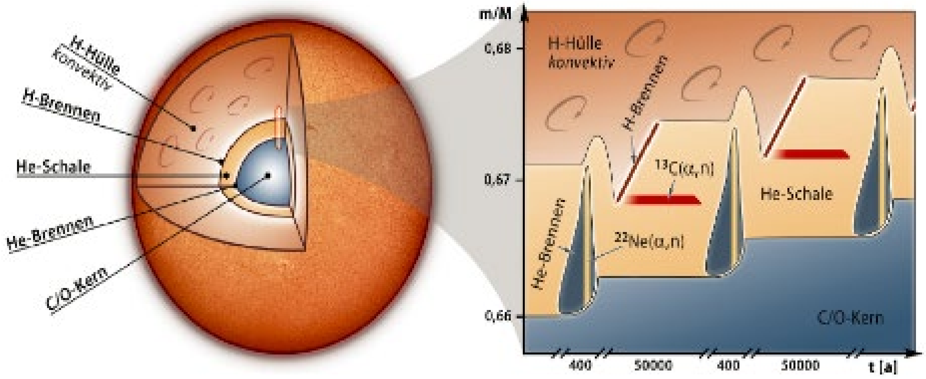

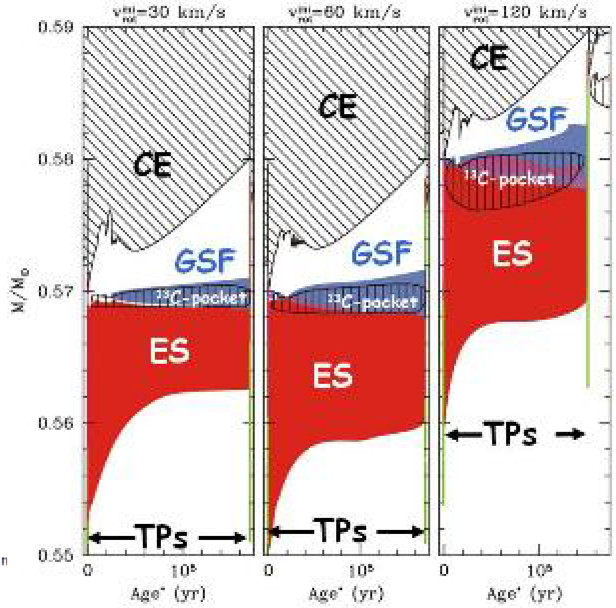

S. Cristallo+2014

- C13-pocket
- Rotation
- Metallicity
- Stellar mass
- Thermal gradients

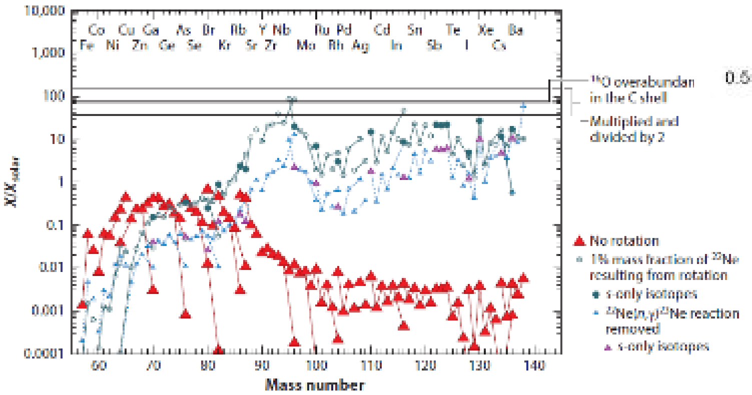

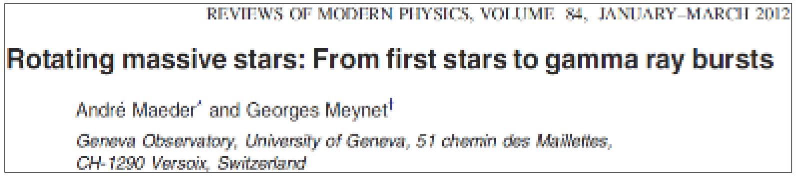

REVIEWS OF MODERN PHYSICS, VOLUME 84, JANUARY–MARCH 2012

Rotating massive stars: From first stars to gamma ray bursts

André Maeder* and Georges Meynet†

Geneva Observatory, University of Geneva, 51 chemin des Maillettes, CH-1290 Versoix, Switzerland

LETTER

Imprints of fast-rotating massive stars in the Galactic Bulge

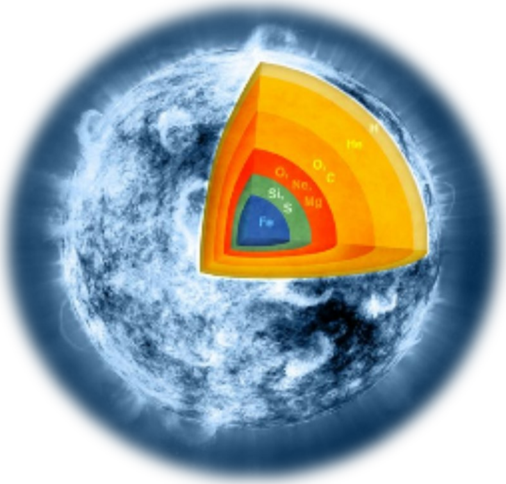

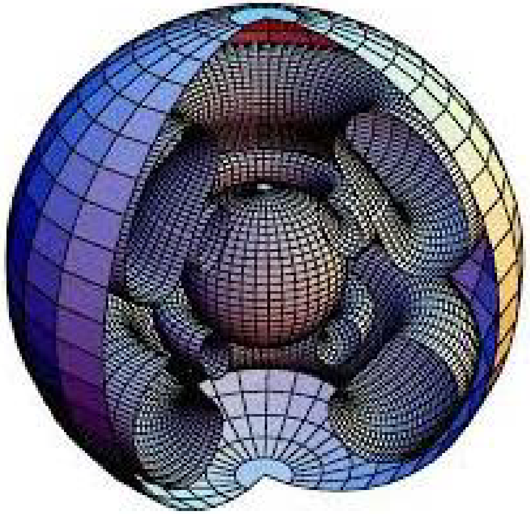

How does it work?

Theory: Stellar model

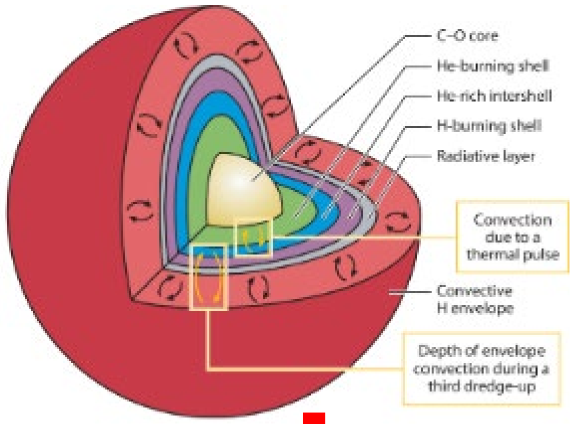

Lugaro M, et al. 2023
Annu. Rev. Nucl. Part. Sci. 73:315–40

+

Experiment: neutron-capture cross sections

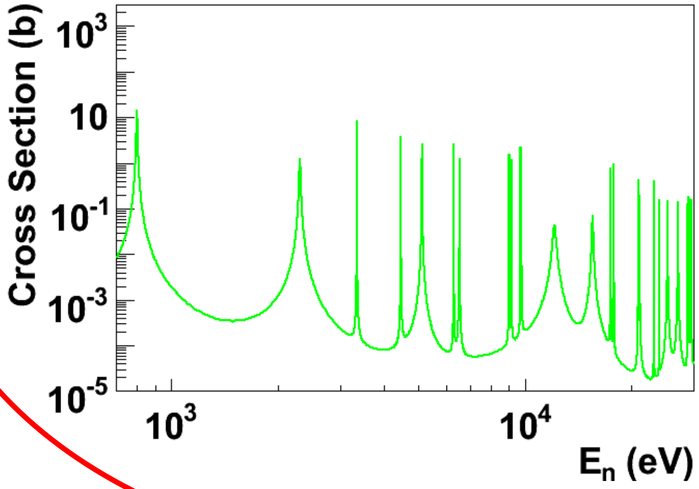

=

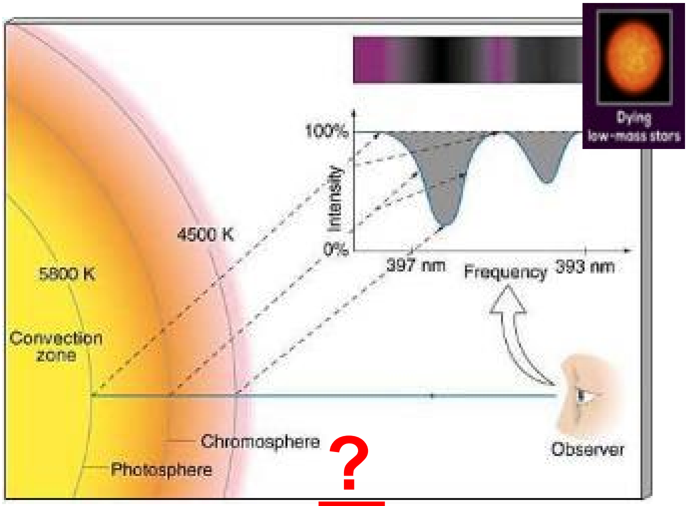

?
=

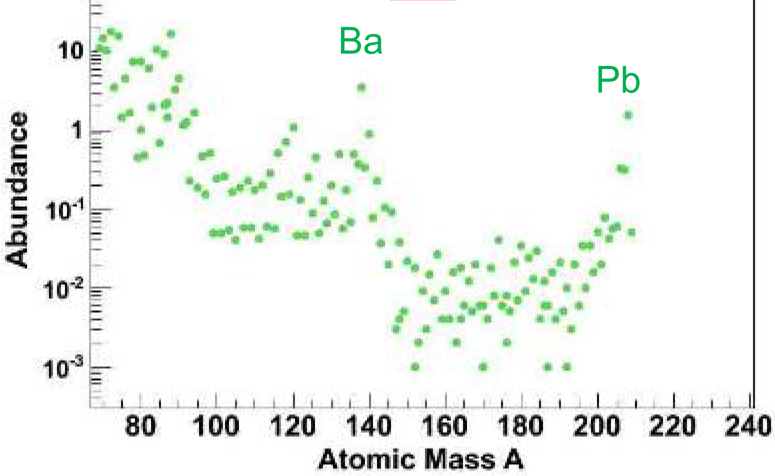

?
=

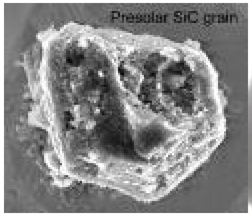

Outline

- Heavy elements nucleosynthesis: How stars make gold (r-process) and lead (s-process)?
- Neutron-capture experiments at CERN n_TOF: Red-Giant stars in the lab
- Enhancing detection sensitivity in neutron capture TOF experiments
- Beyond the limits: r-process neutron-reactions in the lab?
- From stars to tumors: ion-range & dose monitoring in hadron therapy
- Summary & Outlook

The CERN accelerator complex
Complexe des accélérateurs du CERN

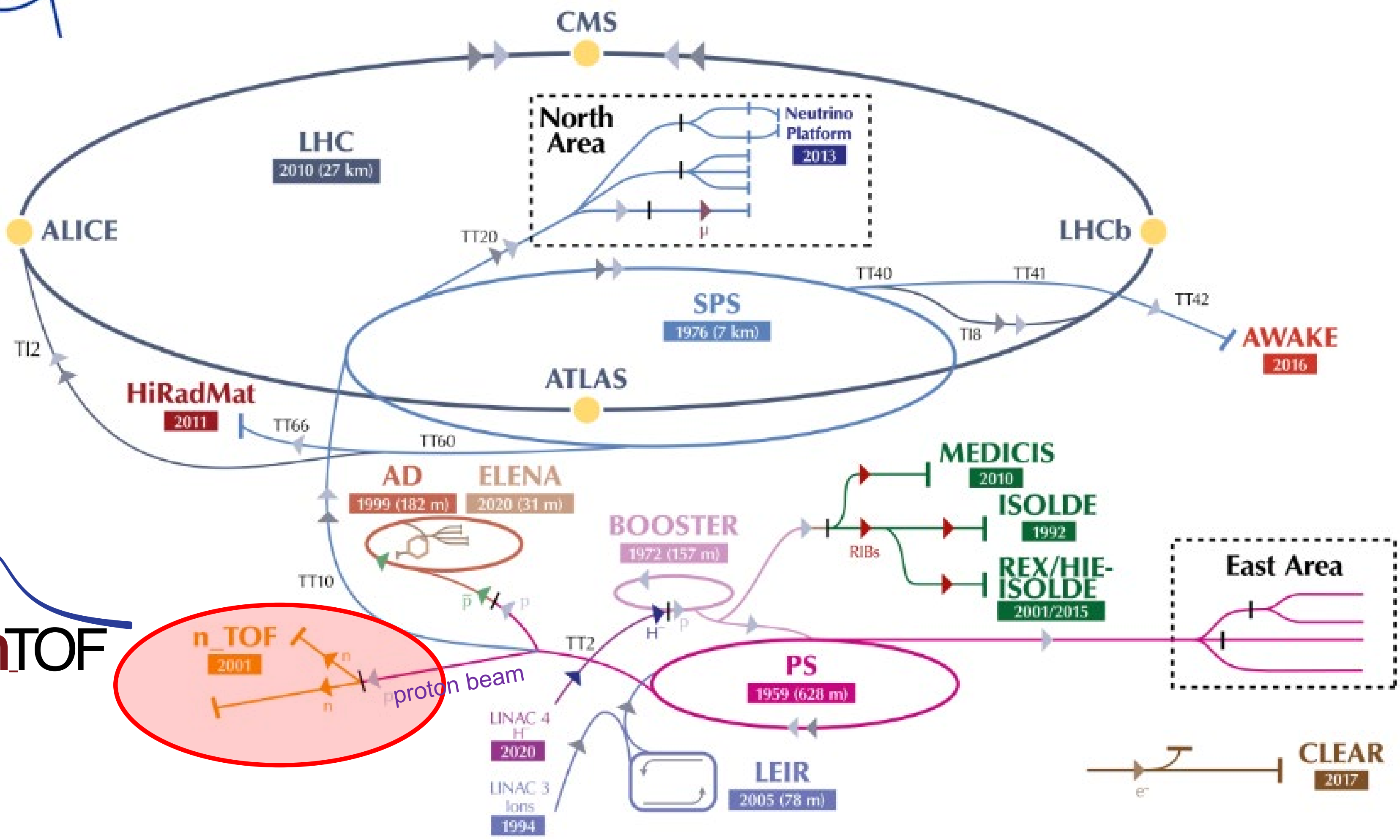

C. Rubbia et al., ***A high resolution spallation driven facility at the CERN-PS to measure neutron cross sections in the interval from 1 eV to 250 MeV***, CERN/LHC/98-02(EET) 1998.

CERN n_TOF Collaboration: 150 scientists, 41 institutions worldwide

n_TOF + ISOLDE = **75% of PS proton Budget (!)**

The CERN n_TOF facility: recreating stellar neutron reactions in the lab

proton beam momentum	20 GeV/c
intensity (dedicated mode)	8.5×10^{12} protons/pulse
repetition frequency	1 pulse/1.2s
pulse width	6 ns (rms)
n/p	300
lead target dimensions	80x80x60 cm^3
cooling & moderation material	N_2 & H_2O (borated)
moderator thickness in the exit face	5 cm
neutron beam dimension in EAR-1 (capture mode)	2 cm (FWHM)

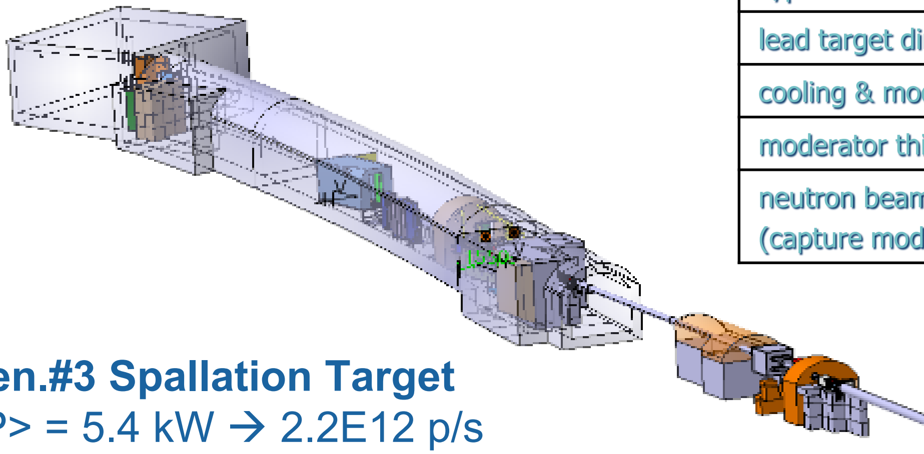

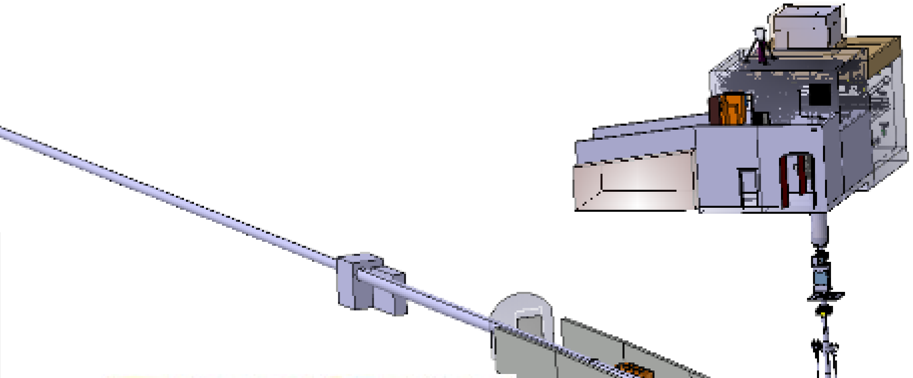

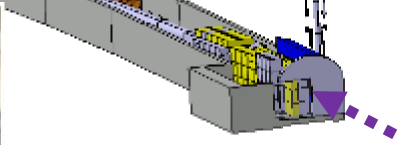

proton beam from the PS

Gen.#3 Spallation Target

<P> = 5.4 kW → 2.2E12 p/s

P_{peak} = 1.6 TW

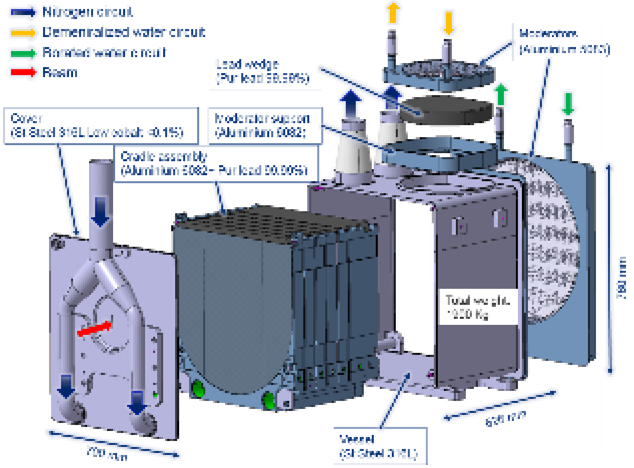

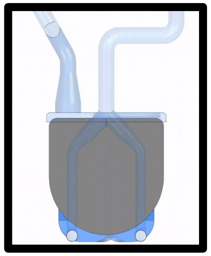

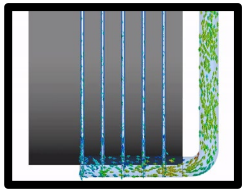

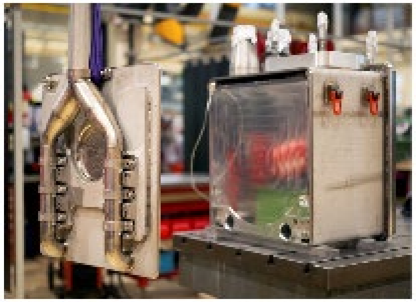

R. Esposito, M. Calviani et al. Phys. Rev. Acc. & Beams 24 (2021)

The CERN n_TOF facility: recreating stellar neutron reactions in the lab

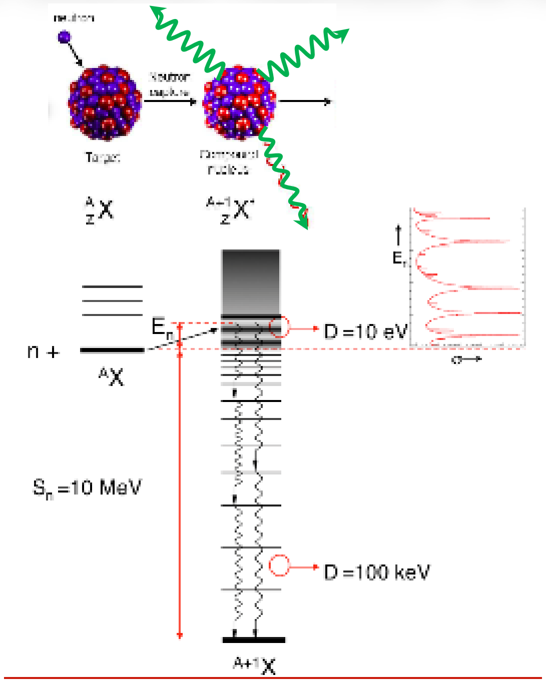

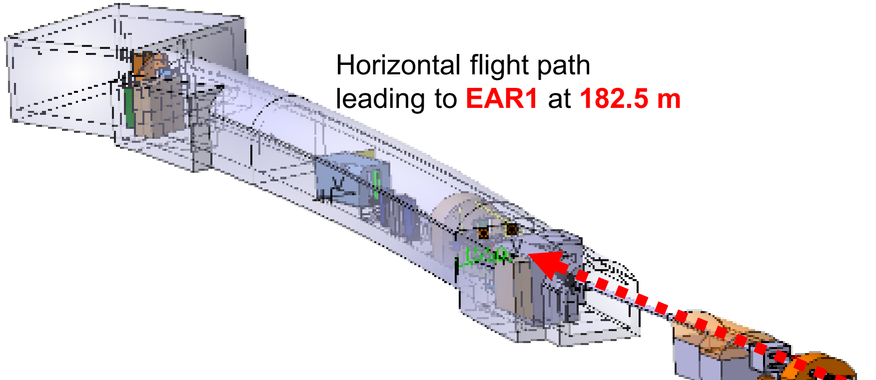

Horizontal flight path leading to **EAR1** at **182.5 m**

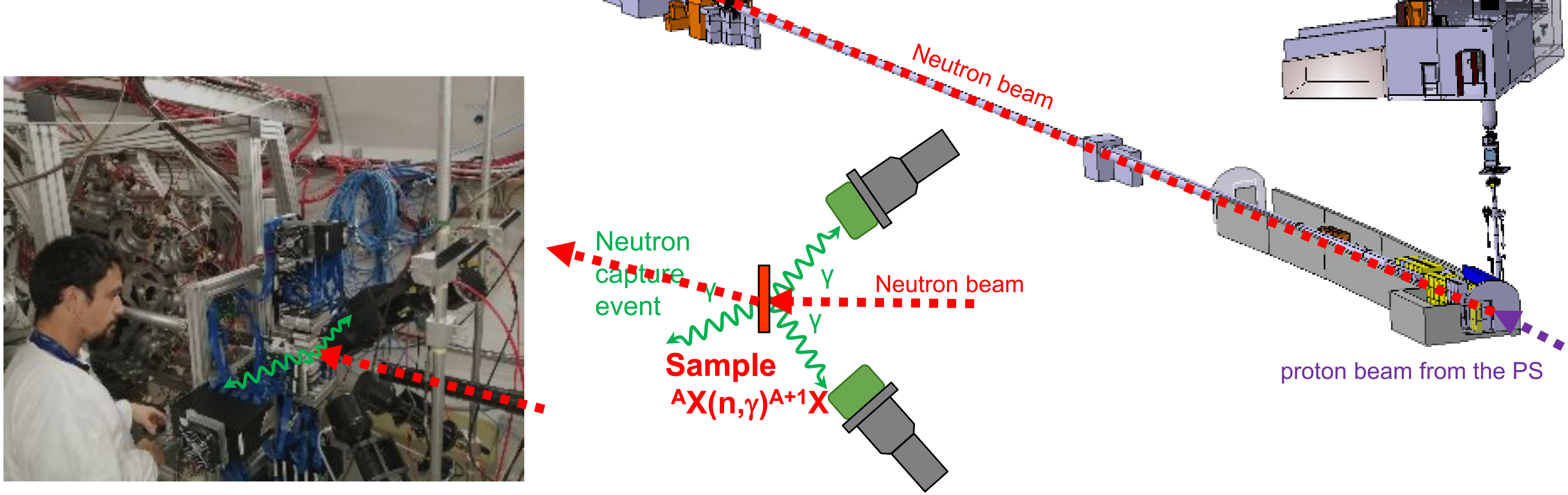

Sample

$^{A}X(n,\gamma)^{A+1}X$

The CERN n_TOF facility: recreating stellar neutron reactions in the lab

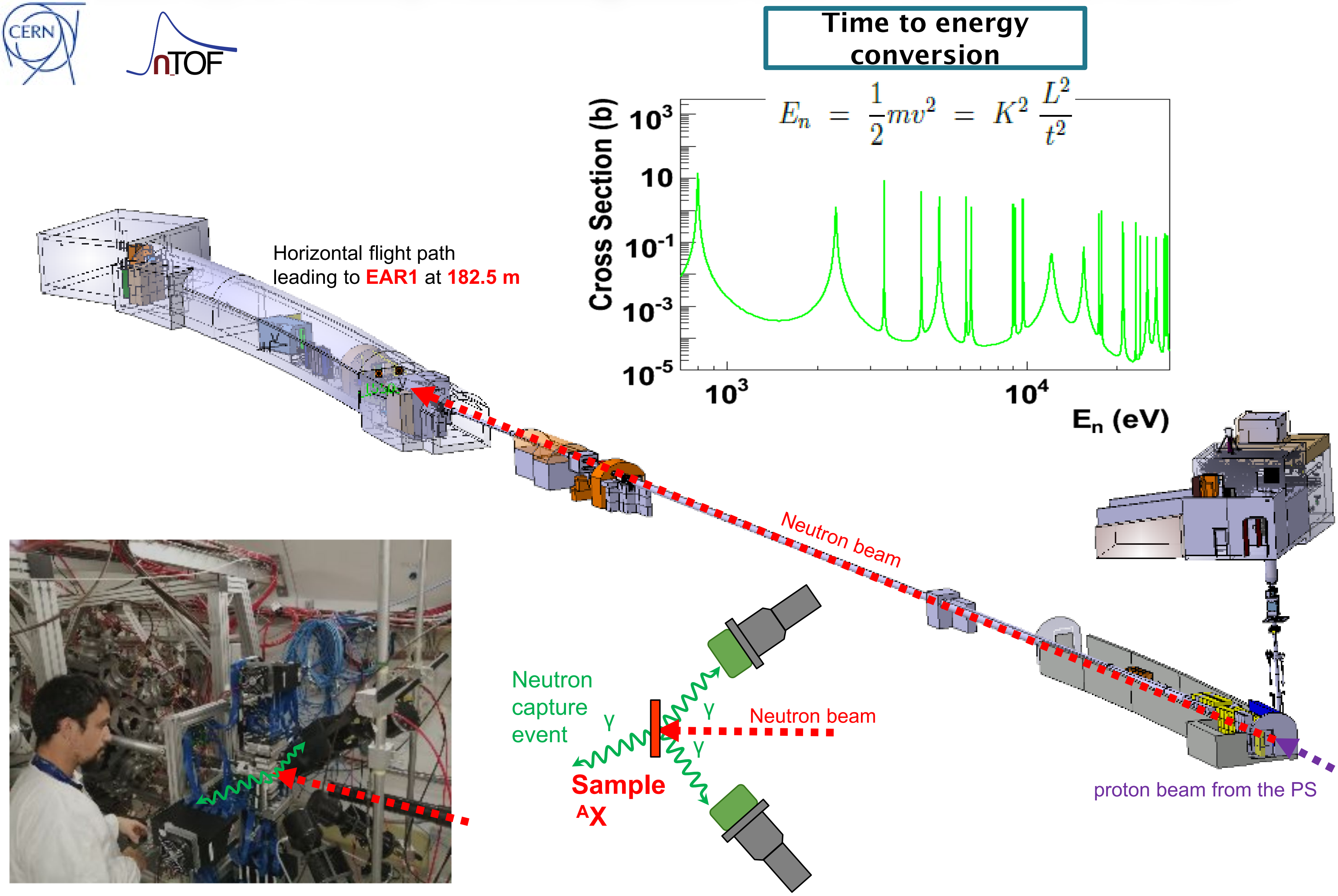

Time to energy conversion

$$E_n = \frac{1}{2}mv^2 = K^2\frac{L^2}{t^2}$$

Horizontal flight path leading to **EAR1** at **182.5 m**

Neutron beam

proton beam from the PS

Neutron capture event

γ

γ

γ

Neutron beam

Sample

^{A}X

The CERN n_TOF facility: recreating stellar neutron reactions in the lab

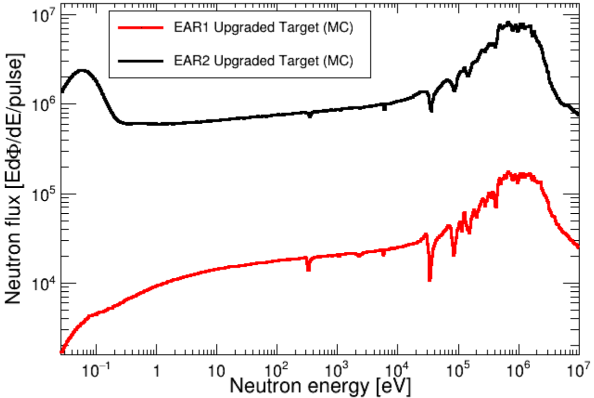

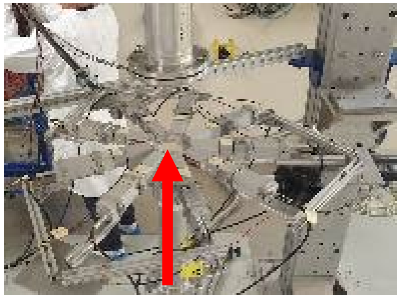

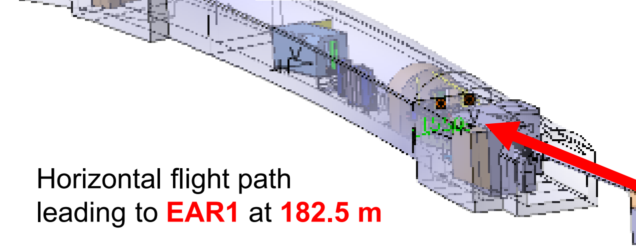

Horizontal flight path
leading to **EAR1** at **182.5 m**

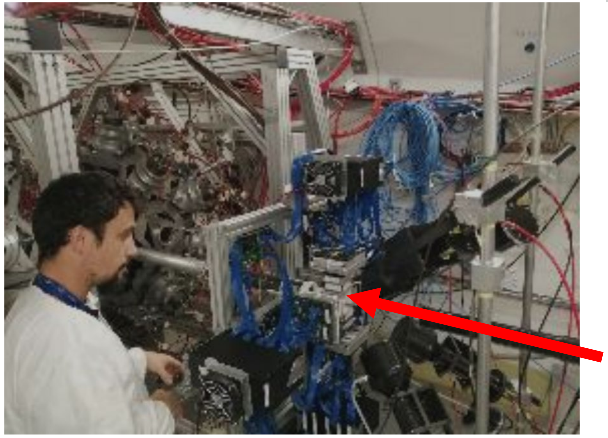

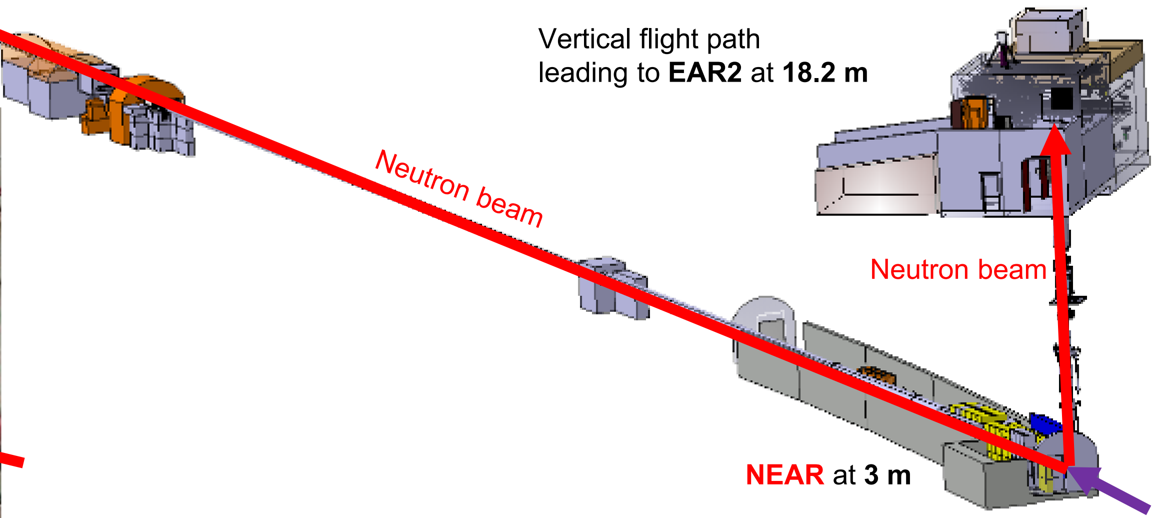

Vertical flight path
leading to **EAR2** at **18.2 m**

NEAR at **3 m**

proton beam from the PS

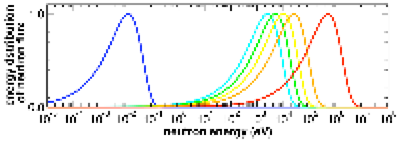

What we have done at n_TOF?

Reaction	Count
Radiative capture reactions (n,γ)	(89)
Fission reactions (n,f)	(37)
Light particle emission reactions (n,lcp)	(11)

The n_TOF Collaboration list of publications:
https://twiki.cern.ch/NTOFPublic/ListOfPublications

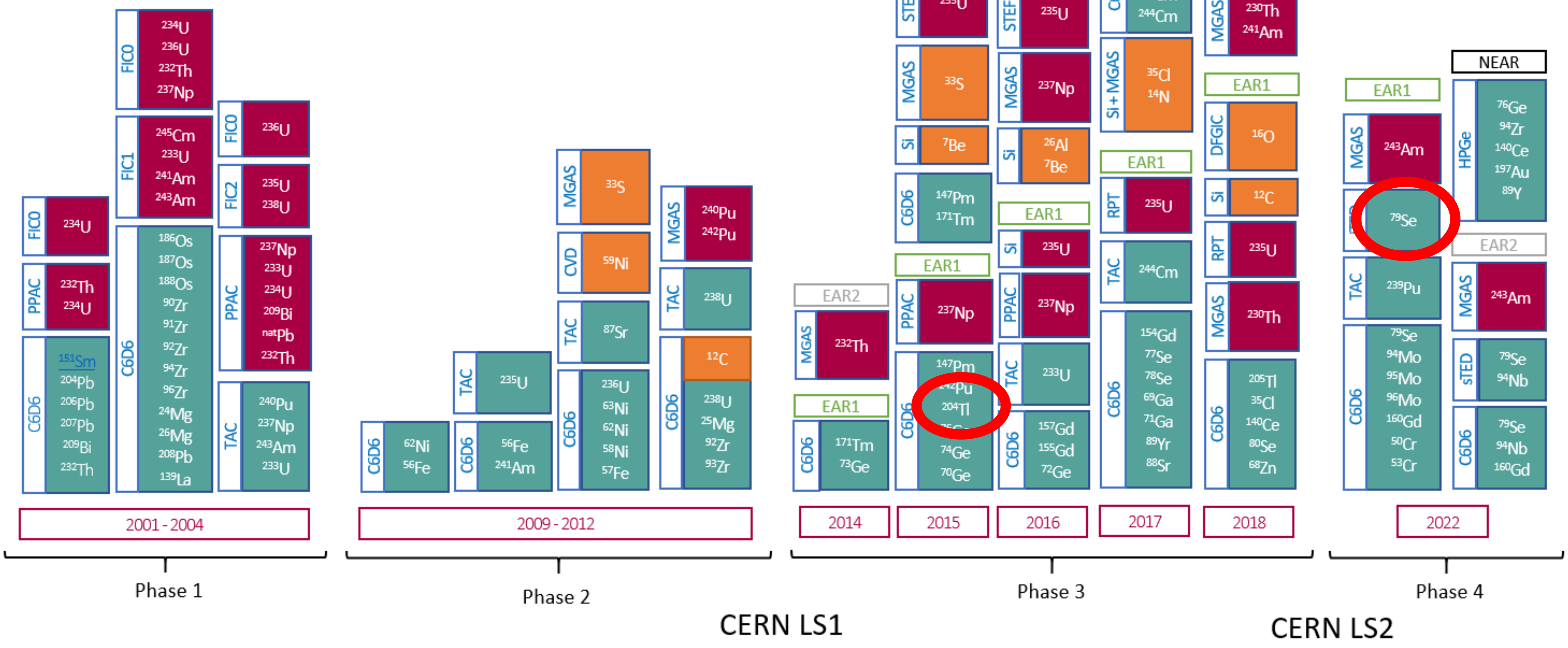

About 50% related to astrophysics

^{204}Pb: Calibrating AGB models & "defining" the age of our Solar System

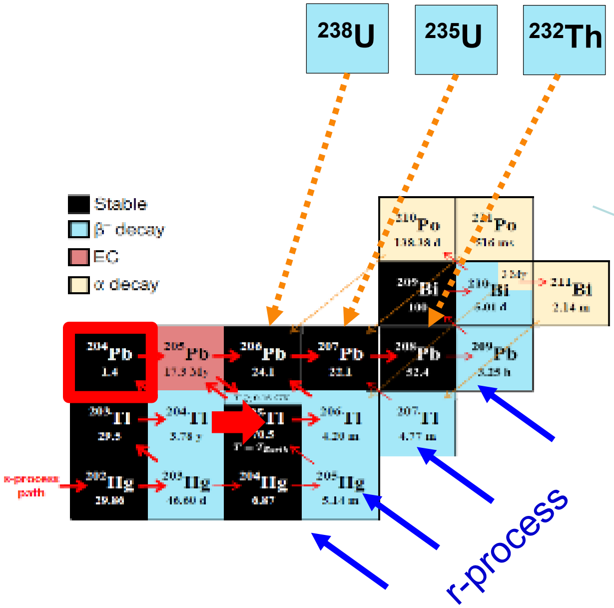

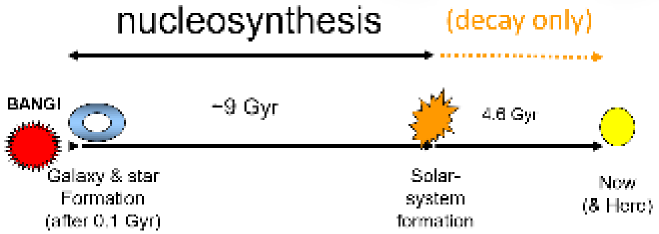

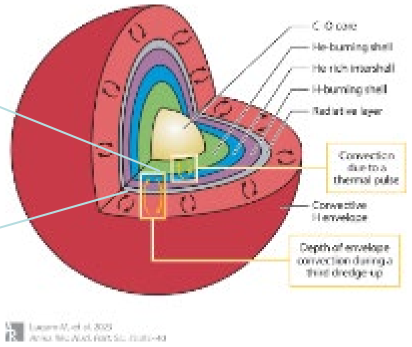

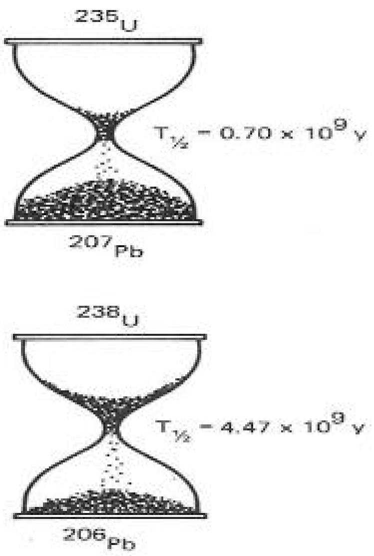

$$\left(\frac{^{206}\mathrm{Pb}}{^{204}\mathrm{Pb}}\right)_{\mathrm{today}} = \left(\frac{^{206}\mathrm{Pb}}{^{204}\mathrm{Pb}}\right)_{t_0} + \left(\frac{^{238}\mathrm{U},\,^{232}\mathrm{Th}}{^{204}\mathrm{Pb}}\right)_{\mathrm{today}} \left(e^{\lambda t} - 1\right)$$

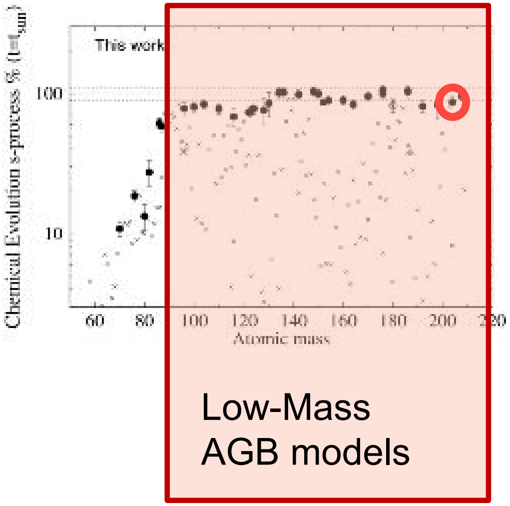

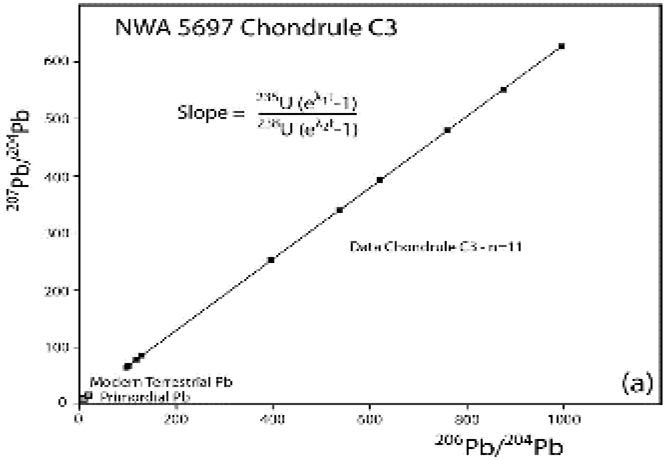

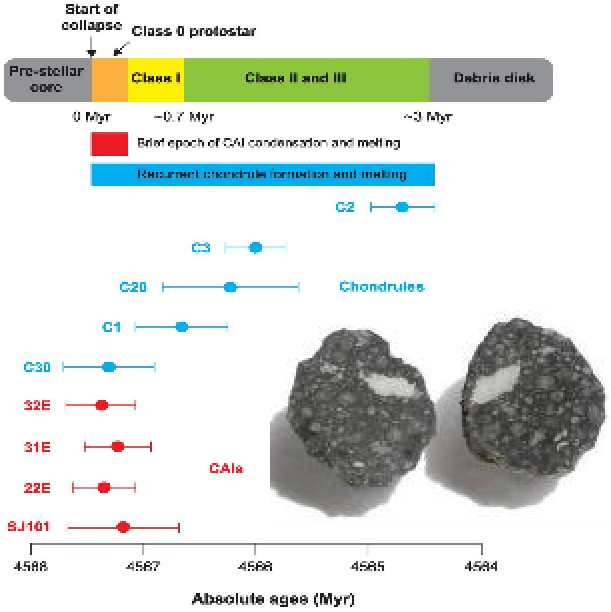

J.N. Connelly et al. Science **338** 2012
DOI: 10.1126/science.1226919

^{204}Pb abundance determined by ^{204}Tl(n,γ)

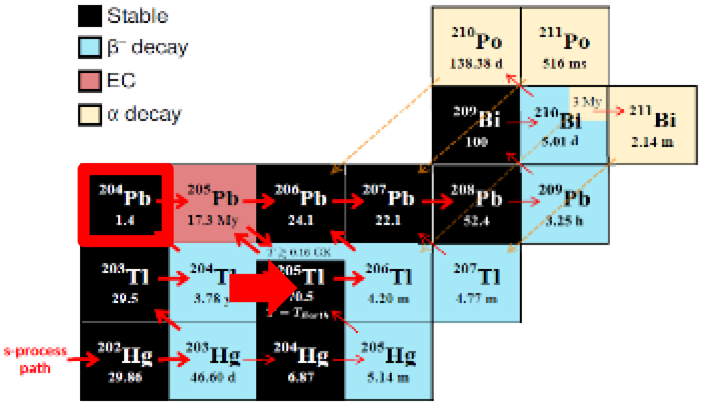

^{203}Tl (225 mg)

^{203}Tl (216 mg)
+
^{204}Tl (9 mg)

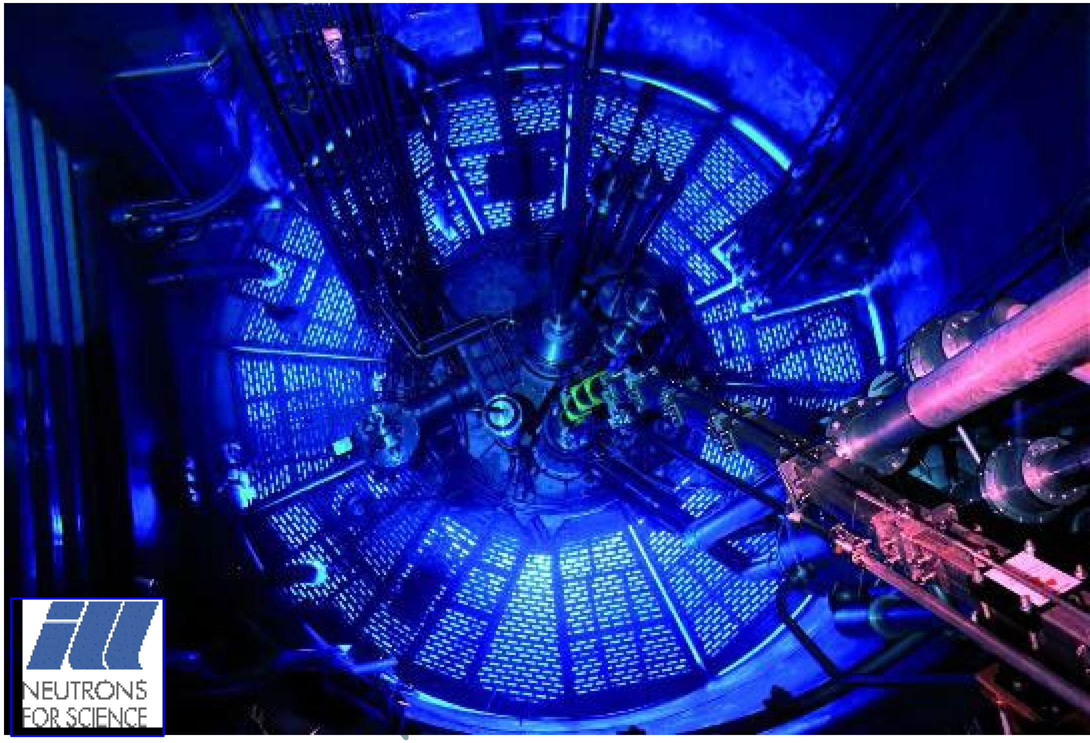

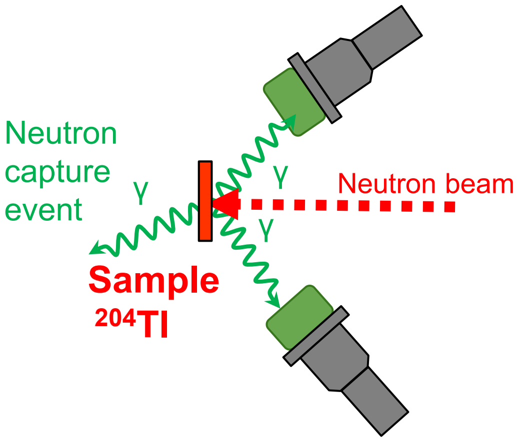

Mimicking stellar nucleosynthesis with a reactor to produce ^{204}Tl

^{204}Tl (3.78y) neutron-capture at CERN n_TOF

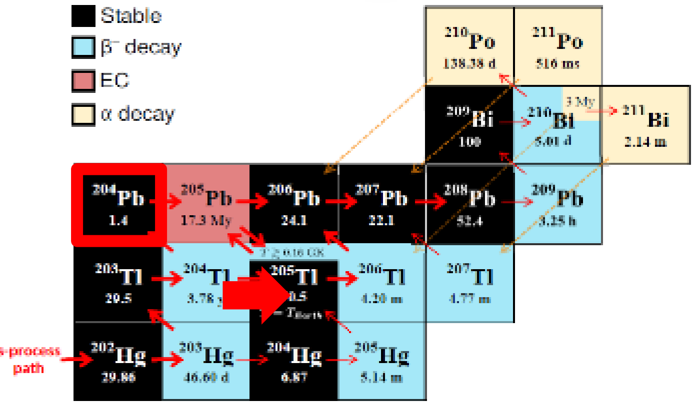

^{203}Tl (216 mg)
+
^{204}Tl (9 mg)

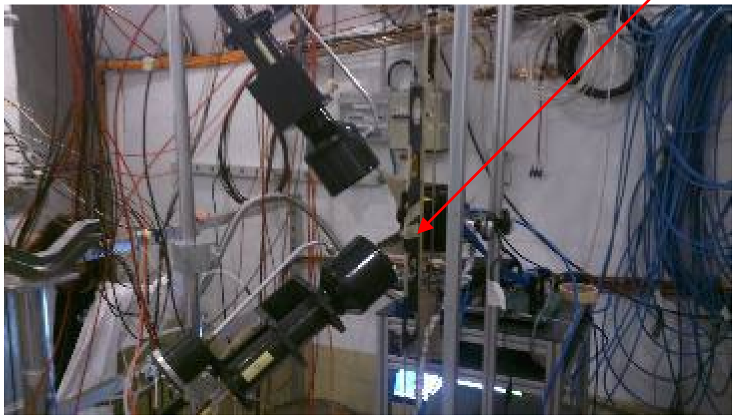

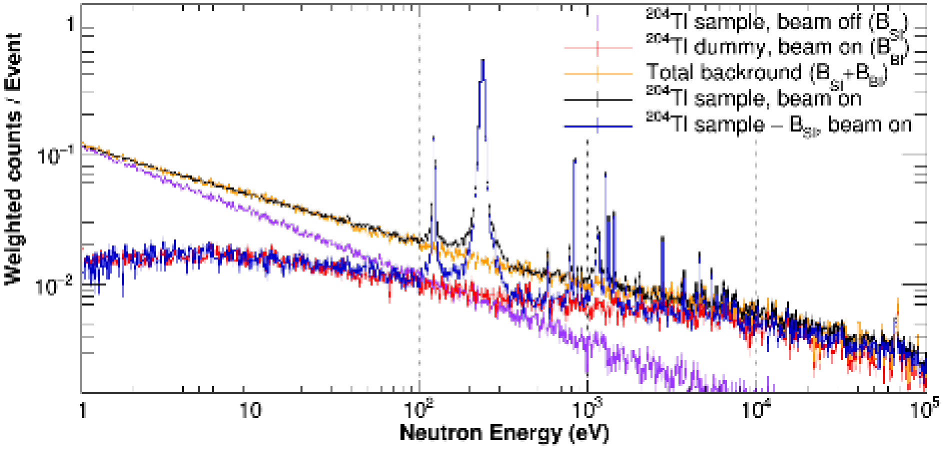

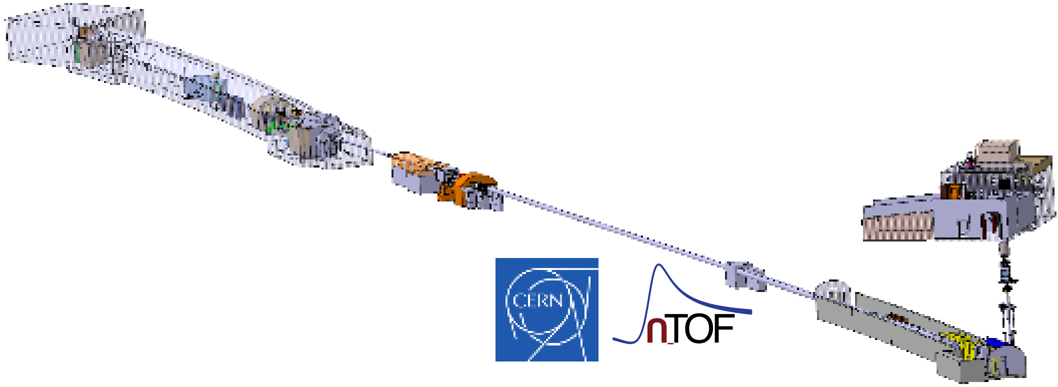

A Casanovas-Hoste *et al.* (n_TOF)
Physical Review Letters **133**, 052702 (2024)
DOI: 10.1103/PhysRevLett.133.052702

^{204}Pb abundance determined by ^{204}Tl(n,γ)

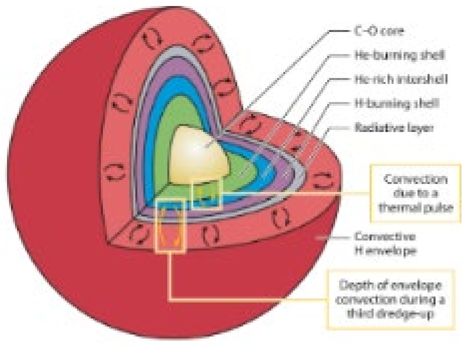

Lugaro M, et al. 2023
Annu. Rev. Nucl. Part. Sci. 73:315–40

+

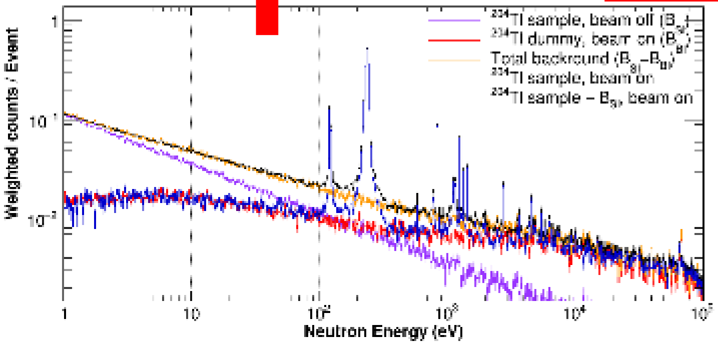

=

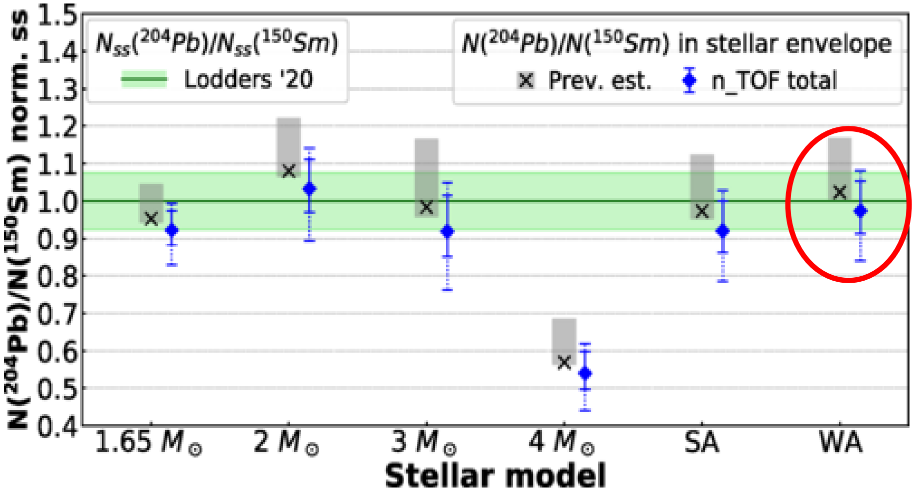

NUGRID

MESA

The uncertainty arising from the ^{204}Tl(n,γ) cross section on the s-process abundance of ^{204}Pb has been reduced from ~30% down to **+8%/−6%**, and the s-process calculations are in agreement with K. Lodders in 2021.

^{204}Pb abundance of pure s-process origin:
→No need for fractionation mechanisms in early Solar system
→No need for invoking gamma-process contributions

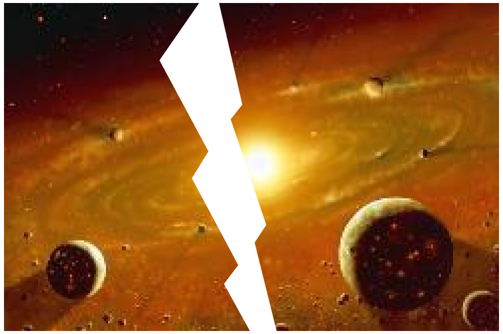

G. Gonzalez 2014

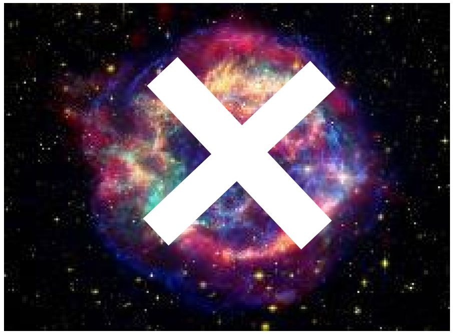

M.Pignatari+ 2016

A Casanovas-Hoste *et al.* (n_TOF)
Physical Review Letters **133**, 052702 (2024)
DOI: 10.1103/PhysRevLett.133.052702

The ^{79}Se(n,γ) stellar thermometer

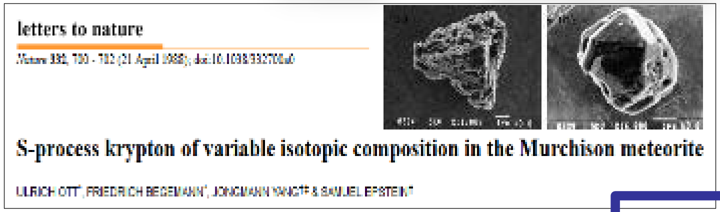
letters to nature

Nature 332, 700 - 702 (21 April 1988); doi:10.1038/332700a0

S-process krypton of variable isotopic composition in the Murchison meteorite

ULRICH OTT*, FRIEDRICH BEGEMANN*, JONGMANN YANG†‡ & SAMUEL EPSTEIN†

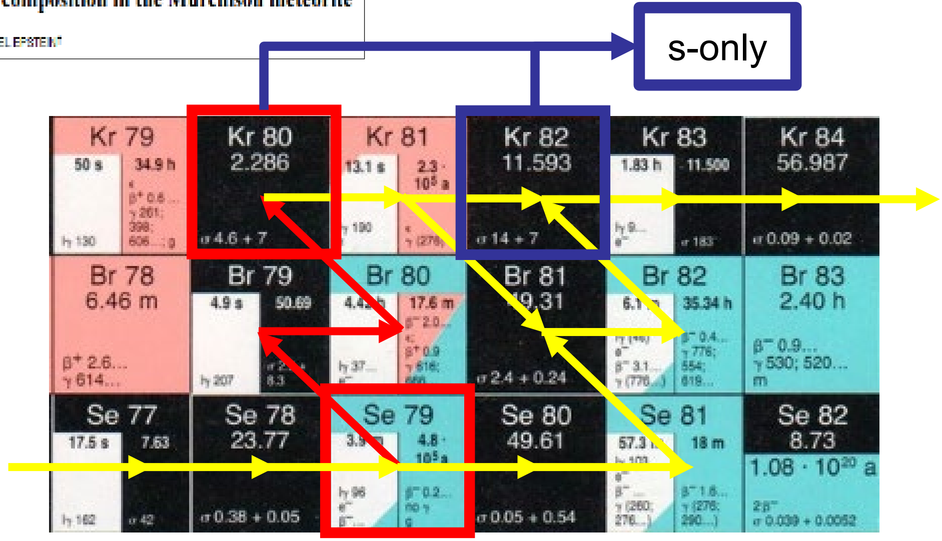

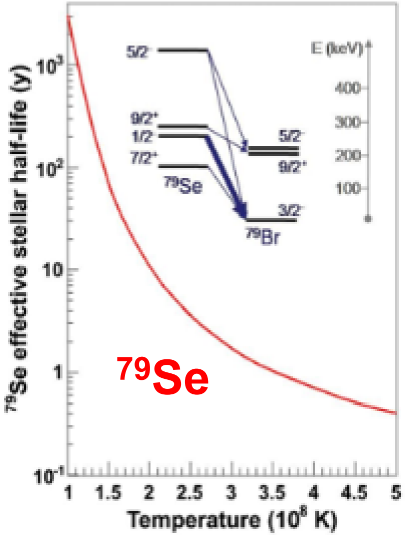

2.8 g of ^{208}Pb
1.0 g of ^{78}Se

3 mg of ^{79}**Se**
1.6 MBq of ^{60}Co
5 MBq of ^{75}Se

PAUL SCHERRER INSTITUT

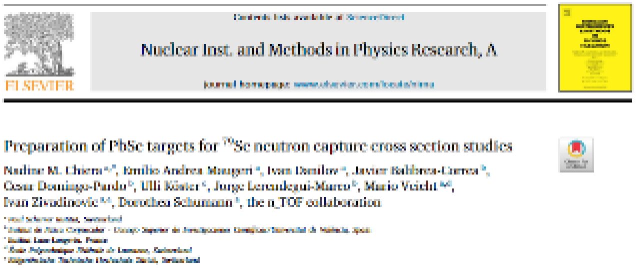
Contents lists available at ScienceDirect

Nuclear Inst. and Methods in Physics Research, A

journal homepage: www.elsevier.com/locate/nima

Preparation of PbSe targets for ^{79}Se neutron capture cross section studies

Nadine M. Chiera, Emilio Andrea Maugeri, Ivan Danilov, Javier Balibrea-Correa, Cesar Domingo-Pardo, Ulli Köster, Jorge Lerendegui-Marco, Mario Veicht, Ivan Zivadinovic, Dorothea Schumann, the n_TOF collaboration

New techniques for enhanced sensitivity in (n,γ) cross-section experiments

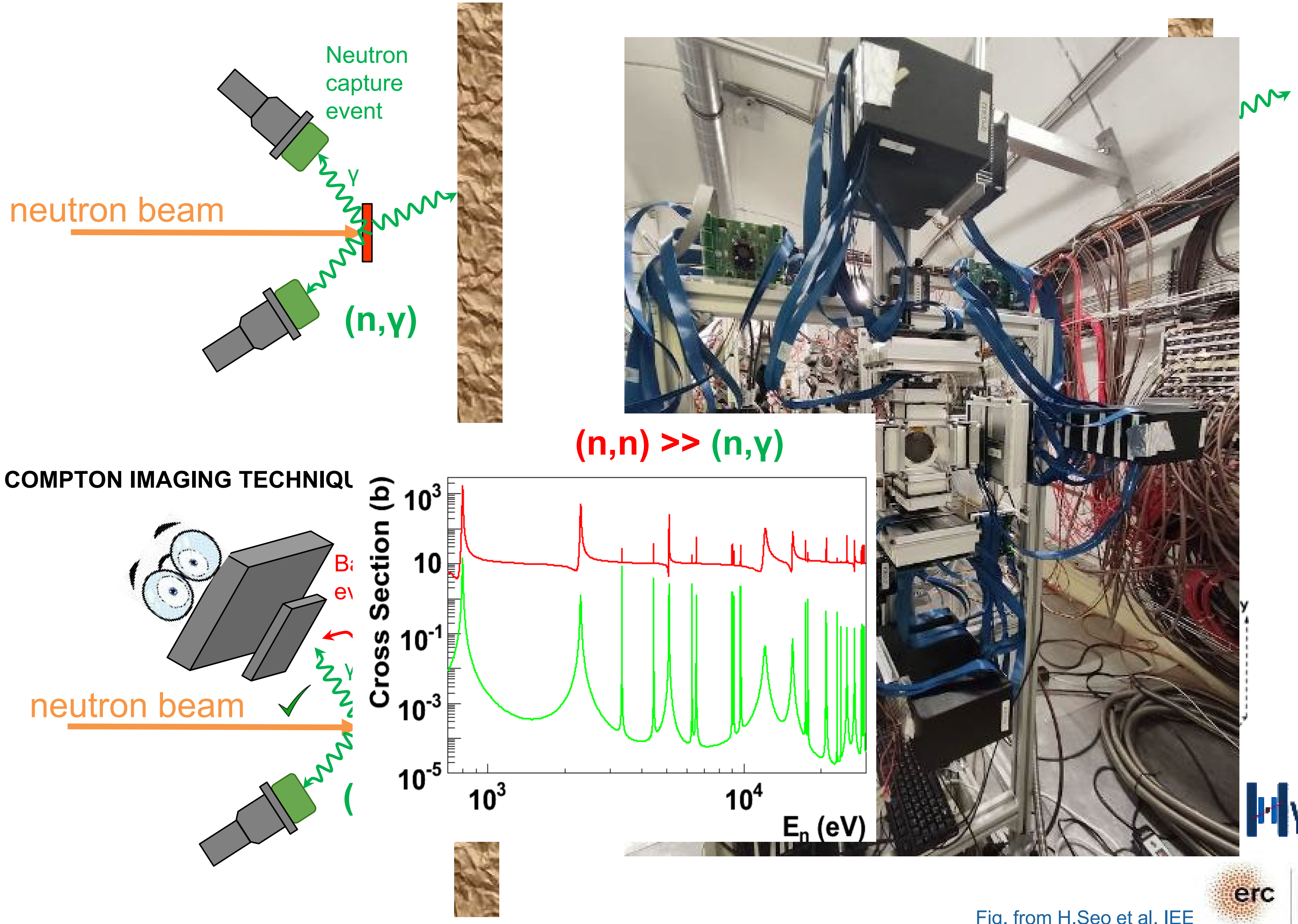

Fig. from H.Seo et al. IEE

European Research Council

Total-Energy Detector with g-ray imaging capability (i-TED):

- Need of **very high detection efficiency** → arrays of large monolithic crystals
- Need of **very low neutron sensitivity** →Customized design with $LaCl_3$(Ce) and ^{6}Li-HD-PE absorbers

3D- Spatial calibration techniques:

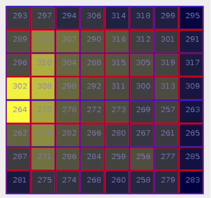

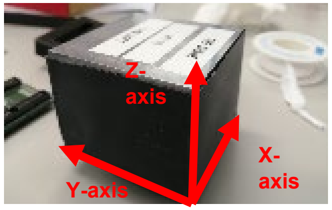

Final i-TED setup @ n_TOF:

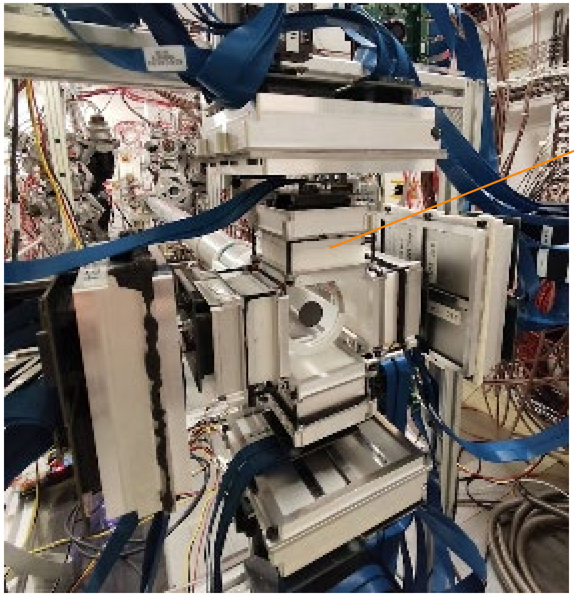

Neutron absorbers based on ^{6}Li-enriched HD-PE: No γ-ray emission after neutron absorption by ^{6}Li (!)

Convolutional Neural Network

3D keras models for the individual crystals

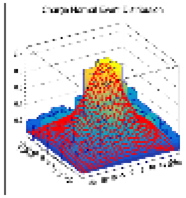

TensorFlow + Keras

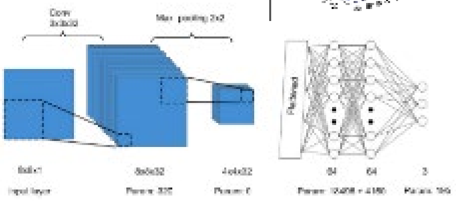

Crystal read-out and electronics:

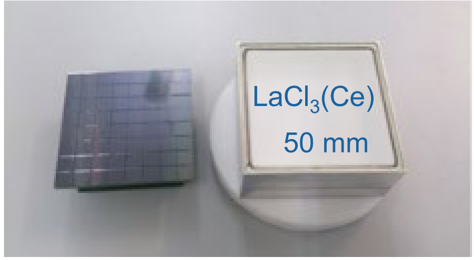

V.Babiano et al, NIM-A 931 (2019)

Optical Photons simulation

P. Olleros *et al.* 2018 JINST13 P03014

ML-aided 3D-position reconstruction

J. Balibrea et al. NIM-A (2020)

- **In total: 20 Position-Sensitive Detectors**
- **1150 cm^3 of LaCl3(Ce)**
- 1280 readout channels (4xKintex FPGA, 20xTOFPET2 **ASIC**s, PETsys)

Testing the gamma-ray vision capability of i-TED

Dynamic image: radioactive source in a remotely controlled XY-gantry imaged at multiple positions

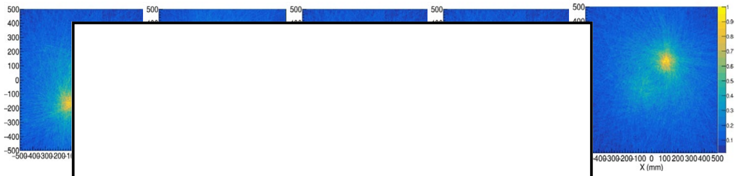

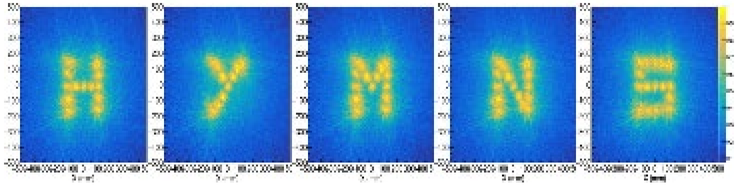

Testing the gamma-ray vision capability of i-TED

Dynamic image: radioactive source in a remotely controlled XY-gantry imaged at multiple positions

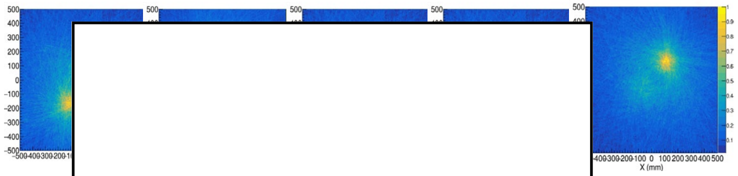

HYMNS

High sensitivitY Measurements of key stellar Nucleo-Synthesis reactions

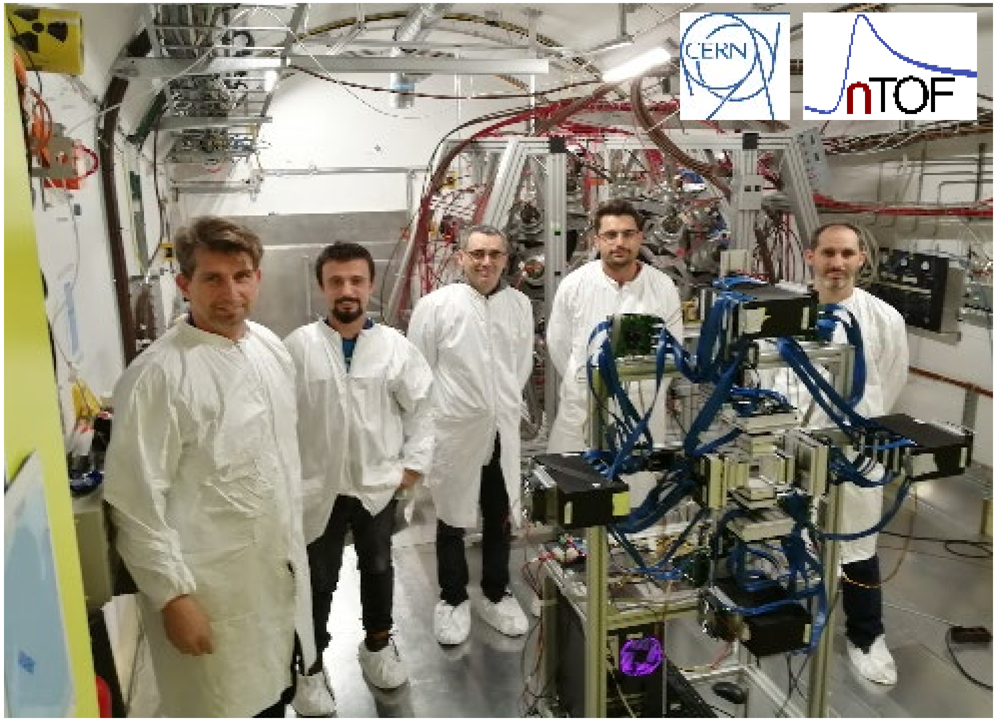

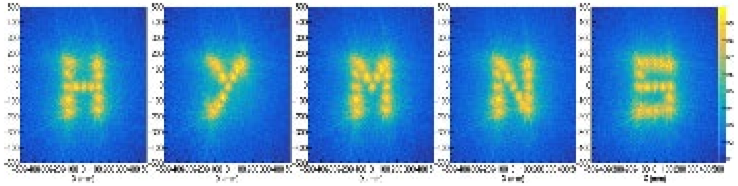

VNIVERSITAT DE VALÈNCIA

CSIC

Consejo Superior de Investigaciones Científicas

erc European Research Council

The ^{79}Se(n,γ) stellar thermometer

Comparison i-TED vs. Conventional C6D6 detectors

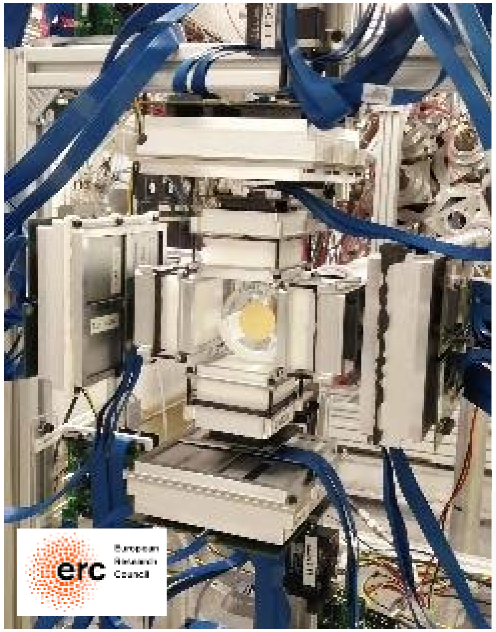

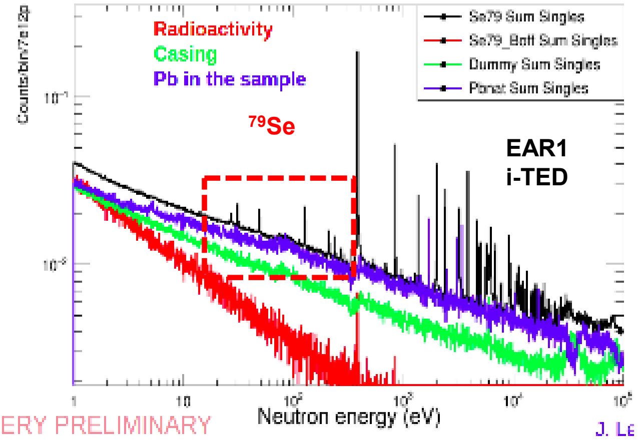

VERY PRELIMINARY

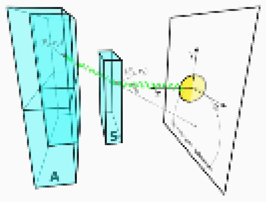

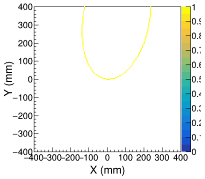

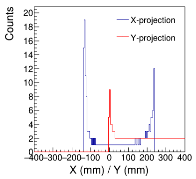

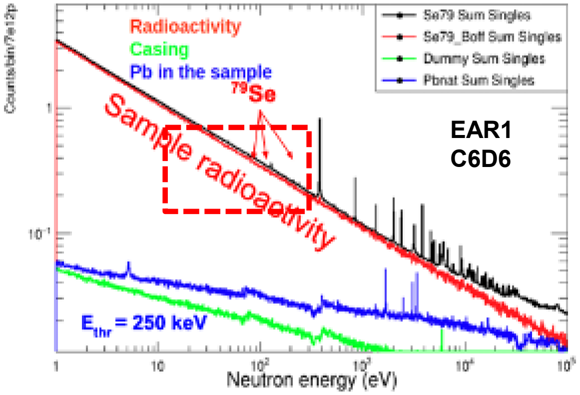

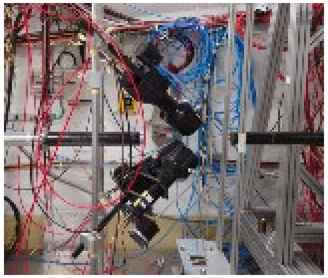

PRELIMINARY RESULTS – DATA ANLYSIS IN PROGRESS-

[CDP, NIM-A 825 (2016)](),
[V.Babiano et al. NIM-A 953 (2020)]()
[V.Babiano-Suarez et al., EPJA, (2022)]()
[J. Lerendegui-Marco et al., EPJWC (2023)]()

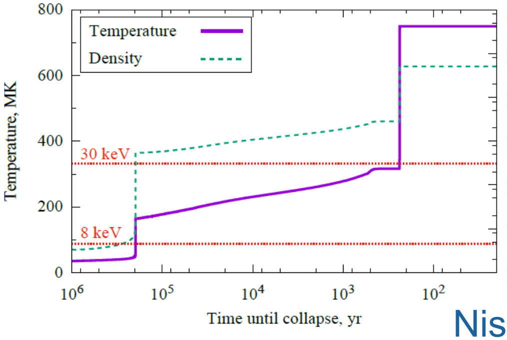

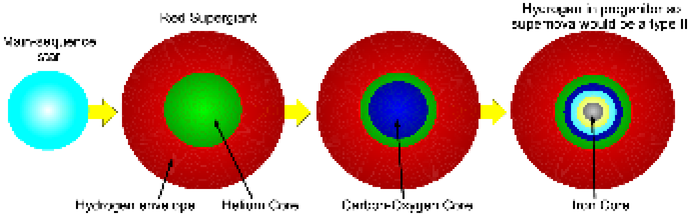

Nishimura+16

Outline

- Heavy elements nucleosynthesis: How stars make gold (r-process) and lead (s-process)?
- Neutron-capture experiments at CERN n_TOF: Red-Giant stars in the lab
- Enhancing detection sensitivity in neutron capture TOF experiments
- Beyond the limits: r-process neutron-reactions in the lab?
- From stars to tumors: ion-range & dose monitoring in hadron therapy
- Summary & Outlook

CSIC

VNIVERSITAT DE VALÈNCIA

erc European Research Council

State-of-the-art TOF neutron-capture measurements: the limit?

EAR1 ^{79}Se(n,γ), 2022

EAR1 ^{205}Tl(n,γ), 2015

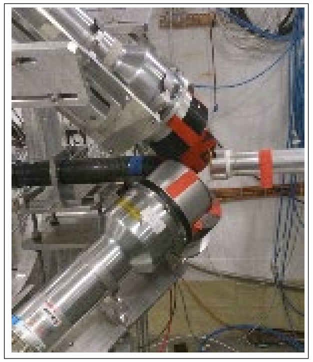

EAR1 ^{151}Sm(n,γ), 2001

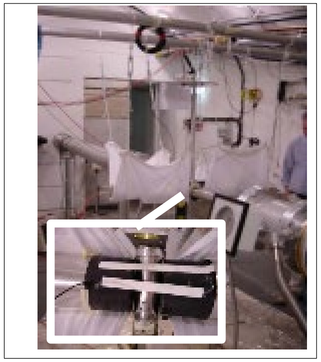

$$FOM = (m_i \cdot \sigma_i \cdot f_e)^{-1}$$

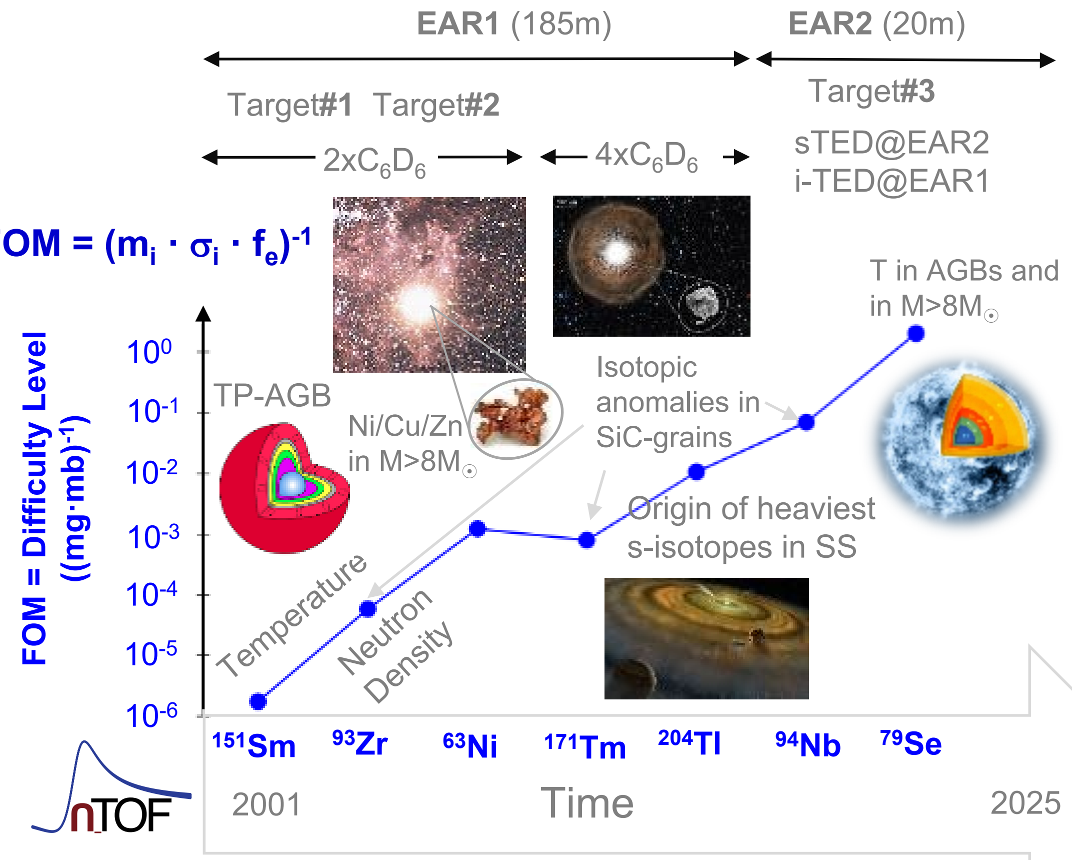

Shortest $t_{1/2}$ = 2-3 years. Still very far from few seconds-minutes half-lives involved in r-process

Target#1 (2000-2004)

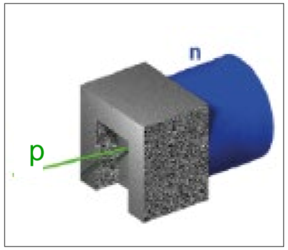

Target#2 (2008-2018)

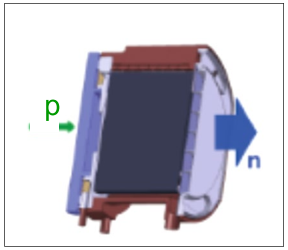

Target#3 (2021-present)

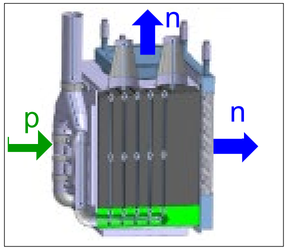

How far are r-nuclei from direct (n, γ) measurements?

Limits in state-of-the-art TOF experiments:

- → Sample > 10^{18} atoms
- → Sample half-life
- → Sample activity < 10 MBq
- → Sample purity / enrichment
- → Neutron-induced backgrounds
- → Detector count rates < 1 MHz

Important neutron-capture isotopes:

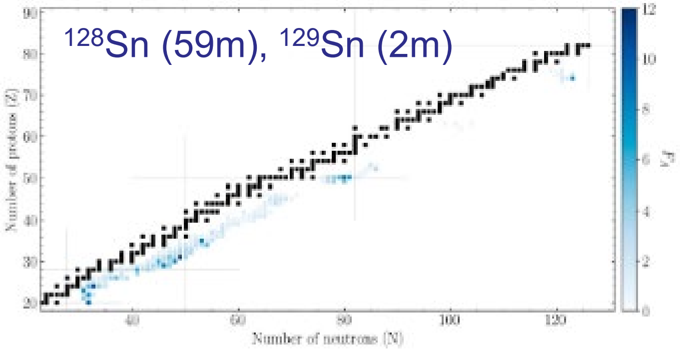

^{128}Sn (59m), ^{129}Sn (2m)

Vescovi+2022

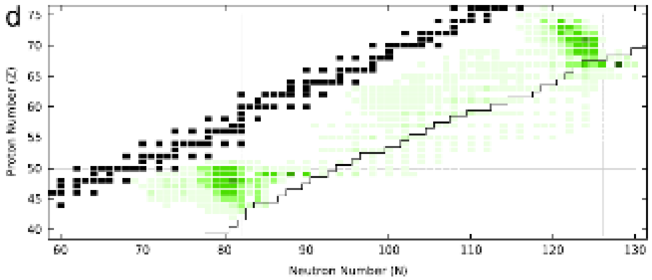

Mumpower+2016

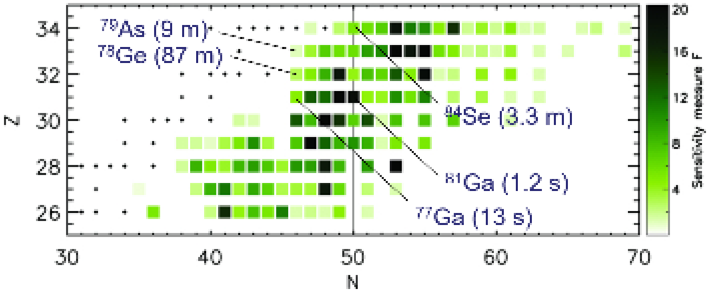

Surman+2014

How far are r-nuclei from direct (n, γ) measurements?

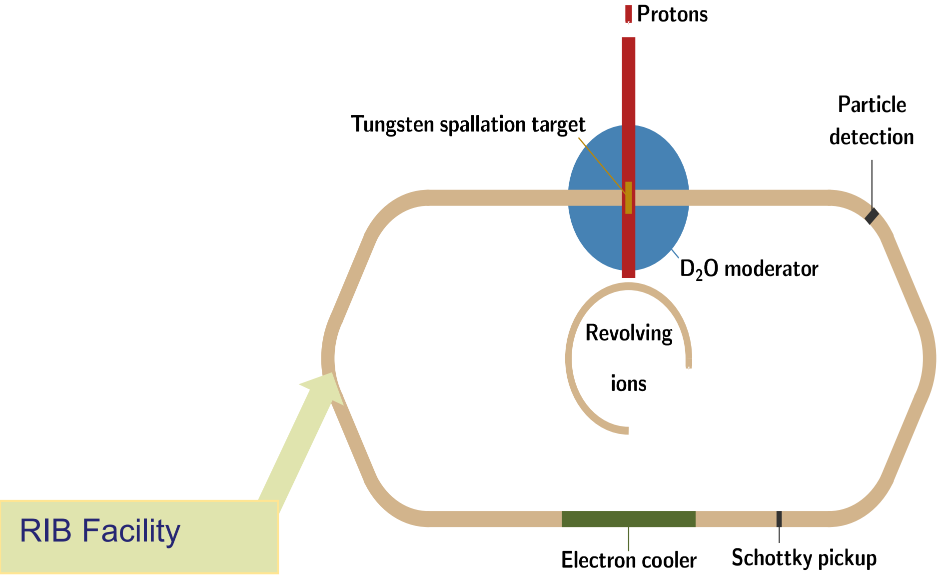

Storage Ring

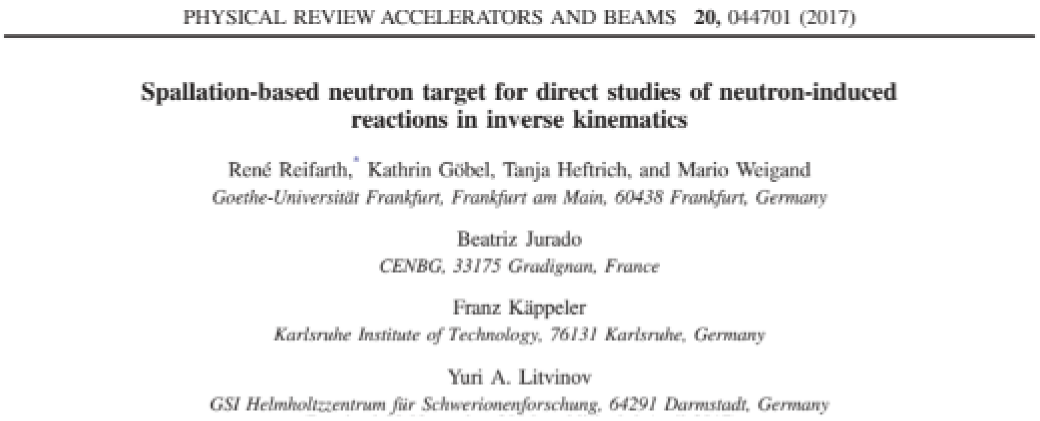

PHYSICAL REVIEW ACCELERATORS AND BEAMS **20,** 044701 (2017)

Spallation-based neutron target for direct studies of neutron-induced reactions in inverse kinematics

René Reifarth,* Kathrin Göbel, Tanja Heftrich, and Mario Weigand
Goethe-Universität Frankfurt, Frankfurt am Main, 60438 Frankfurt, Germany

Beatriz Jurado
CENBG, 33175 Gradignan, France

Franz Käppeler
Karlsruhe Institute of Technology, 76131 Karlsruhe, Germany

Yuri A. Litvinov
GSI Helmholtzzentrum für Schwerionenforschung, 64291 Darmstadt, Germany

Important neutron-capture isotopes:

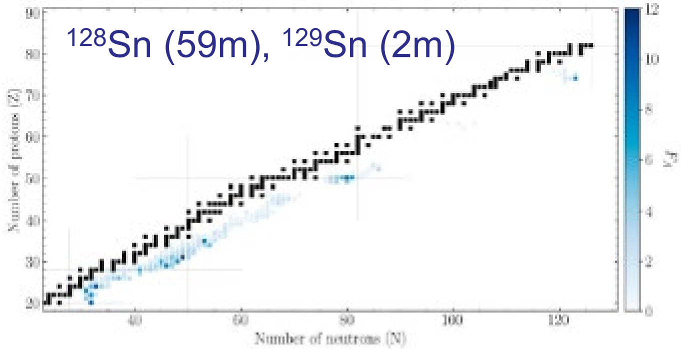

^{128}Sn (59m), ^{129}Sn (2m)

Vescovi+2022

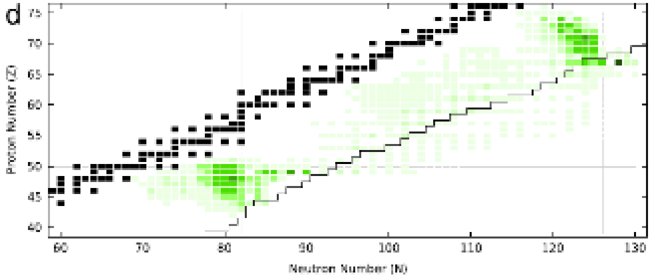

Mumpower+2016

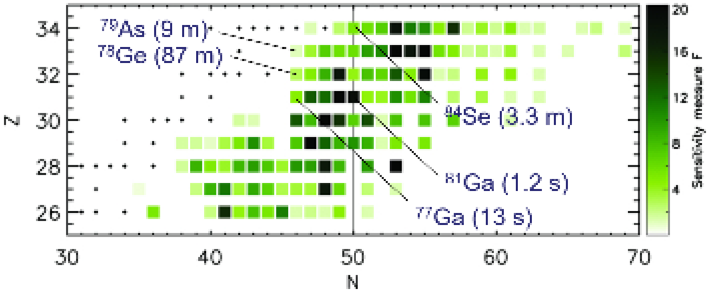

Surman+2014

How far are r-nuclei from direct (n, γ) measurements?

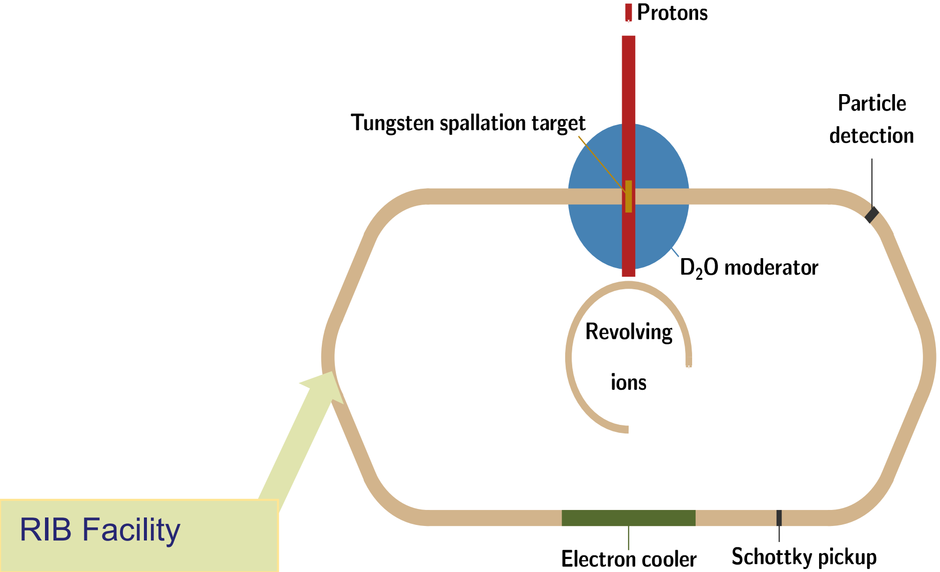

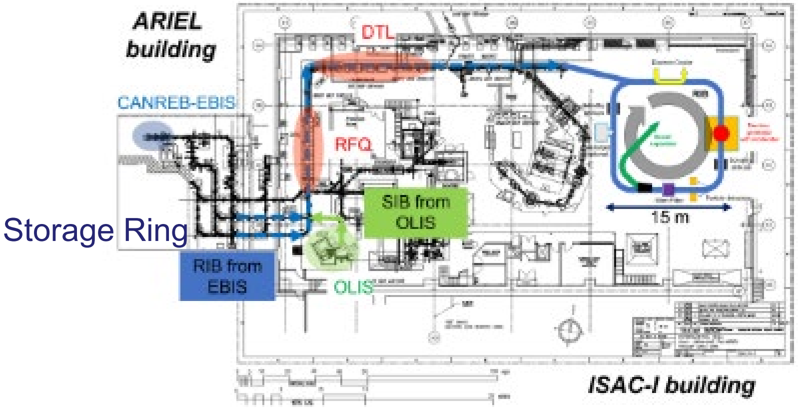

Eur. Phys. J. A (2023) 59:105
https://doi.org/10.1140/epja/s10050-023-01012-9

THE EUROPEAN PHYSICAL JOURNAL A

Regular Article - Experimental Physics

Measuring neutron capture cross sections of radioactive nuclei

From activations at the FZK Van de Graaff to direct neutron captures in inverse kinematics with a storage ring at TRIUMF

Iris Dillmann[1,2,a], Oliver Kester[1,2], Richard Baartman[1,2], Alan Chen[3], Tobias Junginger[1,2], Falk Herwig[2], Dobrin Kalcher[1], Annika Lennarz[1,2], Thomas Planche[1,2], Chris Ruiz[1,2], Nicole Vassh[1]

20th International Conference on Ion Sources — IOP Publishing
Journal of Physics: Conference Series 2743 (2024) 012091 doi:10.1088/1742-6596/2743/1/012091

PHYSICAL REVIEW ACCELERATORS AND BEAMS **20,** 044701 (2017)

Spallation-based neutron target for direct studies of neutron-induced reactions in inverse kinematics

René Reifarth,* Kathrin Göbel, Tanja Heftrich, and Mario Weigand
Goethe-Universität Frankfurt, Frankfurt am Main, 60438 Frankfurt, Germany

Beatriz Jurado
CENBG, 33175 Gradignan, France

Franz Käppeler
Karlsruhe Institute of Technology, 76131 Karlsruhe, Germany

Yuri A. Litvinov
GSI Helmholtzzentrum für Schwerionenforschung, 64291 Darmstadt, Germany

A high-intensity, low-energy heavy ion source for a neutron target proof-of-principle experiment at LANSCE

Andrew L Cooper[1], S Mosby[1], R Reifarth[2], A Couture[1], E Bennett[1], N Gibson[1], D Gorelov[1], C Keith[1], A Lovell[1], G Misch[1], and M Mumpower[1]

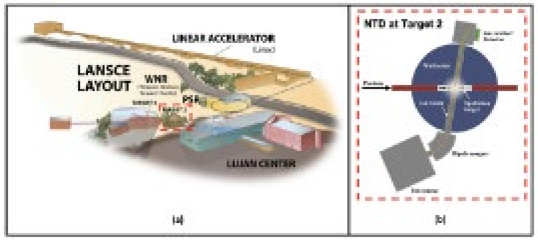

How far are r-nuclei from direct (n, γ) measurements?

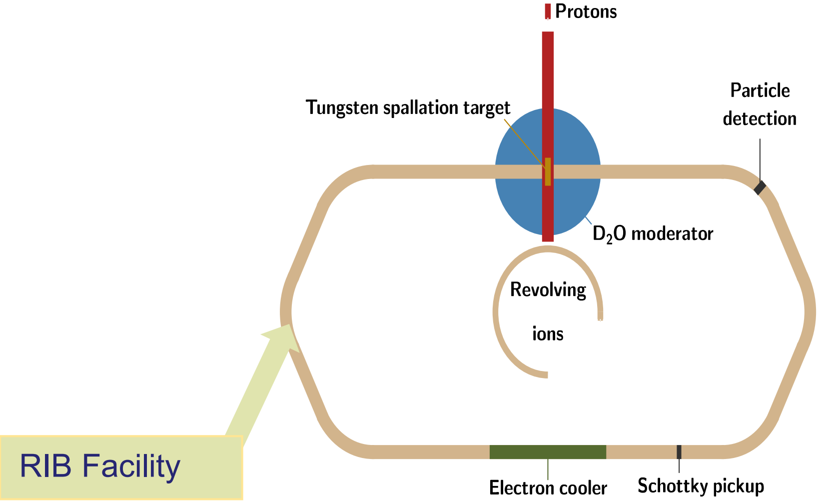

Storage Ring

CERN ISOLDE + nTOF + RING?

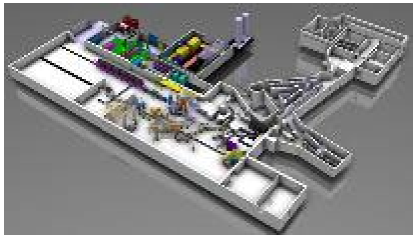

+

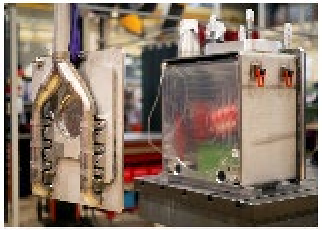

+

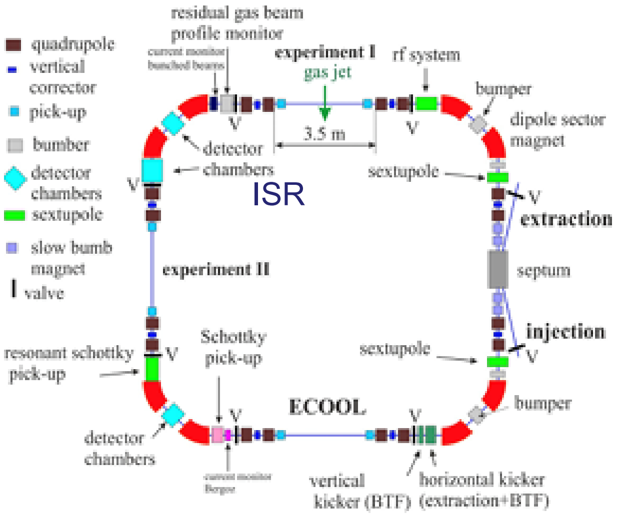

→ISR Project (2030+?)

M. Grieser et al., Eur. Phys. J Spec. Top. 207, 1 (2012)

Outline

- Heavy elements nucleosynthesis: How stars make gold (r-process) and lead (s-process)?
- Neutron-capture experiments at CERN n_TOF: AGB stars in the lab.
- Gamma-ray imaging: Enhancing the sensitivity in neutron capture TOF experiments
- Breaking the limits: r-process neutron reactions in the lab?
- From stars to tumors: ion-range & dose monitoring in hadron therapy
- Summary & Outlook

Artist: Anselm Kiefer
Guggenheim Museum, Bilbao

Therapeutic proton beams for localized tumor treatments

→ Protons: maximum dose deposition at the end of their trajectory (Bragg peak), proposed by R. Wilson in 1946

→ Minimize damage to neighbouring tissues

→ Range uncertainties impose conservative safety margins of 3.5% + 3 mm

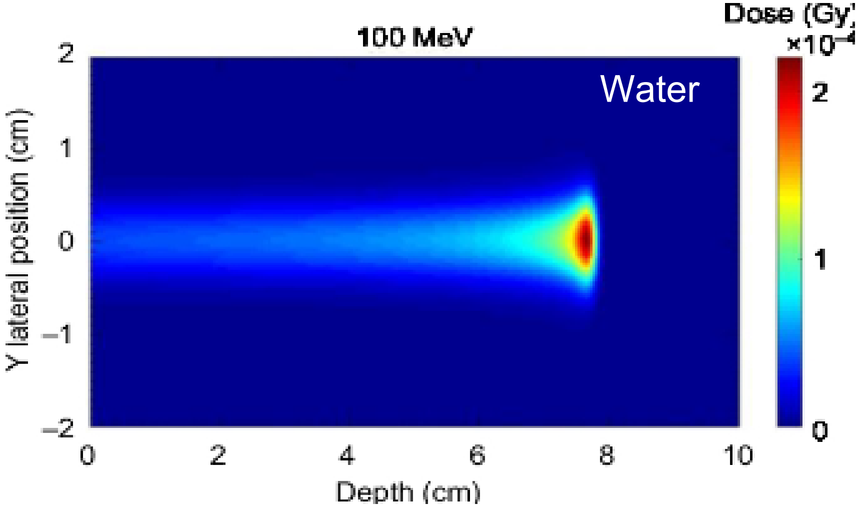

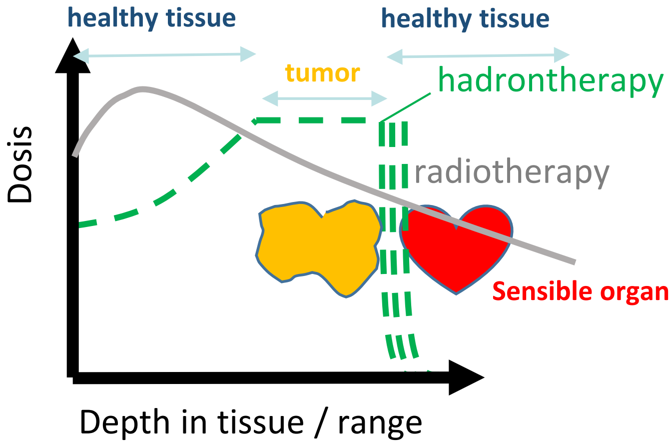

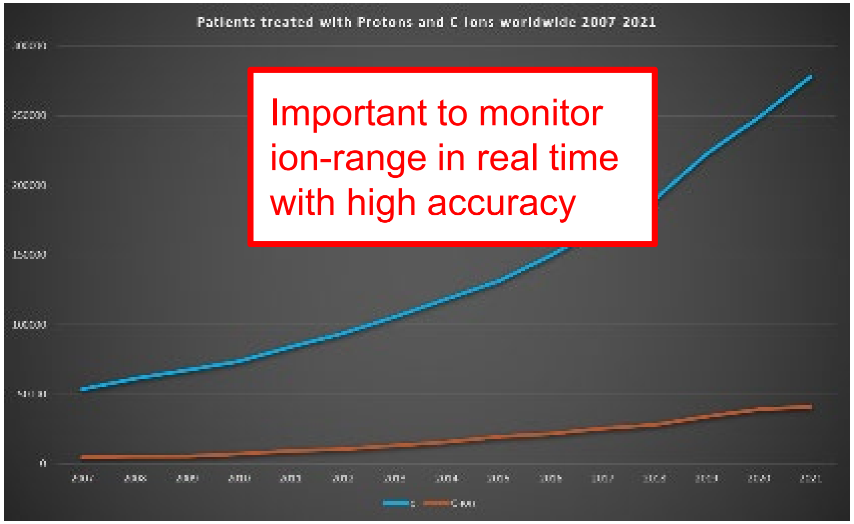

Important to monitor ion-range in real time with high accuracy

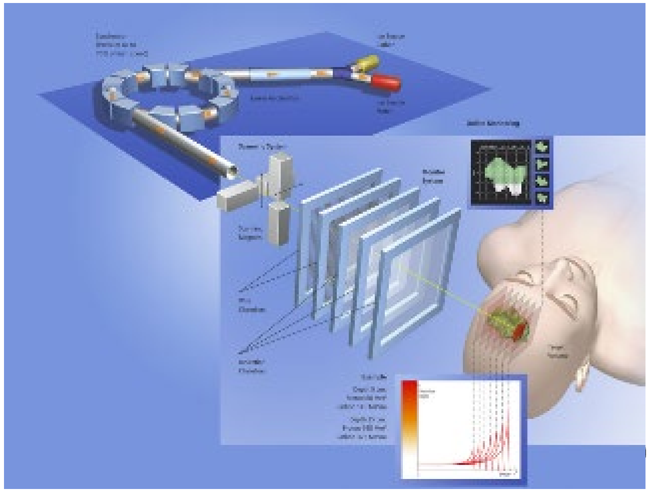

R. Wilson, R.R. (1946); H. Paganetti, Phys. Med. Biol. 57 (2012); U. Amaldi et al., Rep.Prog.Phys. 68 (2005); Zarifi (2019); PTCOG-2022

PET monitoring

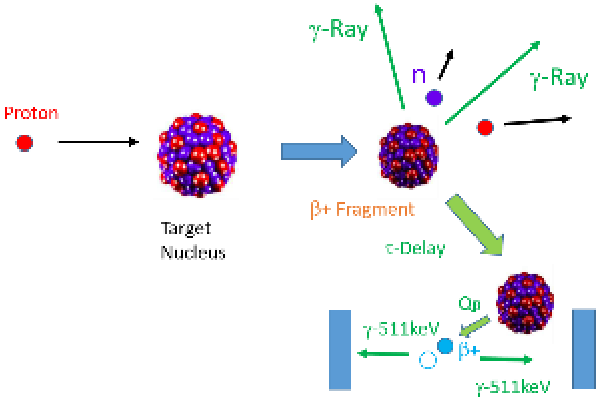

→ Range verification via PET (Llacer, 1979)

- Generally based on ^{15}O (2min), ^{11}C (20min), ^{10}C (20s)
- Sensitive to tissue stoichiometry and mass density
- Functional character: physiological processes and tumour RF
- In-Beam PET: GSI (Enghardt+20, Parodi+02); Excellent sensitivity (**2.5 mm, 10^8p**) with ^{12}N (11ms) and tomographic functionality (KVI-Group, Siemens PET heads)
- Advances with secondary C-beams at GSI+LMU groups (BARB) using radioactive beams of ($^{10\text{-}11}$C) [Kostyleva+23, Boscolo+24, etc], and with $^{14\text{-}\mathbf{15}}$O[Purushothaman+23].

Limitations with "conventional" proton-therapy:

- Delayed (biological washout, organ motion…)
- Not directly coinciding with the Bragg peak
- Low counting statistics (10 Bq/ml) → Low efficiency

Prompt-Gamma Imaging

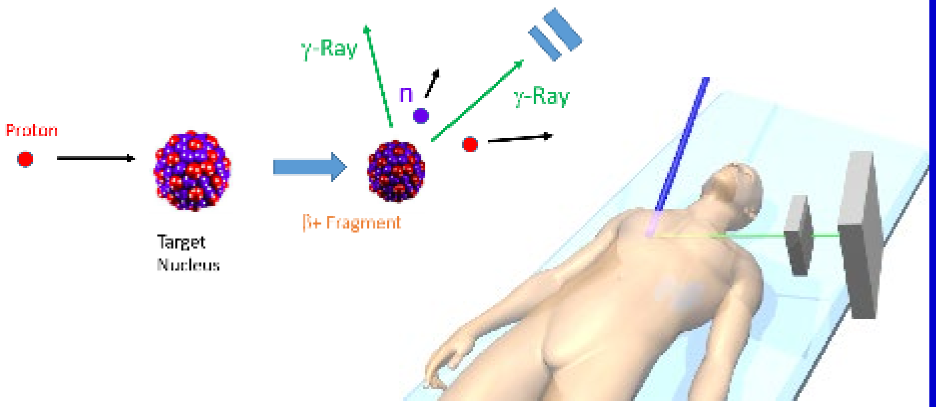

→ Range verification via Prompt Gamma Imaging (Stichelbault&Jongen, 2003)

- Slit camera in clinical use (Smeets+12) → 1-2 mm (1D)
- Most advanced electronic (Compton) imagers: Kabuki+09; Richard+12; Peterson+10; Kormoll+11; Thirolf+14, Llosa+13; etc
- High yield of high-energy γ-rays (2-6 MeV) at the Bragg peak → reliable signature of the ion-range
- Imaging resolution much more limited than in PET
- Low efficiency (particularly for more than two detection planes)
- Large neutron-induced backgrounds (in-beam)

PET monitoring

Prompt-Gamma Imaging

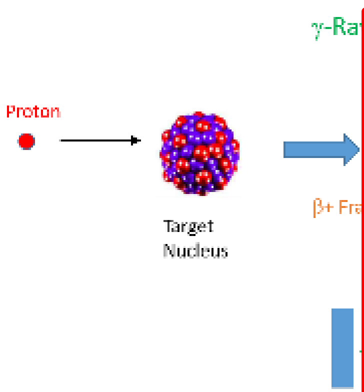

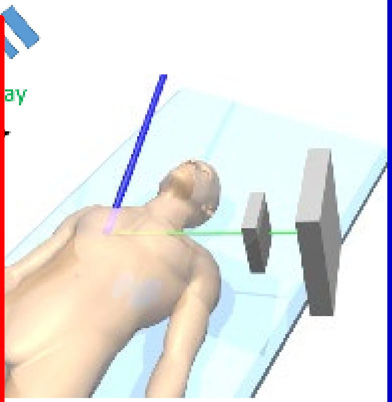

PET

Delayed / Indirect

Efficiency

Image Resolution

Compton

Prompt (Bragg Peak)

Efficiency

Signal/Background

Neutron backgrounds

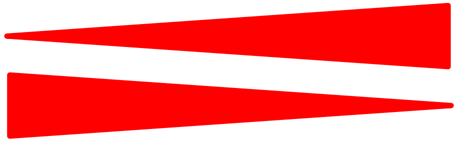

Prompt Gamma Compton & PET together?

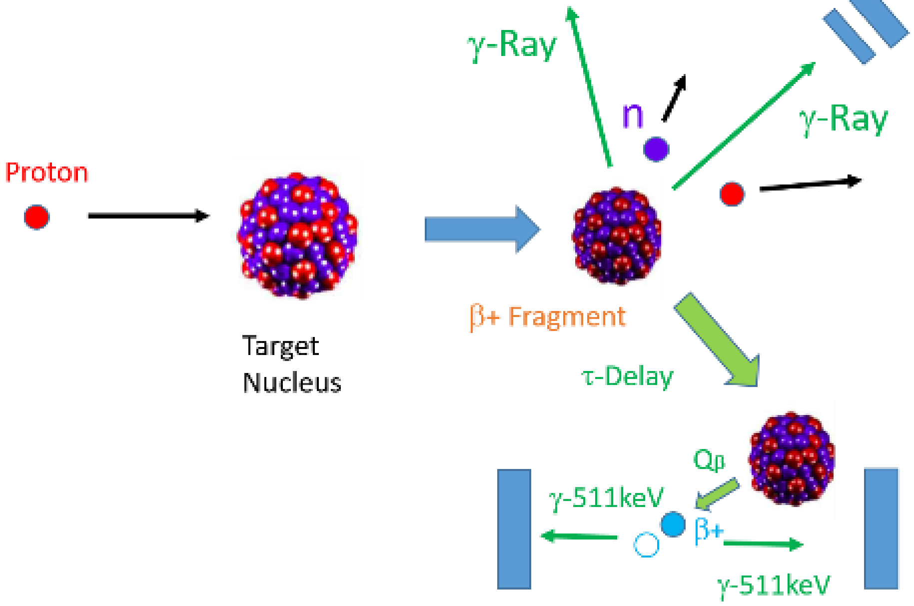

→ Range verification via P

- Generally based on ^{15}O (
- Sensitive to tissue stoich
- Functional character: phy
- In-Beam PET: GSI (Engh
  sensitivity (**2.5 mm, 10^{8}p**
  functionality (KVI-Group,
- Advances with secondary
  (BARB) using radioactive
  Boscolo+24, etc], and wi

Limitations with “conventional

- Delayed (biological wash
- Not directly coinciding wi
- Low counting statistics (1

ompt Gamma Imaging
03)

eets+12) → 1-2 mm (1D)

mpton) imagers: Kabuki+09;

rmoll+11; Thirolf+14,

s (2-6 MeV) at the Bragg

he ion-range

limited than in PET

more than two detection

ounds (in-beam)

Combining PET- and Compton-imaging possible?

K. Parodi, Nucl. Instr. Meth. A (2016)

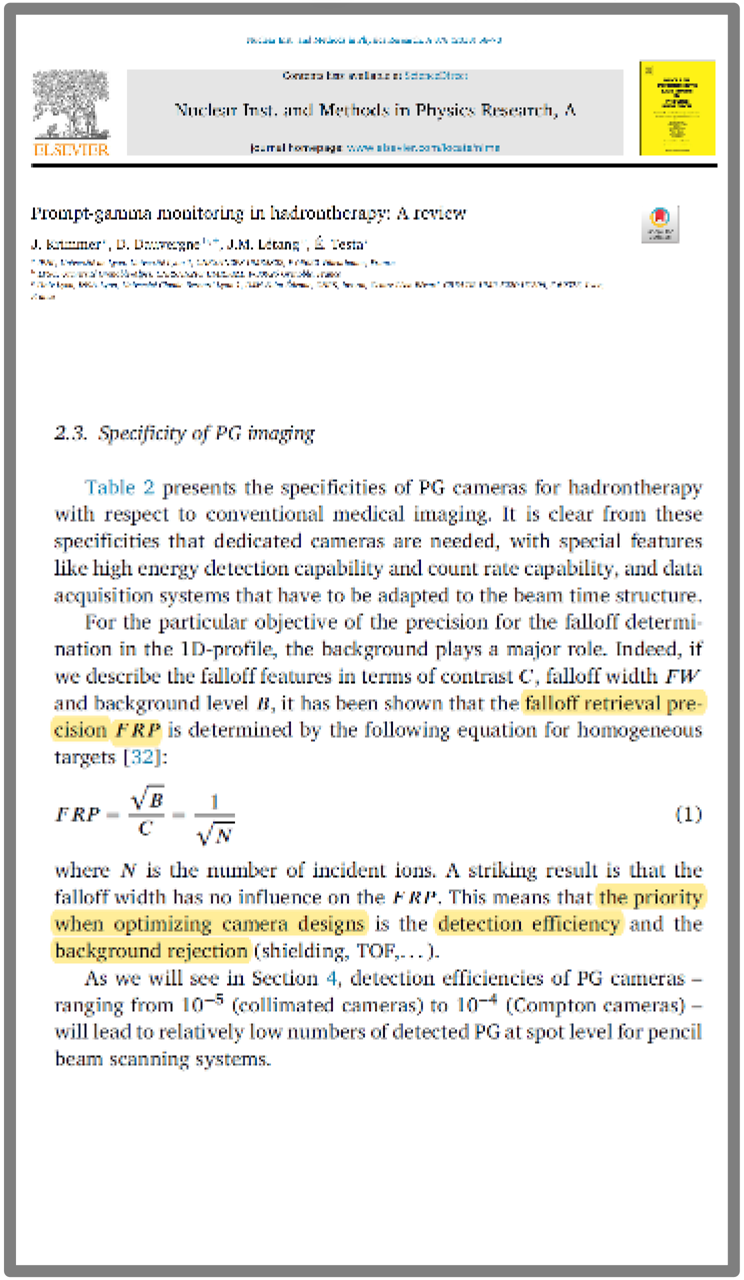

Contents lists available at ScienceDirect

Nuclear Inst. and Methods in Physics Research, A

journal homepage: www.elsevier.com/locate/nima

Prompt-gamma monitoring in hadrontherapy: A review

J. Krimmer, D. Dauvergne, J.M. Létang, É. Testa

2.3. Specificity of PG imaging

Table 2 presents the specificities of PG cameras for hadrontherapy with respect to conventional medical imaging. It is clear from these specificities that dedicated cameras are needed, with special features like high energy detection capability and count rate capability, and data acquisition systems that have to be adapted to the beam time structure.

For the particular objective of the precision for the falloff determination in the 1D-profile, the background plays a major role. Indeed, if we describe the falloff features in terms of contrast C, falloff width FW and background level B, it has been shown that the falloff retrieval precision FRP is determined by the following equation for homogeneous targets [32]:

$$FRP = \frac{\sqrt{B}}{C} = \frac{1}{\sqrt{N}} \qquad (1)$$

where N is the number of incident ions. A striking result is that the falloff width has no influence on the FRP. This means that the priority when optimizing camera designs is the detection efficiency and the background rejection (shielding, TOF,…).

As we will see in Section 4, detection efficiencies of PG cameras – ranging from 10^{-5} (collimated cameras) to 10^{-4} (Compton cameras) – will lead to relatively low numbers of detected PG at spot level for pencil beam scanning systems.

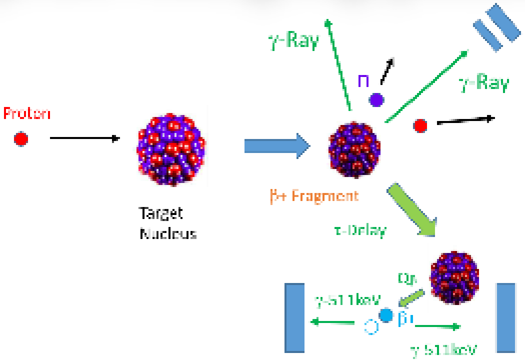

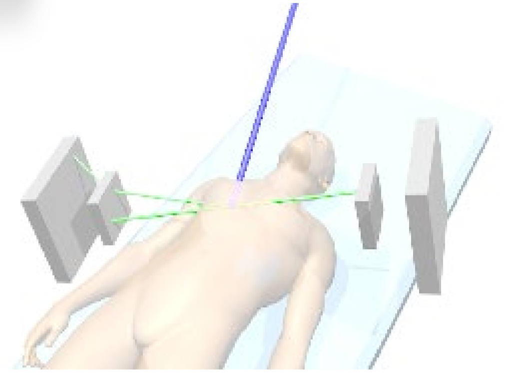

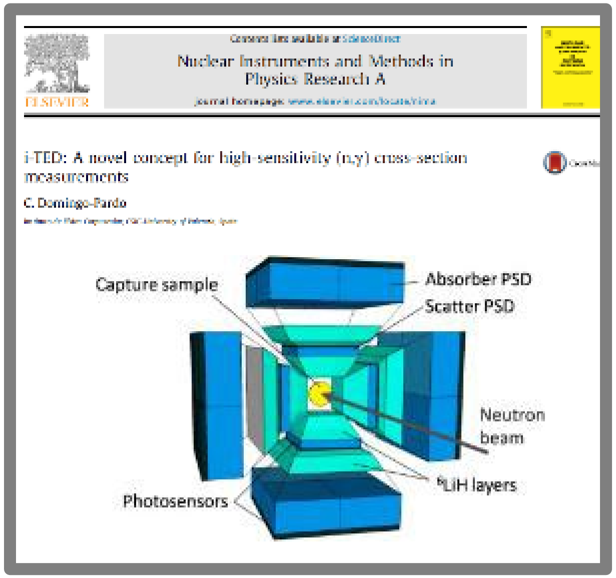

Contents lists available at ScienceDirect

Nuclear Instruments and Methods in Physics Research A

journal homepage: www.elsevier.com/locate/nima

i-TED: A novel concept for high-sensitivity (n,γ) cross-section measurements

C. Domingo-Pardo

- High detection efficiency → Online real-time proton-range verification
- Low sensitivity to n-induced backgrounds → Improved S/B-ratio
- Good performance in the gamma-ray energy range up to 5-6 MeV
- Compact & lightweight → Compatible with clinical environment

First PET-Compton pre-clinical tests at HIT-Heidelberg

Heidelberg Hadrontherapy Center

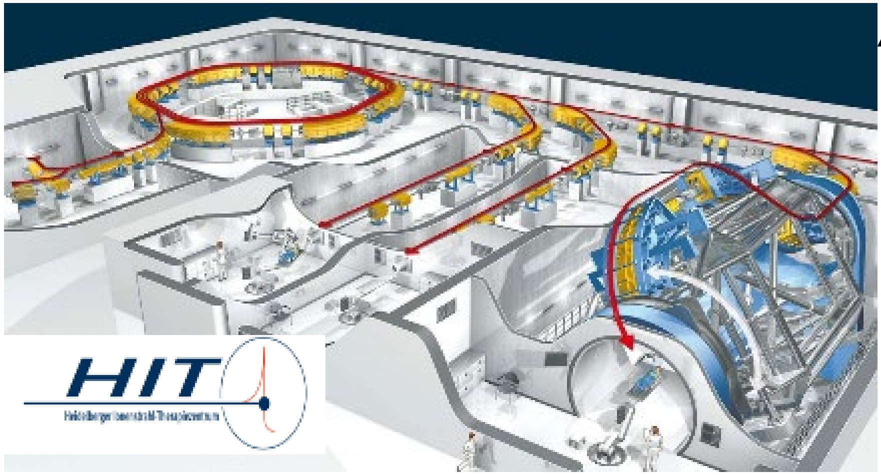

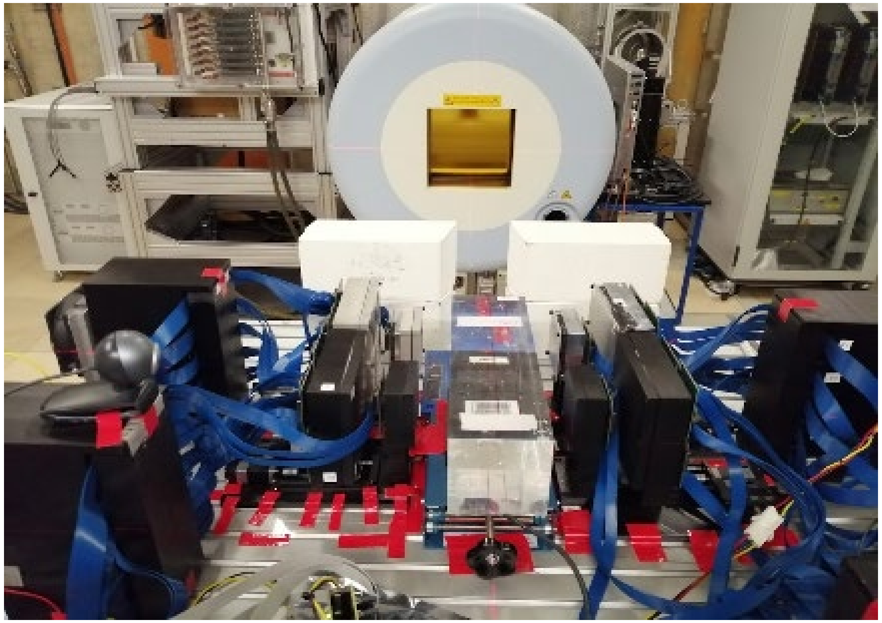

Hybrid **PGI-PET** technique and **pulsed beams**

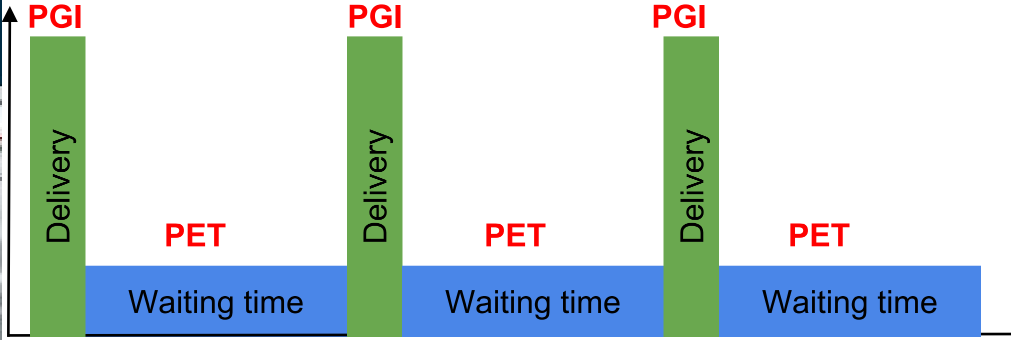

→ Clinical proton-beam energy (55-200 MeV)

→ Clinical proton-intensity (10^8 p/point)

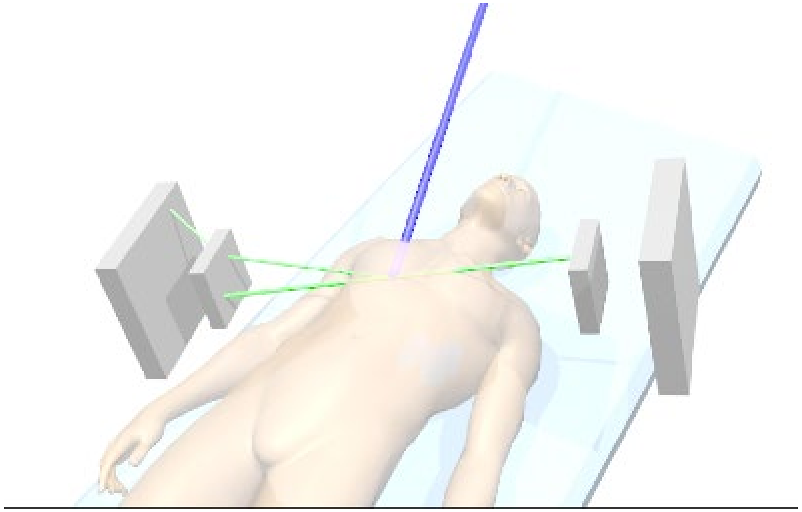

MC-Study: J. Lerendegui-Marco, et al. Nat. Sci. Rep. 12, 2735 (2022)

PoC @ 18 MeV: J. Balibrea-Correa, et al. EPJ-Plus (Nov.2022)

First PET-Compton pre-clinical tests at HIT-Heidelberg

55 MeV p-beam 10^9 p/spot on Graphite Target @ three positions

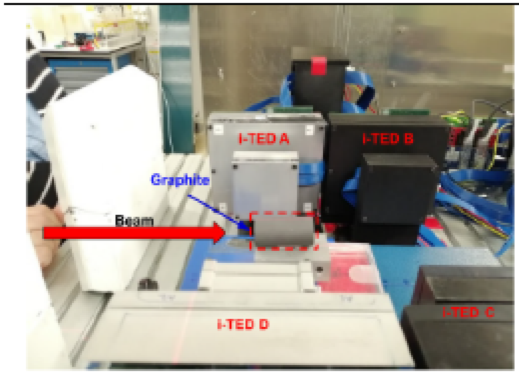

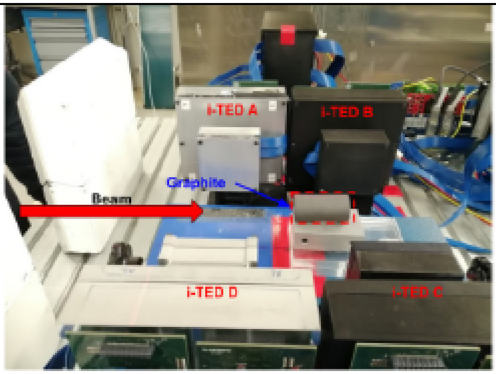

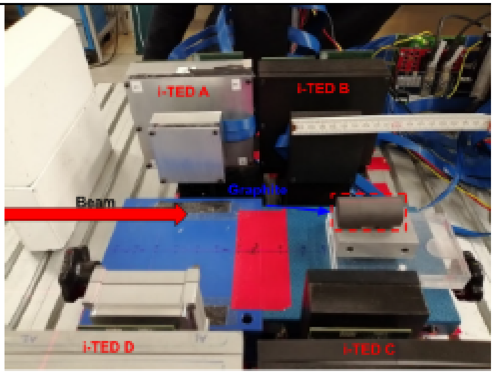

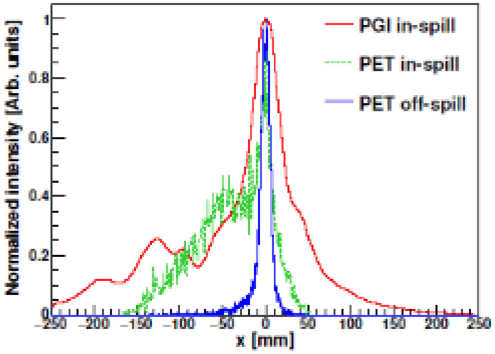

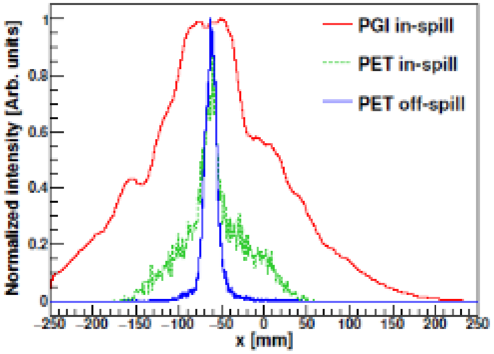

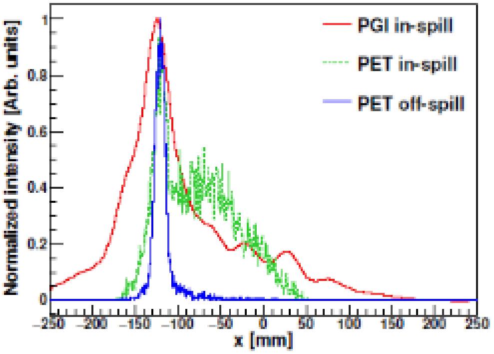

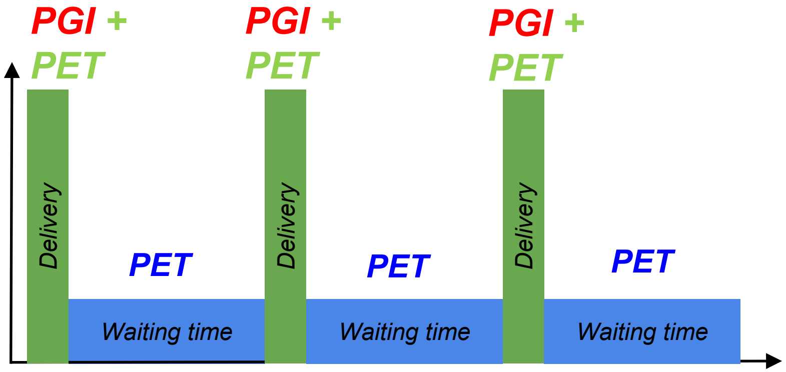

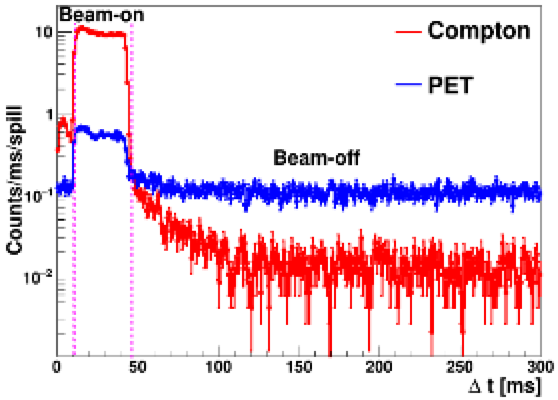

J. Balibrea-Correa, J. Lerendegui-Marco, et al. (HIT, USe) (publication in review)

First PET-Compton pre-clinical tests at HIT-Heidelberg

55 MeV p-beam 10^9 p/spot on Graphite Target @ three positions / Compton PGI:

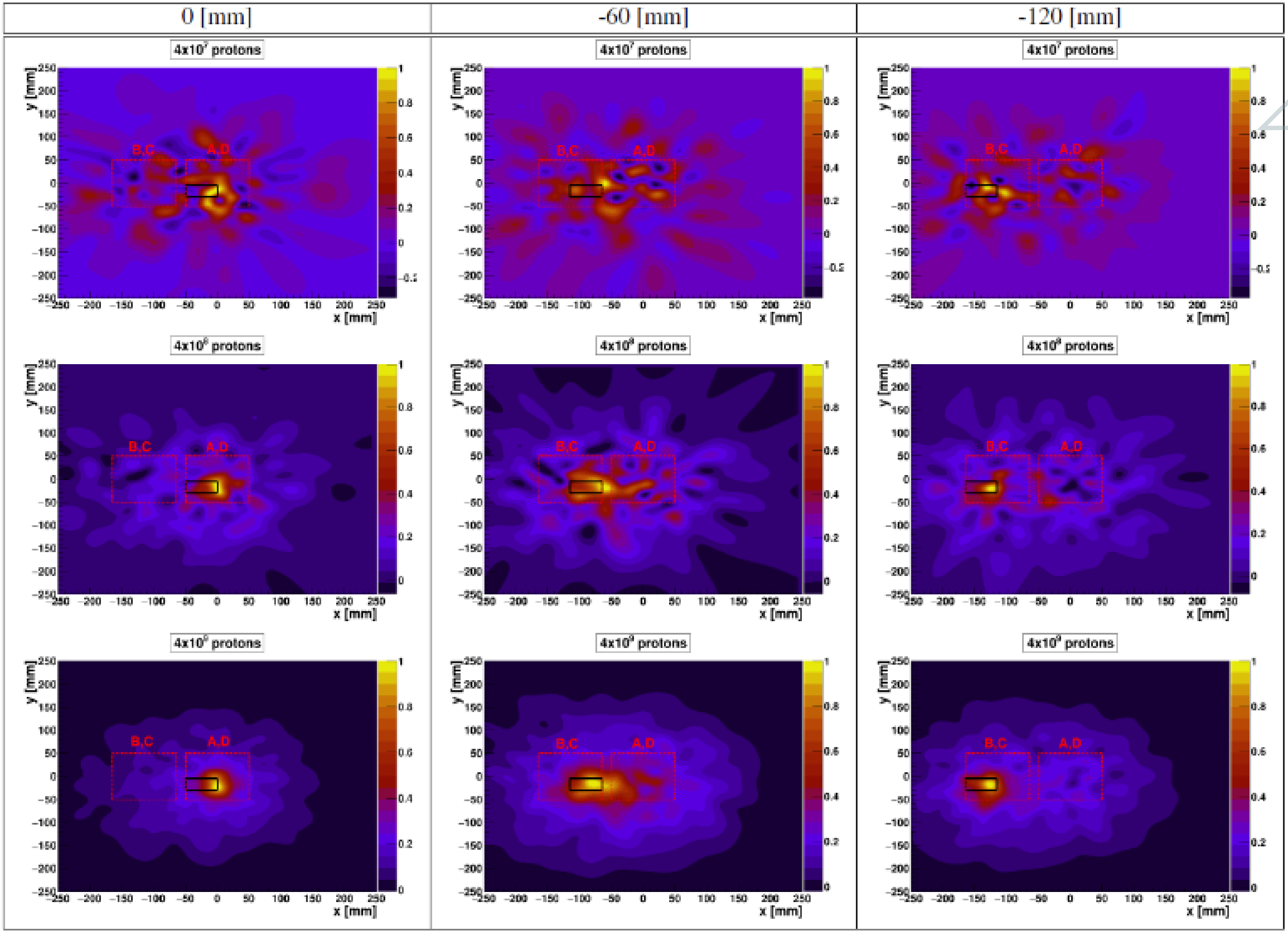

10^7 p/spot

10^8 p/spot

10^9 p/spot

clinical

J. Balibrea-Correa, J. Lerendegui-Marco, et al. (HIT, USe) (publication in review)

First PET-Compton pre-clinical tests at HIT-Heidelberg

150 MeV p-beam 10^9 p/spot on PE-Target @ three positions

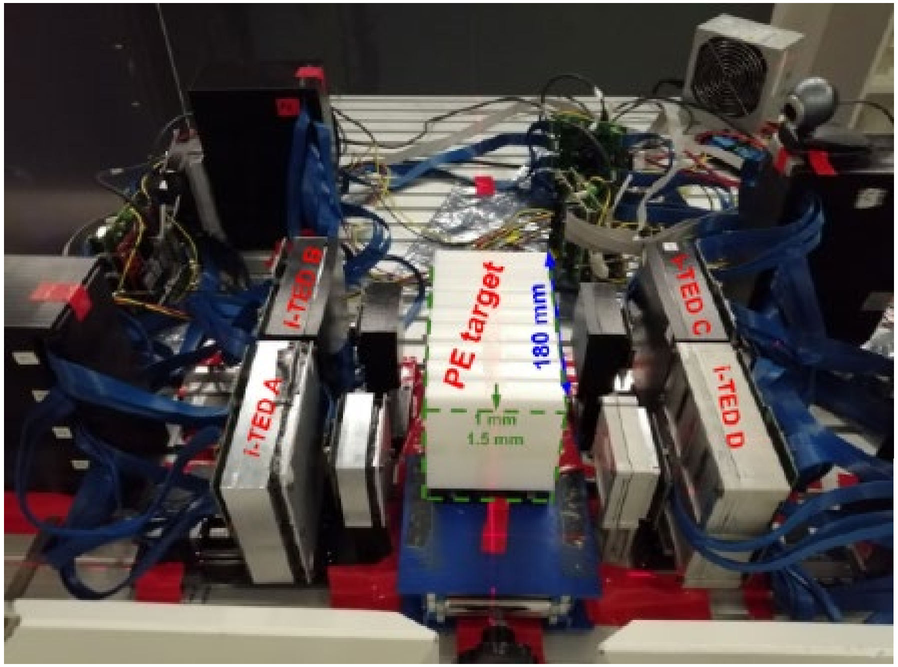

PET in-beam off-spill → mm sensitivity

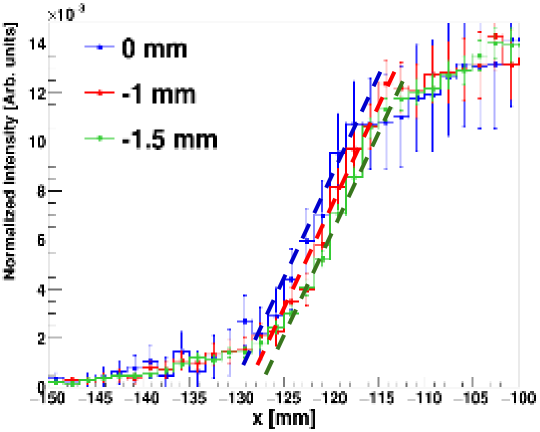

Estimated
Compton PGI
Sensitivity 15mm
at 10^9 p/spot

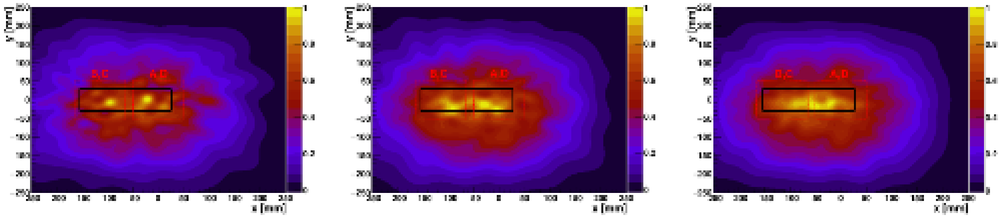

→ Improve geometry → Higher statistics/spot

→ Suppress background → Better S/B

J. Balibrea-Correa, J. Lerendegui-Marco, et al. (HIT, USe) (publication in review)

First PET-Compton pre-clinical tests at WPE

European
Research
Council

ERC-POC
GNVISION

Universitätsmedizin Essen
Universitätsklinikum

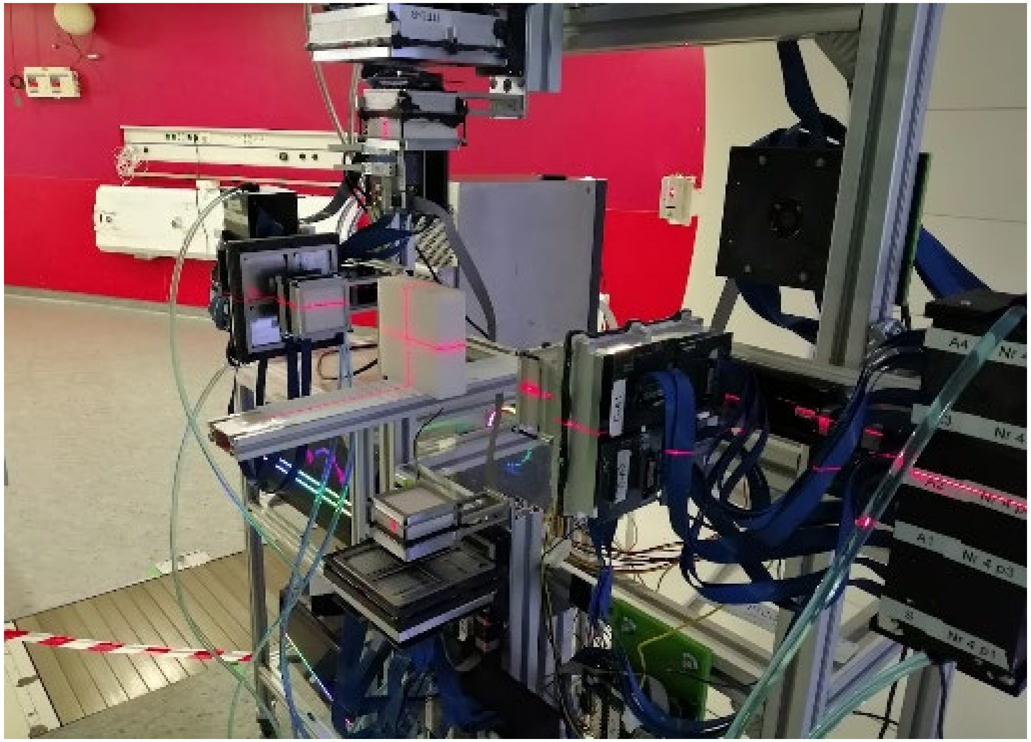

PET Calibration:

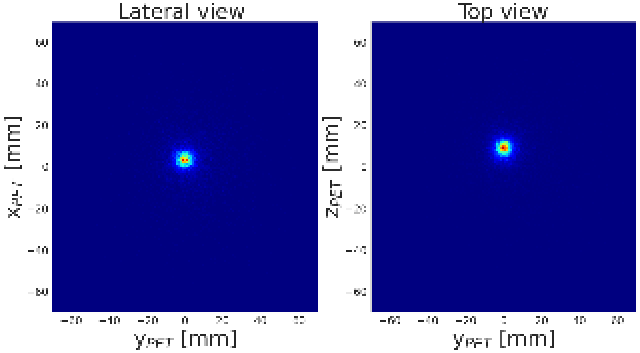

PET in-beam off-spill (range shift):

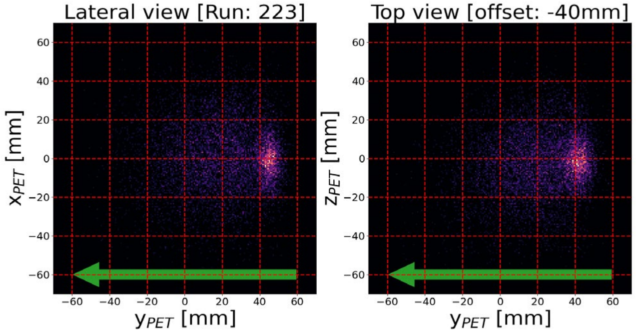

Prel. Est. < 2mm sensitivity for 1E8 p

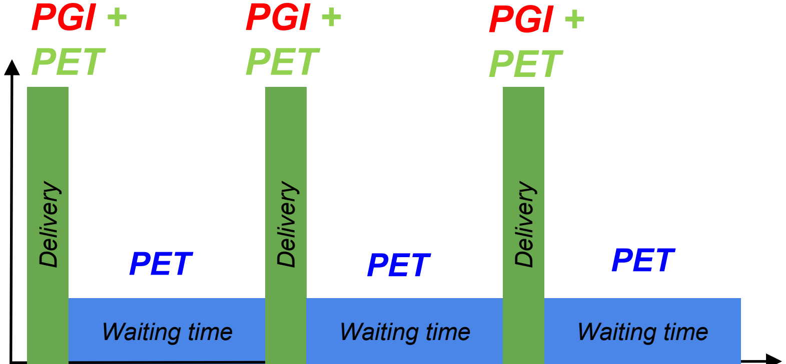

Isochronous Normal Conducting
Cyclotron (**IBA-ProteusPlus**) @ WPE

First PET-Compton pre-clinical tests at WPE

Universitätsmedizin Essen
Universitätsklinikum

European Research Council

ERC-POC
GNVISION

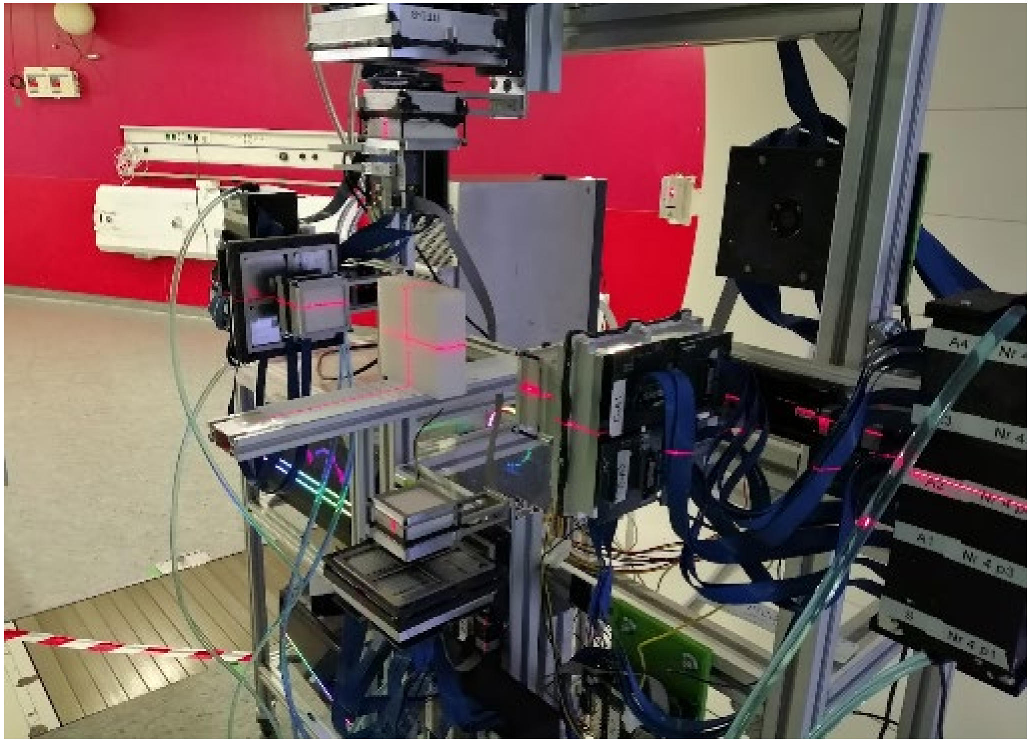

Compton PGI:

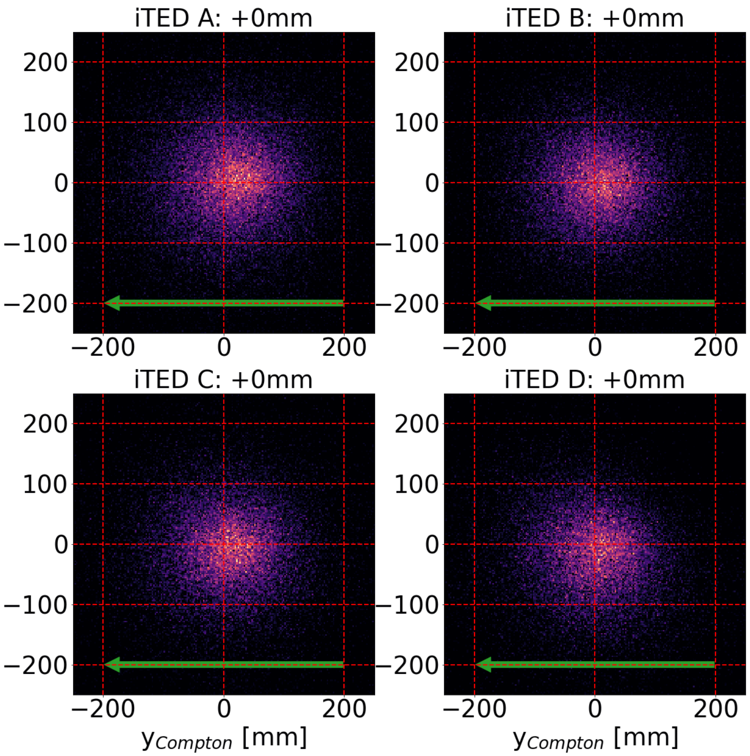

Prel. Est. <4mm sensitivity for 1E8 p

→ Possible to combine Compton & PET with same apparatus using a cyclotron-based machine

→ Data analysis in progress (!)

Dosimetry with therapeutic neutron fields

ERC-POC
AMA

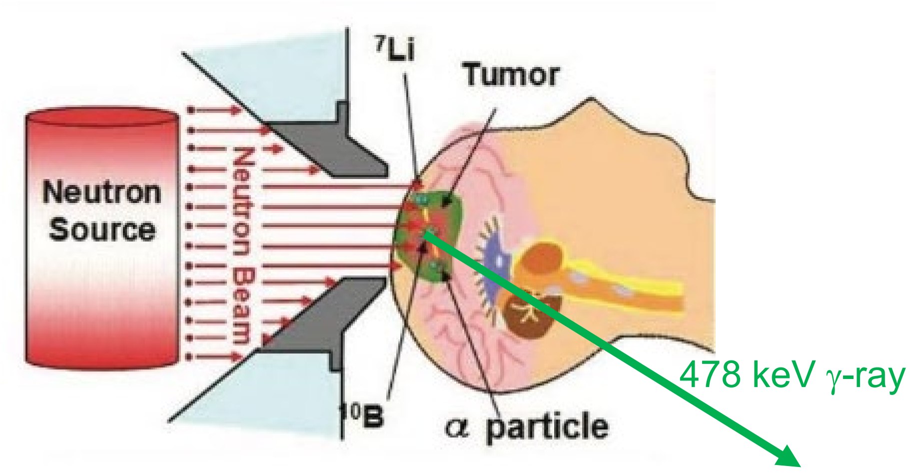

- **BNCT** is an emerging treatment that aims at improving the therapeutic ratio for traditionally difficult to treat tumors.
- Clinically: Glioblastoma multiforme, meningioma, head, neck, lung, breast cancers, etc [Malouff+21]
- **Dosimetry in BNCT presents challenges:**
  - Neutrons interaction within the body
  - Uncertainties associated with the uptake of boron.
- **Current treatment planning:** strong extrapolations of boron uptake by the tumor derived from prior PET scans.

Solution?: online boron-uptake monitoring and spatial distribution via the Compton imaging of the 478 keV line

Challenges:
- Very large count rates (MHz at 50 cm)
- Neutron-induced backgrounds

https://isnct.net/

- Regular patient treatment: 2 (Japan)
- Clinical trial: 6 (Japan, China, Korea, Taiwan)
- Commissioning, Development & Construction

Dosimetry with therapeutic neutron fields

ERC-POC
AMA

- Highly demanding online 3D-reconstruction
- New algorithms required for quasi-real time imaging

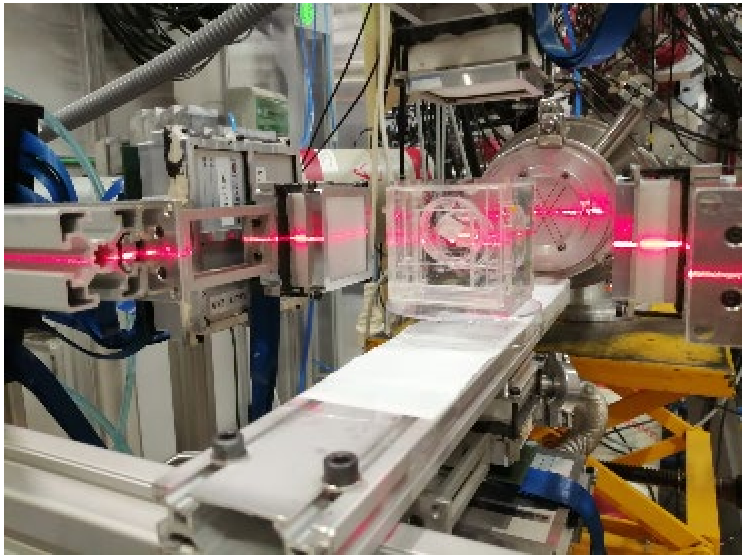

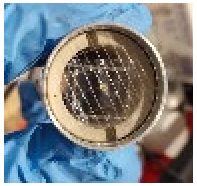

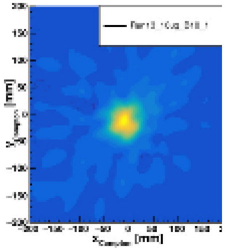

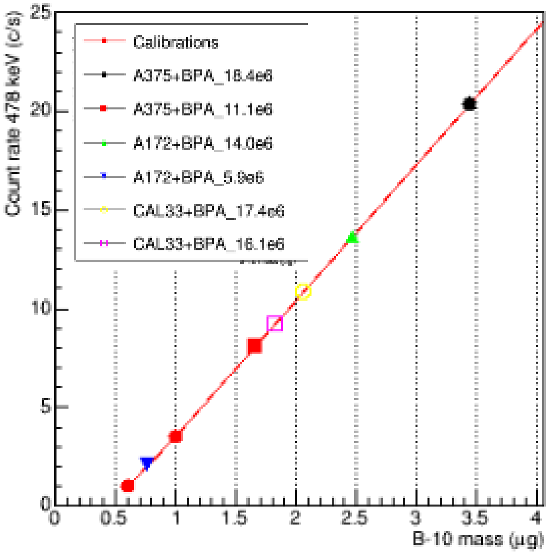

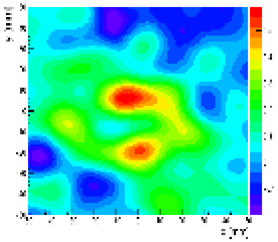

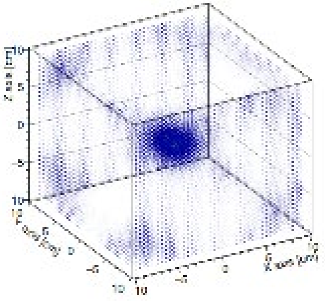

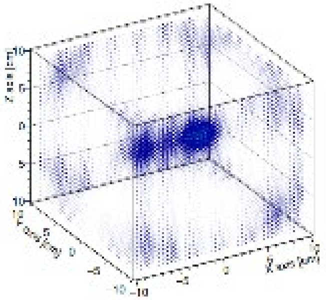

PRELIMINARY RESULTS
WORK IN PROGRESS

Next steps:
- first tests at clinical facility

B. Gameiro et al. (2024) https://doi.org/10.48550/arXiv.2411.04785
P. Torres-Sanchez et al. (2024) https://doi.org/10.1016/j.apradiso.2024.111649
J. Lerendegui-Marco et al. (2024) https://doi.org/10.48550/arXiv.2409.05687

ERC POC-Grant: **A**dvanced imaging system for **M**edical **A**pplications (AMA) (Grant No. 101137646)

Summary & Outlook

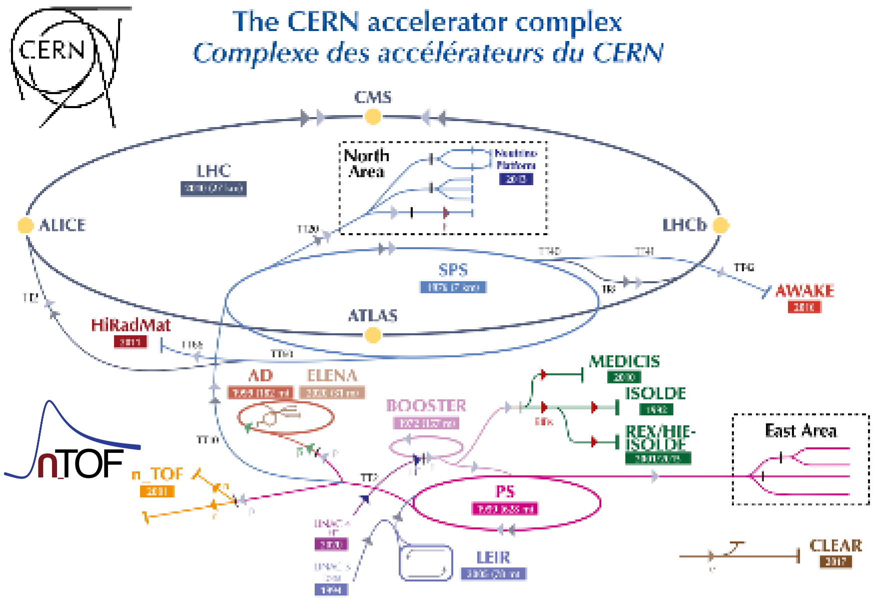

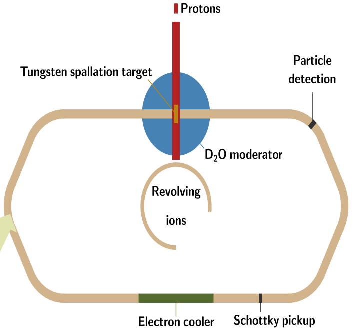

RIB Facility

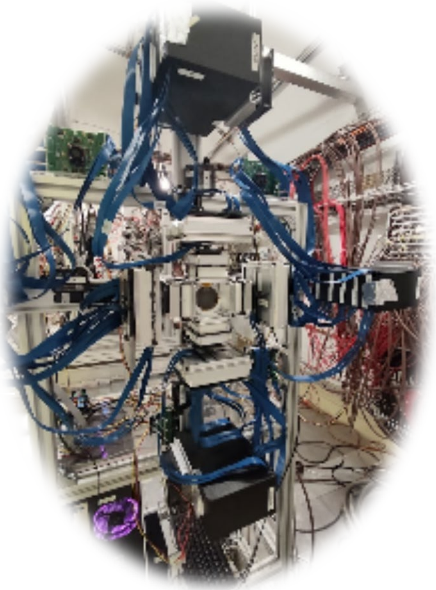

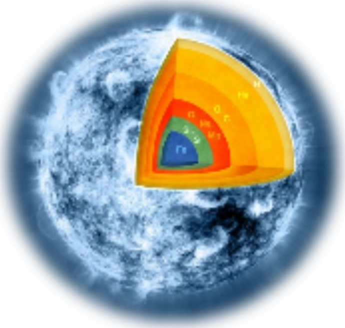

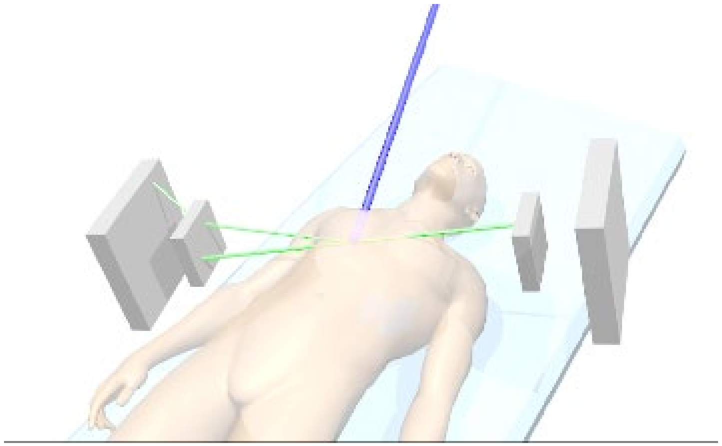

European Research Council

Thanks to all collaborators and funding agencies

O. Aberle[1]
V. Alcayne[2]
S. Amaducci[3,4]
J. Andrzejewski[5]
L. Audouin[6]
V. Babiano-Suarez[7]
M. Bacak[1,8,9]
M. Barbagallo[1,10]
S. Bennett[11]
E. Berthoumieux[9]
J. Billowes[11]
D. Bosnar[12]
A. Brown[13]
M. Busso[10,14,15]
M. Caamaño[16]
L. Caballero-Ontanaya[7]
F. Calviño[17]
M. Calviani[1]
D. Cano-Ott[2]
A. Casanovas[17]
F. Cerutti[1]
E. Chiaveri[1,11]
N. Colonna[10]
G. Cortés[17]
M. A. Cortés-Giraldo[18]
L. Cosentino[3]
S. Cristallo[14,19]
L. A. Damone[10,20]
P. J. Davies[11]
M. Diakaki[21,1]
M. Dietz[24]
C. Domingo-Pardo[7]
R. Dressler[23]
Q. Ducasse[24]
E. Dupont[9]
I. Durán[16]
Z. Eleme[25]
B. Fernández-Domínguez[16]
A. Ferrari[1]
P. Finocchiaro[3]
V. Furman[26]
K. Göbel[27]
R. Garg[22]
A. Gawlik[5]
S. Gilardoni[1]
I. F. Gonçalves[28]
E. González-Romero[2]
C. Guerrero[18]
F. Gunsing[9]
H. Harada[29]
S. Heinitz[23]
J. Heyse[30]
D. G. Jenkins[13]
A. Junghans[31]
F. Käppeler[32]
Y. Kadi[1]
A. Kimura[29]
I. Knapová[33]
M. Kokkoris[21]
Y. Kopatch[26]
M. Krtička[33]
D. Kurtulgil[27]
I. Ladarescu[7]
C. Lederer-Woods[22]
H. Leeb[8]
J. Lerendegui-Marco[18]
S. J. Lonsdale[22]
D. Macina[1]
A. Manna[34,35]
T. Martínez[2]
A. Masi[1]
C. Massimi[34,35]
P. Mastinu[36]
M. Mastromarco[1]
E. A. Maugeri[23]
A. Mazzone[10,37]
E. Mendoza[2]
A. Mengoni[38]
V. Michalopoulou[21,1]
P. M. Milazzo[39]
F. Mingrone[1]
J. Moreno-Soto[9]
A. Musumarra[3,40]
A. Negret[41]
R. Nolte[24]
F. Ogállar[42]
A. Oprea[41]
N. Patronis[25]
A. Pavlik[43]
J. Perkowski[5]
L. Persanti[10,14,19]
C. Petrone[41]
E. Pirovano[24]
I. Porras[42]
J. Praena[42]
J. M. Quesada[18]
D. Ramos-Doval[6]
T. Rauscher[44,45]
R. Reifarth[27]
D. Rochman[23]
Y. Romanets[28]
C. Rubbia[1]
M. Sabaté-Gilarte[18,1]
A. Saxena[46]
P. Schillebeeckx[30]
D. Schumann[23]
A. Sekhar[11]
A. G. Smith[11]
N. V. Sosnin[11]
P. Sprung[23]
A. Stamatopoulos[21]
G. Tagliente[10]
J. L. Tain[7]
A. Tarifeño-Saldivia[17]
L. Tassan-Got[1,21,6]
Th. Thomas[27]
P. Torres-Sánchez[42]
A. Tsinganis[1]
J. Ulrich[23]
S. Urlass[31,1]
S. Valenta[33]
G. Vannini[34,35]
V. Variale[10]
P. Vaz[28]
A. Ventura[34]
D. Vescovi[10,14]
V. Vlachoudis[1]
R. Vlastou[21]
A. Wallner[47]
P. J. Woods[22]
T. Wright[11]
P. Žugec[12]

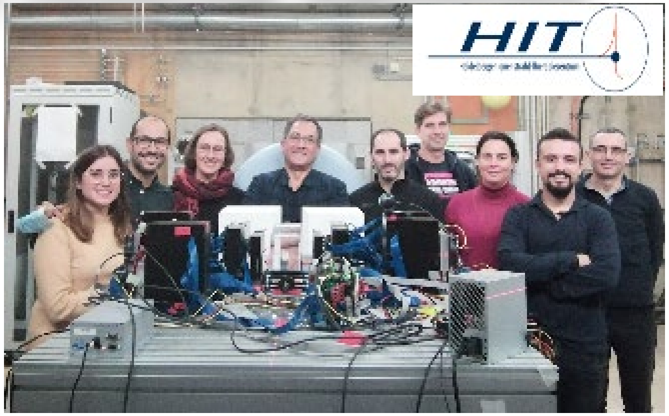

The n_TOF Collaboration

nTOF

European Research Council

erc

ERC-CoG HYMNS Grant Id. 681740

ERC-POC AMA Grant Id. 101137646

ERC-POC GNVISION Grant Id.101113330

CSIC

Universitat de València

PAUL SCHERRER INSTITUT PSI

NEUTRONS FOR SOCIETY

MINISTERIO DE CIENCIA E INNOVACIÓN

Financiado por la Unión Europea NextGenerationEU

Plan de Recuperación, Transformación y Resiliencia

Agencia Estatal de Investigación